NEWLY SYNTHESIZED mRNA ESCAPES TRANSLATIONAL REPRESSION DURING THE ACUTE PHASE OF THE MAMMALIAN UNFOLDED PROTEIN RESPONSE

By

MOHAMMED RUBAYYI ALZAHRANI

Submitted in partial fulfillment of the requirements for

the degree of Doctor of Philosophy

Department of Biochemistry

Advisor: Maria Hatzoglou

CASE WESTERN RESERVE UNIVERSITY

January, 2023

CASE WESTERN RESERVE UNIVERSITY

SCHOOL OF GRADUATE STUDIES

We hereby approve the thesis/dissertation of

Mohammed Rubayyi Alzahrani

candidate for the degree of **Doctor of Philosophy ***

Committee Chair

William Merrick

Advisor

Maria Hatzoglou

Committee Member

Kristian Baker

Committee Member

Richard Padgett

Committee Member

Boaz Tirosh

Date of Defense

November 16th, 2022

*We also certify that written approval has been

obtained for any proprietary material contained therein

DEDICATION

To my parents, sisters, and brothers, especially Abdullah, for their continuous support throughout my scientific journey. To the love of my life, Shouruq, for her shared emotions and assistance in raising our wonderful kids, Rema and Rabie. To my kids who brought joy, built memories, and made life easier and less stressful throughout this scientific journey.

TABLE OF CONTENTS

LIST OF TABLES

LIST OF FIGURES

ACKNOWLEDGEMENTS

In the beginning, I cannot forget King Saud bin Abdulaziz University for Health Sciences (KSAU-HS) in Saudi Arabia who believed in me and gave me the opportunity to study abroad and broaden my horizon in learning science. Therefore, I am indebted for their generosity and support throughout my graduate studies.

This work would not have seen the light without the support of my advisor, Dr. Hatzoglou and my laboratory mates. Here, I would like to thank Dr. Hatzoglou for allowing me to conduct my research in her laboratory and being a friend and mentor at the same time. She has taught me how to address scientific questions and problems and asked me to explore the molecular mechanisms underlying a branch of the integrated stress response pathways. I would like to show my gratitude to my colleagues; Dr. Guan, Dr. Jobava, Dr. Gao, Dr. Chukwurah, Dr. Chen, Dr. Zagore, and Mrs. Wu, a research assistant III, for their support, scientific discussion and teaching me different experimental skills and techniques.

I am filled with gratitude to the members of my PhD research committee (Dr. Baker, Dr. Padgett, Dr. Merrick, and Dr. Tirosh) for their mentorship. I am especially grateful to Dr. Baker for her help with the manuscript and PhD thesis revisions, guidance, and support. Special thanks to Dr. Padgett for his scientific discussion and suggestions, and to Dr. Merrick and Dr. Tirosh for their help with the PhD thesis preparations and revisions. Also, I would like to show my gratitude to Dr. Licatalosi for his guidance, experimental suggestions, and mentorship that ended prior to my thesis defense due to his new position in a different institution and city.

I would like to express my deepest appreciation to the faculty members of the Biochemistry Department at CWRU for their discussion and providing constructive criticism after each seminar I presented in Wood Building-428 Classroom and to the department staff for their assistance and support with administrative papers.

I would like to take this opportunity to express my gratitude to Dr. Wek who was my mentor for my master's degree in Biochemistry and Molecular Biology Department at Indiana University-Purdue University Indianapolis. When I began in Dr. Wek's Laboratory, I had no clue how RNA isolation could be performed. Therefore, I thank Dr. Wek and his laboratory personnel for developing my laboratory skills that helped me to be the person I am today and paved the way to pursue and finish my PhD degree.

Finally, I would like to thank my family: my parents, brothers, and sisters. I was raised among them with infinite love, care, and support. On an equivalent scale, I am grateful for my other half, my wife, who has supported me through my scientific journey since the beginning when I started learning English as a second language. She eased and reduced homesickness while we were abroad. In addition, I thank my children [Rema (9 years) and Rabie (3 years) born in Long Beach and Cleveland cities, respectively]. By raising them in the USA, we had great times to run away from stressful moments of life.

LIST OF ABBREVIATIONS

A	Adenosines
aa	Amino Acids
ABCE1	ATP-Binding Cassette Subfamily E Member 1
ADP	Adenosine Diphosphate
ALYREF	Aly/REF Export Factor
APA	Alternative Polyadenylation
A-Site	Ribosomal Amino-Acylated tRNA-Site
Asn	Asparagine (N)
Asp	Aspartic acid (D)
ATF	Activating Transcriptional Factor
ATF4	Activating Transcriptional Factor 4
ATF6α	Activating Transcriptional Factor 6-α
ATF6β	Activating Transcriptional Factor 6-β
ATP	Adenosine Triphosphate
ATP5B	ATP Synthase F1 Subunit-β
ATPase	Adenosine Triphosphatase
BiP	B-cell Immunoglobulin Binding Protein
BLOS1	Biogenesis of Lysosomal Organelles Complex 1 Subunit 1
BPS	Branchpoint Sequence
bZIP	Basic Leucine Zipper Transcription Domain
C	Cytosine

°C	Celsius Degree
Ca^{2+}	Calcium
Caf1	CCR4-Associated Factor 1
CBS	Cap-Binding Protein Complex
CCR4-NOT	Carbon Catabolite Repression 4-Negative on TATA
CCTα	CTP:phosphocholine Cytidylyltransferase
CDK	Cyclin-Dependent Kinase
cDNA	Complementary DNA
CDS	Coding Sequence
CERT	Ceramide Transfer Protein
CF I	Cleavage Factors I
CF II	Cleavage Factors II
CHOP	CCAAT/Enhancer-Binding Protein Homologous Protein
Con	Control or Cells Treated with DMSO
COPI	Coat Protein Complex I
COPII	Coat Protein Complex II
CPA	Cyclopiazonic Acid
CPAC	Cleavage and Polyadenylation Complex
CPEB4	Cytoplasmic Polyadenylation Element-Binding 4
CPSF	Cleavage and Polyadenylation Specificity Factor
CRAC	Ca^{2+} Release-Activated Channels
CREB	cAMP-Response Element-Binding

CREB3	cAMP-Response Element-Binding Protein 3
CReP	Constitutive Repressor of eIF2α-P
CRM1	Chromosomal Maintenance 1
Cryo-EM	Cryogenic Electron Microscopy
CstF	Cleavage Stimulation Factor
CTD	Carboxyl (C)-Terminal Domain
CTE	Constitutive Transport Element
Cys	Cysteine (C)
DAG	Diacyl Glycerol
DCP1	Decapping Protein 1
DCP2	Decapping Protein 2
DDX	DEAD-Box Helicase
DELE1	DAP3 Binding Cell Death Enhancer 1
DIS3L2	DIS3-Like 3′-5′ Exoribonuclease 2
DMSO	Dimethyl Sulfoxide
DNA	Deoxyribonucleic Acid
DRB	5,6-Dichloro-1-Beta-D-Ribofuranosylbenzimidazole
DSIF	DRB Sensitivity-Inducing Factors
dsRBM	Double-Stranded Ribonucleic Acid Binding Motifs
dsRNA	Double-Stranded Ribonucleic Acid
DTT	Dithiothreitol
DXO	Non-Canonical Decapping Exoribonuclease

E-complex	Early Complex of Spliceosome Assembly
E Fraction	Eluted or 5EU-Labeld RNAs
4E-BP	eIF4E-Binding Proteins
EDC	Enhancer of mRNA Decapping Proteins
EDEM	ER Degradation-Enhancing α-Mannosidase-Like Proteins
EDTA	Ethylenediaminetetraacetic Acid
eEF1A	Eukaryotic Translation Elongation Factor 1 A
eEF1B	Eukaryotic Translation Elongation Factor 1 B
eEF2	Eukaryotic Translation Elongation Factor 2
eEF2K	eEF2 Kinase
eEF3	Eukaryotic Elongation Factor 3
eIF2	Eukaryotic Translation Initiation Factor 2
eIF2B	Eukaryotic Translation Initiation Factor 2 B
eIF2Bε	Eukaryotic Translation Initiation Factor 2 B Subunit ε
eIF2α	Eukaryotic Translation Initiation Factor 2 Subunit α
eIF2α-P	Eukaryotic Translation Initiation Factor 2 Subunit α-Phosphorylation
eIF3	Eukaryotic Translation Initiation Factor 3
eIF4A	Eukaryotic Translation Initiation Factor 4 A
eIF4B	Eukaryotic Translation Initiation Factor 4 B
eIF4E	Eukaryotic Translation Initiation Factor 4 E
eIF4F	Eukaryotic Translation Initiation Factor 4 F
eIF4G	Eukaryotic Translation Initiation Factor 4 G

eIF5A	Eukaryotic Translation Initiation Factor 5 A
eIF5B	Eukaryotic Translation Initiation Factor 5 B
EJC	Exon-Junction Complex
ER	Endoplasmic Reticulum
ERAD	ER-Associated Degradation System
ERES	ER Exit Sites
eRF1	Eukaryotic Release Factor 1
eRF3	Eukaryotic Release Factor 3
eRNA	Enhancer RNAs
ERSE-I	ER Stress Response Element-I
ERSE-II	ER Stress Response Element-II
E-Site	Ribosomal Deacylated tRNA Exit-Site
E-Syts	Extended-Synaptotagmins
5EU	5-Ethynyl Uridine
EXO	Exosome
F Fraction	Polyribosome-Free Fractions
FFAT	Two Phenylalanines in an Acidic Tract
FT Fraction	Flow-Through or Unlabeled mRNA
G	Guanosines
G domain	GTP-Binding Domain
GADD34	Growth Arrest and DNA-Damage-Inducible Protein 34
GANP	Germinal Center-Associated Nuclear Protein

GAP	GTPase Activating Proteins
GAPDH	Glyceraldehyde 3-Phosphatase Dehydrogenase
GCN2	General Control Nonderepressible-2
GDP	Guanosine Diphosphate
GEF	Guanine Nucleotide-Exchange Factor
GI-Oligo Tail	Guanosine/Inosine Oligo Tail
GLE1	GLE1 RNA Export Mediator
Gln	Glutamine (Q)
Glu	Glutamic acid (E)
Gly	Glycine (G)
GMD	Glucocorticoid Receptor-Mediated Decay
GMP	Guanosine Monophosphate
GPI	Glycosyl Phosphatidyl Inositol
GPI-AP	GPI- Anchored Proteins
GTP	Guanosine Triphosphate
GU	Guanosine-Uridine
H	Hour
H Fraction	Heavy Polyribosome Fractions
H3K4me3	Tri-Methylation of Histone 3 on Lys-4
H44	18S rRNA Helix
HEAT	Huntingtin, Elongation Factor 3, Protein Phosphatase 2A, Tor1
HEPES	4-(2-Hydroxyethyl)-1-Piperazineethanesulfonic Acid

HEXIM1	Hexamethylene-Bis-Acetamide-Inducible Protein
His	Histidine (H)
His-RS	Histidyl-tRNA Synthetase Like Domain
HR	Hydrophobic Regions
HRI	Heme-Regulated Inhibitor Kinase
HRSP12	Heat-Responsive Protein 12
HSP40	Heat Shock Protein 40
HSP90	Heat Shock Protein 90
IDR	Intrinsically Disordered Regions
IER3IP1	Immediate Early Response 3 Interacting Protein 1
IFN	Interferons
INSIG	Insulin-Induced Gene
IP3	Inositol (1,4,5)-Trisphosphate
IRE1α	Inositol-Regulated Enzyme 1-α
IRE1β	Inositol-Regulated Enzyme 1-β
ISR	Integrated Stress Response
ISRIB	ISR Inhibitor
KD	Kinase Domain
kDa	Kilodalton
KO	Knockout
KOH	Potassium Hydroxide
L Fraction	Light Polyribosome Fractions

LARP	La-Related Proteins
lncRNA	Long Non-Coding RNA
LSM	Sm-Like Proteins
LSM 14	LSM14A mRNA processing body assembly factor
Lys	Lysine (K)
m^6A	N-6 Methylation of Adenosine
m^7G	7-Methylguanosine
MAFA	MAF bZIP Transcription Factor A
MCS	Membrane Contact Sites
MEF cells	Mouse Embryonic Fibroblasts
Met	Methionine (M)
Mg^{2+}	Magnesium
Min	Minutes
MIN6	Mouse Pancreatic β Cells
miRNA	MicroRNAs
mL	Milliliter
mM	Millimolar
mm	Millimeter
mRNA	Messenger Ribonucleic Acids
mRNP	Messenger Ribonucleoproteins
mTOR	Mammalian Target of Rapamycin
mTORC1	Mammalian Target of Rapamycin Complex 1

NADPH	Nicotinamide Adenine Dinucleotide Phosphate
NCBP1	Nuclear Cap-Binding Protein 1
NCBP2	Nuclear Cap-Binding Protein 2
NELF	Negative Elongation Factors
NF-κB	Nuclear Factor-κB
NGD	No-Go mRNA Decay
NIR	PI-Transfer Protein Membrane Associated
NKX2-2	NK2 Homeobox 2
nM	Nanomolar
nm	Nanometer
NMD	Nonsense-Mediated mRNA Decay
NPC	Nuclear Pore Complex
NS	Non-Significance
NSD	Non-Stop mRNA Decay
nt	Nucleotides
NTC	Nineteen Complex
NTD	Amino (N)-Terminal Domain
NTF2	Nuclear Transport Factor 2
NTR	Nineteen-Related Proteins
NUDIX	Nudix Hydrolases
NUP	Nucleoporins
NXF1	Nuclear RNA Export Factor 1

NXT1	Nuclear Transport Factor 2 Like Export Factor 1
OH	Hydroxyl groups
ORP	OSBPs-Related Proteins
OSBP	Oxysterol Binding Proteins
PA	Phosphatidic Acid
PAB1	Poly(A)-Binding Protein
PABPC	Cytoplasmic Poly(A)-Binding Proteins
PABPN	Nuclear Poly(A)-Binding Proteins
PACT	Protein Kinase R Activator
PAM2	PABP-Interacting Motif 2
PAN2	Poly(A)-Specific Ribonuclease Subunit 2
PAN3	Poly(A)-Specific Ribonuclease Subunit 3
PAP	Poly(A) Polymerase
PARN	Poly(A)-Specific Ribonuclease
PAS	Polyadenylation Signal
PATL1	PAT1 homolog 1 Processing Body mRNA Decay Factor
PBS	Phosphate-Buffer Saline
PC	Phosphatidylcholine
PDI	Protein Disulfide Isomerase
PDIA3	PDI Family A Member 3
PDIA6	PDI Family A Member 6
PDX1	Pancreas/Duodenum Homeobox Protein 1

PE	Phosphatidylethanolamine
PERK	Protein Kinase R-Like Endoplasmic Reticulum Kinase
PERKi	The GSK2656157 molecule known as PERK Inhibitor
PH	Pleckstrin Homology
PI	Phosphatidyl Inositol
PIC	Pre-Initiation Complex
PI3K	Phosphoinositide 3-Kinase
PIP2	Phosphatidylinositol (4,5)-bisphosphate
PI4P	Phosphatidylinositol 4-monophosphate
pKD	Partial protein Kinase Domain
PKR	Protein Kinase R
Pol	RNA Polymerase
Pol II-CTD	CTD of RNA Polymerase II
PP1	Protein Phosphatase 1
Pro	Proline (P)
PRR	Pattern Recognition Receptors
PSC	Premature-Stop Codons
P-SITE	Ribosomal Peptidyl tRNA-Site
PTC	Peptidyl Transferase Center
P-TEFb	Positive Transcription Elongation Factor B
Puro	Puromycin
Ran	RAS-Related Nuclear Proteins

RBD	RNA-Binding Domain
RBP	RNA-Binding Proteins
RIDD	Regulated IRE1-Dependent Decay
RISC	RNA-Induced Silencing Complex
RNA	Ribonucleic Acids
RNase	Endoribonuclease
RNP	Ribonucleoproteins
ROS	Reactive Oxygen Species
rRNA	Ribosomal RNAs
RT-PCR	Reverse Transcription-Polymerase Chain Reaction
RT-qPCR	Reverse Transcription-quantitative Polymerase Chain Reaction
SAR1	Secretion Associated RAS-related GTPase 1
SCAP	SREEBP-Cleavage Activating Proteins
SDS	Sodium Dodecylsulfate
SDS-PAGE	Sodium Dodecylsulfate-Polyacrylamide Gel Electrophoresis
SEC24D	COPII Coat Complex Component, Homolog D
Ser	Serine (S)
SERCA	Sarcoendoplasmic Reticular Ca^{2+} Adenosine Triphosphatase
SF1	Splicing Factor 1
SF3	Splicing Factor 3
SGs	Stress Granules
S6K	70-kDa Ribosomal Protein S6 Kinase

SMG	NMD-Associated Factors
SMP	Synaptotagmin-Like Mitochondrial and Lipid-Binding Protein
snRNA	Small Nuclear RNA
snRNP	Small Nuclear Ribonucleoprotein
SOCE	Store Operated Ca^{2+} Entry
SREBF1	Sterol Regulatory Element Binding Transcription Factor 1
SREBF2	Sterol Regulatory Element Binding Transcription Factor 2
SREBP	Sterol Regulatory Element-Binding Proteins
SRL	Sarcin-Ricin Loop
SRP	Signal Recognition Particles
3′-SS	3′ Splice Site
5′-SS	5′ Splice Site
SSC	Saline-Sodium Citrate
SSP	Signal Sequence Peptidase
$t_{1/2}$	Half-lives
T1D	Type 1 Diabetes
TAG	Triacyl Glycerides
TC	Ternary Complex
TCA	Trichloroacetic acid
Tg	Thapsigargin
TGN	Trans-Golgi Network
THOC	THO Complex

Thr	Threonine (T)
Tn	Tunicamycin
TOB	Transducer of ERB-B2 Receptor Tyrosine Kinase
TRAF2	Tumor Necrosis Factor Receptor-Associated Factor 2
TRBP	TAR RNA Binding Protein
TREX	Transcription/Export
tRNA	transfer RNA
$tRNAi^{Met}$	Initiator tRNA Charged with Methionine
TRP	Translocated Promoter Region
TTP	Tristetraprolin
U	Uridines
U2AF	U2 Auxiliary Factor
uORF	upstream Open Reading Frames
UPF	NMD Regulators
UPR	Unfolded Protein Response
UTR	Untranslated Regions
UV	Ultraviolet
V	Volts
VAP	Vesicle-Associated Membrane Protein-Associated Proteins
VAP-A	Vesicle-Associated Membrane Protein-Associated Protein-A
VWM	Vanishing White Matter
WRS	Wolcott-Rallison Syndrome

WT	Wild Type
XBP1	X-Box Binding Protein 1
XBP1s	X-Box Binding Protein 1-Spliced
XBP1u	X-Box Binding Protein 1-Unspliced
XRN1	Cytoplasmic 5′-3′ Exoribonuclease 1
β-ME	Beta-mercaptoethanol
µCi	Microcurie
4µ8C	IRE1α Inhibitor
µg	Microgram
µL	Microliter
µM	Micromolar
%	Percent

Newly Synthesized mRNA Escapes Translational Repression during the Acute Phase of the Mammalian Unfolded Protein Response

Abstract

by

MOHAMMED RUBAYYI ALZAHRANI

Endoplasmic Reticulum (ER) stress, caused by the accumulation of misfolded proteins in the ER, elicits a homeostatic mechanism known as the Unfolded Protein Response (UPR). The UPR reprograms gene expression to promote adaptation to chronic ER stress. The UPR comprises an acute phase involving inhibition of bulk protein synthesis and a chronic phase of transcriptional induction coupled with the partial recovery of protein synthesis. However, the role of transcriptional regulation during the acute phase of the UPR is not well understood. In this study (Alzahrani et al., 2022), I analyzed the fate of newly synthesized mRNA encoding the protective and homeostatic transcription factor X-box binding protein 1 (XBP1) during this acute phase of UPR.

Global translational repression induced during the acute UPR was documented and characterized by decreased translation and increased stability of *XBP1* mRNA. My data suggest this stabilization of *XBP1* mRNA is independent of new transcription. In contrast, newly synthesized *XBP1* mRNA is shown to accumulate with long poly(A) tails and escapes translational repression during the acute phase of UPR. Inhibition of nascent RNA polyadenylation during the acute phase

decreased cell survival with no effect in unstressed cells. During the chronic phase of the UPR, *XBP1* mRNA abundance and long poly(A) tails decreased in a manner consistent with co-translational deadenylation.

Finally, additional pro-survival, transcriptionally-induced genes show similar regulation, supporting the broad significance of the pre-steady state UPR in translational control during ER stress. I conclude that the biphasic regulation of poly(A) tail length during the UPR represents a previously unrecognized pro-survival mechanism of mammalian gene regulation.

CHAPTER 1: AN OVERVIEW OF THE CELLULAR RESPONSE TO STRESS

Mammalian cells are exposed to diverse environmental stress stimuli that disrupt protein homeostasis through the phosphorylation of the alpha subunit of eukaryotic Translation Initiation Factor 2 (eIF2α), leading to inhibition of bulk protein synthesis. The phosphorylation of eIF2α (eIF2α-P) also activates signaling pathways to cope with cellular stresses and maintain proteomic integrity. In mammalian cells, there are four eIF2α Serine (Ser)/Threonine (Thr) kinases that phosphorylate eIF2α at Ser-51 residue. The eIF2α kinases include the Heme-Regulated Inhibitor Kinase (HRI or EIF2AK1), Protein Kinase R (PKR or EIF2AK2), PKR-Like Endoplasmic Reticulum Kinase (PERK or EIF2AK3), and General Control Nonderepressible-2 (GCN2 or EIF2AK4) (Figure 1.1) (Costa-Mattioli & Walter, 2020; Wek, 2018). Upon the activation of eIF2α kinases, eIF2α-P controls the intracellular concentration of active Ternary Complex (TC) required for translation initiation. The TC is composed of the heterotrimeric translation factor eIF2, Guanosine Triphosphate (GTP), and the Initiator tRNA Charged with Methionine ($tRNAi^{Met}$). Following eIF2-GTP hydrolysis in the first round of translation initiation, eIF2- Guanosine Diphosphate (GDP) is exchanged to eIF2-GTP by another translation factor, known as eukaryotic Translation Initiation Factor 2 B (eIF2B), which functions as a Guanine Nucleotide-Exchange Factor (GEF). Importantly, eIF2B-mediated exchange of eIF2-GDP to eIF2-GTP is considered as the rate-limiting step for the assembly of active TC. When eIF2α is phosphorylated, the eukaryotic Translation Initiation Factor 2 (eIF2) stays bound by eIF2B leading

to eIF2B inhibition and a decreased GEF activity. The inhibitory function of eIF2α-P is obtained by a strong affinity binding to eIF2B at different sites, displacing eIF2 from the catalytic epsilon domain of eIF2B (eIF2Bε). Thus, eIF2α-P traps and inactivates available eIF2B that is of lower abundance than eIF2 (Adomavicius et al., 2019; Costa-Mattioli & Walter, 2020). Meanwhile, select messenger Ribonucleic Acids (mRNA) such as a transcription factor, known as the *Activating Transcriptional Factor* 4 (*ATF4)*, escape the stress-induced translation inhibition. ATF4 acts as a master transcriptional regulator of the stress-specific transcriptome during stress conditions (Guan et al., 2017; Wek, 2018). Since the various eIF2α kinases induce eIF2α-P in response to different stress conditions, this pathway has been referred as the Integrated Stress Response (ISR) (Figure 1.1). The activation of ISR is transient, as ATF4 downstream targets include the Growth Arrest and DNA-Damage-Inducible Protein 34 (GADD34), a regulatory component of Protein Phosphatase 1 (PP1), that dephosphorylates eIF2α-P and turns off the ISR. During chronic stress, ISR inhibition allows a recovery in protein synthesis and the expression of the adaptive transcriptome. The ISR ensures the expression of GADD34 by two synergistic mechanisms: First, GADD34 is transcriptionally enhanced by ATF4. Second, GADD34 is selectively translated during ISR-mediated translational recovery (Costa-Mattioli & Walter, 2020; Wek, 2018). Although partial recovery of the acute phase translational inhibition is necessary for adaptation to chronic ER stress (Guan et al., 2017), recovery of protein synthesis to normal pre-stress levels decreases adaptation to chronic ER stress

via mechanisms involving the UPR-induced transcription program (Han et al., 2013; Krokowski et al., 2013). The increased recovery of protein synthesis by the combinatory effect of these stress regulatory genes can adversely affect cell survival through Adenosine Triphosphate (ATP) depletion and oxidative stress. In addition, CCAAT/Enhancer-Binding Protein Homologous Protein (CHOP), a stress transcriptional factor, is another ATF4 downstream target that promotes cell death during chronic stress conditions. Therefore, the stress specific genes may dictate the cell fate by adaptive functions in response to acute/early stress conditions or apoptotic functions during chronic/late stress conditions (Almanza et al., 2019; Guan et al., 2017; Wek, 2018)

Regulation of eIF2α phosphorylation

The levels of eIF2α-P are not only controlled by the eIF2α kinases, but also by two mammalian phosphatase complexes of the PP1 phosphatase. These phosphatase complexes contain either the stress-induced GADD34 or the Constitutive Repressor of eIF2α-P (CReP), as regulatory components that recruit the phosphatase complex to dephosphorylate eIF2α-P (Figure 1.1) (Guan et al., 2017; Wek, 2018). In the dephosphorylation mechanism of eIF2α-P, the dynamic G-actin monomers have been suggested to stabilize phosphatase complexes for their actions. The involvement of G-actin proteins indicates that ISR is connected to cellular processes such as actin polymerization (Costa-Mattioli & Walter, 2020). In addition, phosphatase complexes have been targeted by pharmacological inhibitors to understand their role during ISR. For instance, salubrinal and its

derivative, Sal003, have been shown to inhibit both phosphatase complexes without a clear mechanism for their actions. In addition, two inhibitors, Guanabenz and sephin1, inhibit phosphatases bound to GADD34, whereas raphin1 is more specific inhibitor to phosphatases bound by CReP (Almanza et al., 2019; Costa-Mattioli & Walter, 2020). Since eIF2α-P inactivates eIF2B, as previously explained, a recently developed drug, known as ISR Inhibitor (ISRIB) was shown to enhance the assembly of eIF2B complexes for recycling eIF2-GDP to the active eIF2-GTP. This drug inhibits the ISR at low eIF2α-P and loses activity as the levels of stress increases (Almanza et al., 2019; Costa-Mattioli & Walter, 2020; Wek, 2018).

The integrated stress response regulators

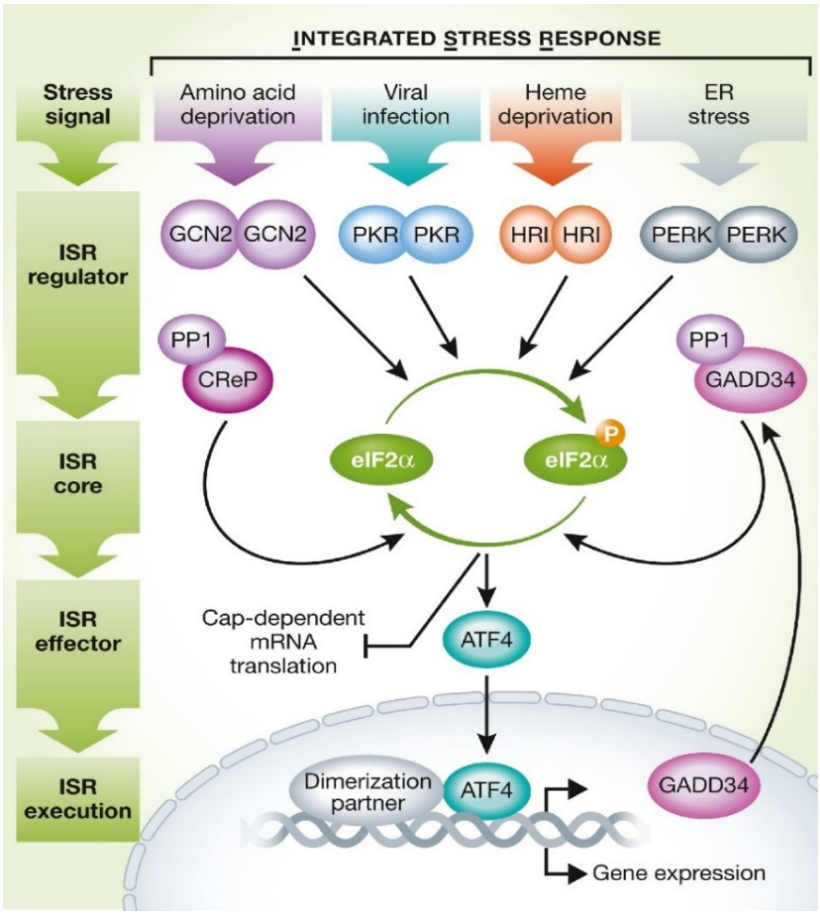

Figure 1. 1. Overview of integrated stress response pathway in eukaryotes. Diverse stress stimuli activate the four eIF2α kinases, PERK, PKR, HRI and GCN2 to phosphorylate eIF2α that inhibits global cap-dependent translation. However, some ISR-specific transcripts, including *ATF4* transcripts, are preferentially translated. ATF4 represents the downstream effector of ISR to convey the signals by promoting the adaptive gene expression. Meanwhile, CReP and GADD34 expression downregulate the ISR by dephosphorylation of eIF2α. Reprinted with permission from John Whiley and Sons, the publisher of (Pakos-Zebrucka et al., 2016).

PERK pathway

Earlier studies discovered PERK in pancreatic islets of rats and later described as Ser/Thr kinase protein (Almanza et al., 2019). PERK is an ER

transmembrane protein that is ubiquitously expressed among tissues with the highest levels in pancreas (Zhang et al., 2002). PERK consists of two domains; the N-terminal-sensing domain locates in the ER lumen and the C-terminal kinase domain presents in the cytosol (Almanza et al., 2019). PERK is activated by ER stress, discussed in detail below, including disruption of Calcium (Ca^{2+}) balance, protein folding and glycosylation in the ER. The prevailing mechanism of PERK regulation involves an ER-resident chaperon, known as B-cell Immunoglobulin Binding Protein (BiP) (Zhang et al., 2002). Under unstressed conditions, PERK has been proposed to associate with BiP in an inactive form. During ER stress, the accumulation of misfolded proteins is recognized by the molecular chaperone BiP. As a result, BiP dissociates from the PERK luminal ER sensor domain and thus, allows oligomerization and trans-autophosphorylation of Thr-980 residues (W. Cui, Li, Ron, & Sha, 2011). Consequently, PERK-mediated eIF2α-P inhibits global protein synthesis to preserve energy and nutrients and decrease the burden on ER protein synthesis and folding machinery (Almanza et al., 2019; Wek, 2018). Although PERK-Knockout (KO) mice experience prenatal death accounting to 40 Percent (%), the survived mice are characterized by sever postnatal growth retardation, skeletal abnormalities, and development of hyperglycemia. PERK-KO mutants exhibit severe loss of pancreatic insulin-secreting beta cells and glucagon-secreting alpha cells leading to the development of diabetes mellitus (Zhang et al., 2002). PERK mutations leading to a lack of the kinase activity result in the development of Wolcott-Rallison Syndrome (WRS). The characteristics of this disease involve neonatal diabetes, osteoporosis, digestive dysfunctions, hepatic

complications, and ultimately early death due to absence of translational control (Wek, 2018).

PERK activation is involved in many tumors and has been targeted by inhibitory molecules to limit its cytoprotective function and increase cell death in cancer cell lines. The discovery of GSK2656157 molecule (PERKi) has been shown to inhibit PERK enzymatic activity and PERK downstream targets such as eIF2α-P and ATF4 (Atkins et al., 2013). Recently, PERKi was used to delineate PERK contribution to the translational reprogramming during chronic ER stress. For example, *ATF4* mRNA translation is upregulated during acute ER stress due to increased eIF2α-P and consequently suppressed eIF2B activity that is critical for translation initiation. During chronic ER stress, ATF4 was still expressed in agreement with the sustained low eIF2B activity and the translation of *ATF4* mRNA was shown to be dependent on the eukaryotic Translation Initiation Factor 3 (eIF3) (Guan et al., 2017). Together, these data indicate a PERK control over the translational reprogramming during chronic ER stress in an eIF3-dependent manner for translation initiation.

GCN2 pathway

The eIF2α kinase GCN2, was first identified by Hinnebusch's study in budding yeast (Garcia-Barrio, Dong, Ufano, & Hinnebusch, 2000). Interestingly, GCN2 is not listed as an essential gene because its depletion in mice does not affect embryonic viability. However, Amino Acids (aa)-starved GCN2-KO mice show signs of increased morbidity including production of abnormal proteins in

the liver and loss of skeletal muscle. *GCN2* mutations have been reported as the underlying cause of the pulmonary veno-occlusive disease characterized by narrow pulmonary veins and venules due to increased cellular proliferation. In addition, the activation of GCN2 is involved in lipid metabolism, learning and memory, pro-survival in cancers, immunity, and Deoxyribonucleic Acid (DNA) repair under the effect of Ultraviolet (UV) irradiation (Anda, Zach, & Grallert, 2017; Castilho et al., 2014; Eyries et al., 2014). GCN2-KO is linked to pulmonary disorders, such as pulmonary arterial hypertension, pulmonary veno-occlusive disease, and pulmonary capillary hem-angiomatosis. Although GCN2 has been thought to promote angiogenesis during nutrient deprivation, the direct link of GCN2 to pulmonary diseases remains poorly understood (Costa-Mattioli & Walter, 2020).

The human GCN2 is a 190-Kilodalton (kDa) protein with multiple conserved domains. GCN2 domains include the Amino (N)-Terminal Domain (NTD), the Partial protein Kinase Domain (pKD), the catalytic protein Kinase Domain (KD), the histidyl-transfer RNA synthetase Like Domain (His-RS), and the Carboxyl (C)-Terminal Domain (CTD). In addition, studies of GCN2 domains have illustrated a linker region encompassing charged residues between the pKD and RWD domains. Under physiological conditions, GCN2 domains form inhibitory interactions between the CTD and KD and His-RS domain rendering the protein inactive. However, upon activation, usually by deacylated transfer RNAs (tRNAs), GCN2 domains undergo conformational changes to release the inhibitory interactions between GCN domains. In addition to the limited

availability of amino acids, osmotic stress, glucose starvation, and UV radiation have been reported to activate GCN2 (Anda et al., 2017; Castilho et al., 2014; Masson, 2019)

GCN2 activation is regulated by deacylated tRNAs, the dimeric GCN1-GCN20 complex, ribosomes and ribosomal P-stalk. First, tRNA synthetases cannot aminoacylate tRNA under amino acid-deprivation leading to accumulation of deacylated tRNAs in the cytosol. Several studies have shown that the His-RS domain can distinguish between charged and uncharged tRNAs and represents an essential domain in the mechanism of GCN2 activation. Secondly, GCN1 and GCN20 are other key regulators of the eIF2α kinase, GCN2, in yeast. GCN1 plays a critical role in GCN2 activation because its deletion in yeast inhibits GCN2 activation in response to low amino acid availability *in vivo*, but not *in vitro*. GCN1 is a larger protein than GCN2 with a sequence homology to the eukaryotic Elongation Factor 3 (eEF3), while the central region of GCN1 protein composed of a Huntingtin, Elongation Factor 3, Protein Phosphatase 2A, TOR1 (HEAT) repeat. The C-terminal domain of GCN1 has been documented to interact with GCN2. On the other hand, GCN20 was initially discovered in yeast together with GCN1 and GCN2. So far, no mammalian homolog to GCN20 has been found. The N-terminal domain of GCN20 interacts with the HEAT region of GCN1 forming a stable complex. Similar to GCN1 structure, GCN20 contains a sequence homology to eEF3 that exhibits weaker ribosomal interactions than GCN1. Thus, the ribosomal interactions mediated by the eEF3-like sequence of GCN1-GCN20 complex, GCN2 co-activators, was hypothesized to facilitate

recognition of deacylated tRNAs. Finally, initial studies have assessed ribosomal interaction based on GCN2 co-migration with ribosomes in yeast. However, this observation is absent in mice. The difference between yeast and mouse GCN2 migration was attributed to the potential various mechanisms employed for mouse GCN2 activation. In addition, mutational and deletion studies within GCN2 domains highlight three critical GCN2 domains, including pKD, KD, His-RS like domains, for ribosomal interactions. Recently, GCN2-ribosome interactions were mapped using hydrogen deuterium exchange mass spectrum. The study findings indicate that association of GCN2 with ribosomes is via the NTD of P-stalk protein that is adjacent to the Ribosomal Amino-acylated tRNA-Site (A-Site). The P-stalk, also known as P0, associates with ribosomes, P1 and P2 proteins, involved in translational fidelity, to form a dynamic complex. In addition, the P-stalk represents a core element in the GTPase-associated center for recognition and GTP hydrolysis of elongation factor. These P-stalk proteins, P0, P1 and P2, contain a conserved 12-residue motif within the CTD involved in recruiting translational factors during protein synthesis (Masson, 2019).

In response to amino acid deprivation, uncharged tRNAs are accumulated in the cytosol and bind the HisRS domains. Consequently, this binding releases the inhibitory contacts among GCN2 domains and the rearranged GCN2 structure favors the activation of GCN2. The rearrangement of GCN2 domains allows auto-phosphorylation of the two conserved Thr residues within the activation loop of GCN2-KD in mice, Thr-898 and Thr-903. The GCN2-NTD is believed to assist docking of the GCN1-GCN20 complex, and its deletion

interferes with the nutrient stress-induced GCN2 activation. The GCN1-GCN20 complex has been thought to associate with ribosomes and thus, facilitate GCN2 binding to uncharged tRNAs. The encoded kinase in GCN2-pKD is catalytically inactive due to missing critical residues required for the kinase function. However, the GCN2-pKD allosterically enhances the GCN2 activation through the neighboring GCN2 domains (Castilho et al., 2014; Masson, 2019).

GCN2 has been well studied in yeasts. Studies of GCN2 in mammalian cells are still emerging. Therefore, establishing a model for GCN2 activation is difficult. For example, UV-irradiated cells in fission yeasts and mammals have been documented to activate GCN2. In fission yeast, UV radiation has been reported to inhibit protein synthesis by GCN2 activation via a GCN1-dependent mechanism due to unaltered deacylated tRNAs. In addition, the reported uncharged tRNA-independent GCN2 activation has been hypothesized to be based on a dysregulated translation represented by stress-mediated ribosomal stalls. Together, these data suggest alternative mechanisms of GCN2 activation including ribosome-mediated regulation of GCN2 activation (Masson, 2019).

PKR pathway

In 1990, PKR was discovered and identified as an innate immune protein against viral infection. PKR expression is constitutive and PKR-KO mice develop normally. The PKR protein is expressed at low levels and has a molecular weight of 68 kDa. PKR is composed of the Double-Stranded Ribonucleic Acid (dsRNA)-Binding Motifs (dsRBM) in the NTD and a catalytic kinase in the CTD. dsRBM1 is connected to dsRBM2 by a 23-aa linker. dsRBMs are linked to the CTD via a

flexible linker. Although the structure of the PKR kinase domain is like other protein kinases, its interaction with eIF2α requires a unique α-helix within the C-terminal lobe of the PKR catalytic domain. Moreover, dsRBMs have been found to interact with other proteins such as the TAR RNA Binding Protein (TRBP) and the PKR Activator (PACT, RAX is the murine homolog). These proteins regulate PKR in mammalian cells under stress conditions. For example, stress-induced PACT phosphorylation at Ser-287 is essential for PACT-PKR association and subsequently PKR activation, while TRBP interaction with PKR has been suggested to inactivate PKR (Chukwurah, Farabaugh, Guan, Ramakrishnan, & Hatzoglou, 2021; Gal-Ben-Ari, Barrera, Ehrlich, & Rosenblum, 2018; Lancaster et al., 2016; Watanabe, Imamura, & Hiasa, 2018).

PKR proteins are localized predominantly in the cytosol, where viral dsRNA accumulates upon infections, and interact with ribosomes. Upon viral infections, PKR expression is induced via several proteins that bind specifically to the PKR promoter sequence, named IFN-stimulated response element. The induced PKR binds to dsRNA causing PKR oligomerization and autophosphorylation at several Ser and Thr residues known as the activation loop/segment. Among these residues, Thr-446 and Thr-451 are constantly phosphorylated to stabilize PKR dimerization for maximal PKR catalytic activity. In addition, the active PKR phosphorylates its substrate, eIF2α, and subsequently blocks protein synthesis. As part of the PKR anti-viral function, apoptosis is induced in an eIF2α-dependent

or -independent mechanism (Chukwurah et al., 2021; Gal-Ben-Ari et al., 2018; Watanabe et al., 2018).

In addition to the canonical viral dsRNA mediated PKR activation, several stress stimuli have been reported to activate PKR such as cytokines including Interferons (IFN), interleukin 1, and tumor necrosis factor alpha, bacterial lipopolysaccharides, Heat Shock Protein 90 (HSP90), misfolding protein or oxidative stress agents such as Tunicamycin (Tn), Thapsigargin (Tg), arsenic acids, and hydrogen peroxides. Also, PKR activation through several signaling pathways has been reported including the Toll-interleukin 1 receptor domain-containing adaptor protein and Toll-like receptor 4 signaling pathways, and platelet-derived growth factor through signal transducer and activator of transcription 3 and extracellular signal-regulated protein kinase 1/2 phosphorylation. Together, these PKR activation-related pathways highlight the crosstalk between stress pathways and indicate the central role of PKR in multiple cellular functions including translational and transcriptional regulations, cellular proliferation, and cell death via apoptosis (Chukwurah et al., 2021; Gal-Ben-Ari et al., 2018; Watanabe et al., 2018).

HRI pathway

Initial studies of HRI have restricted HRI expression to reticulocytes and bone marrow in rabbits. Subsequent studies have profiled HRI expression in many tissues indicating its ubiquitous expression. HRI deletion in mice shows it is not essential for development but demonstrates abnormal response to iron and heme deficiency (Burwick & Aktas, 2017). The protein of HRI migrates on Sodium

Dodecylsulfate-Polyacrylamide Gel Electrophoresis (SDS-PAGE) at a molecular weight of 90 kDa and structurally composed of the NTD, containing a heme-binding site, the catalytic region including Kinase I and Kinase II domains interspaced by a kinase insertion domain that also binds to heme reversible, and the CTD of HRI (Bhavnani et al., 2017; Sreejith et al., 2012). HRI proteins are critical in hemoglobin synthesis, especially in erythrocytes. Like other eIF2α kinases, HRI proteins are activated by autophosphorylation under low heme concentrations. In addition, other stress conditions contribute to HRI activation including osmotic stress, heat shock mediated by HSP90 and HSP70 proteins, oxidative stress, proteosome inhibition, aggregated proteins in the cytoplasm, and recently, mitochondrial stress (Girardin, Cuziol, Philpott, & Arnoult, 2021).

HRI functions as a sensor for cytosolic misfolded proteins during innate immunity, proteotoxicity and mitochondrial stress. Since PKR governs innate immune response to viral infections, bacterial infections have been suggested to activate ISR determined by increased expression of ISR markers such as eIF2α-P. *Shigella* infection has been reported to activate HRI via a heme-independent mechanism involving HSP70 dissociation mechanism, similar to BiP dissociation from PERK. Upon *shigella* infections, HRI is responsible for ISR-mediated upregulation of pro-inflammatory genes. The inflammatory response is mediated by nod1 and nod2, innate immune receptors, that activate the Nuclear Factor-κB (NF-κB), an inflammatory transcription factor. In addition, activation of NF-κB is reduced in HRI-knockdown cells and HRI-KO mice characterized by a decreased

inflammatory response. Together, these findings reinforce the requirement of HRI activation in response to bacterial infections. In addition to an HRI role in the inflammatory response, HRI monitors the cytosolic proteotoxicity. Defective mechanisms of cytosolic protein clearance, including autophagy and proteosome-ubiquitin proteolysis, result in protein accumulations and proteotoxicity. For example, the accumulation of multimeric α-synuclein proteins forming amyloid fibrils is one of the hallmarks of Parkinson's disease. The multimeric α-synuclein proteins are degraded via the proteosome-ubiquitin proteolysis. Several reports have indicated the cytosolic accumulation of α-synuclein proteins in cell lines that do not express the Wild Type (WT) HRI. Therefore, HRI downregulation may augment neurodegenerative diseases. In addition to HRI control of protein aggregations, mitochondrial dysregulation has been linked to HRI activation. Recent studies have illustrated the activation of ISR is mediated by HRI in response to mitochondrial stress. HRI activation is mediated by mitochondrial proteins, named DAP3 Binding Cell Death Enhancer 1 (DELE1), that is cleaved by another mitochondrial protease, named OMA1 Zinc Metallopeptidase, upon mitochondrial stress. Thus, the cleaved DELE1 is accumulated in the cytosol and binds HRI leading to its activation (Girardin et al., 2021).

Stress granules

eIF2α-P as a result of stress conditions is associated with cytoplasmic foci rich in Ribonucleic Acids (RNA) and RNA-Binding Proteins (RBP), known as stress granules. Stress Granules (SGs) are intracellular and membrane-less structures discovered first in mammalian cells during stress conditions. SGs are condensates

assembled under different stresses, including oxidative stress and nutrient deprivation, and are formed by interactions between RNAs and proteins that contain Intrinsically Disordered Regions (IDR). These regions are believed to assemble SGs and can be regulated by post-translational modification and chaperones. The formation of SGs is due to inhibition of 48S Pre-Initiation Complex (PIC), while the inhibition of 60S recruitment does not induce SGs. Since SGs are noticed during translation initiation, the molecular composition of SGs is rich with translational factors, RNAs, or other translation regulators including RBPs. However, the composition of SG varies depending on the type of stress. Among these proteins, TIA-1 and G3BP1 have been proposed to be core components of SGs. The function of SGs is originally thought to store translationally repressed mRNA. The discovery of bidirectional movement of SG components through these structures has opened for alternative SG functions including Ribonucleoprotein (RNP) remodeling. Interestingly, SGs have been reported to interact with another RNA granule, known as processing bodies, that contain RNA decay factors. Therefore, this interaction may support the proposed SG function of RNP remodeling. In addition, SGs contain components that are not involved in RNA metabolism. For example, apoptotic and signaling regulators, such as Tumor Necrosis Factor Receptor-Associated Factor 2 (TRAF2), have been reported as residents of SG. Therefore, SG is not limited to mRNA sorting, but also involves in apoptosis and signaling regulations (Fan & Leung, 2016; Wolozin & Ivanov, 2019).

Dysregulated ISR is associated with diseases

Phosphorylation-resistant mutations of eIF2 associates with postnatal lethality in mice indicating their important roles in normal physiology. In overactivated ISR conditions, mice without the function of the two eIF2 phosphatase complexes cannot survive due to persistent inhibition of protein synthesis required during embryogenesis. In addition, CReP mutations destabilizing the phosphatase complex can lead to early-onset diabetes, growth retardation, microcephaly and learning disabilities, and liver pathologies, while its deletion in pancreatic β cells decreases insulin synthesis and triggers apoptosis upon ER stress (Costa-Mattioli & Walter, 2020).

Other ISR dysregulations result in various diseases. Vanishing White Matter (VWM), for example, is characterized by childhood ataxia with central nervous system hypomyelination. This VWM disease is caused by mutations in genes encoding eIF2B subunits. As a result of eIF2B mutations, the exchange of eIF2-GDP to eIF2-GTP is lowered and thus, activates ISR independent of external stress. When combined with stress, increased levels of eIF2α-P further amplify ISR leading to its destructive features. Interestingly, ISRIB has positive effects in cells and mice bearing the VWM mutations. In addition, eIF2γ mutations are documented in MEHMO patients characterized by mental deficiency, epilepsy, hypogenitalism, microcephaly, and obesity, an X-linked disability syndrome. Although eIF2 function is impaired by different eIF2B and eIF2γ mutations, they contribute to the reduced levels of active TC (Costa-Mattioli & Walter, 2020; Wek, 2018).

Other ISR components deletion can lead to deleterious outcomes. For example, the mutations of an ER co-chaperone, $P58^{IPK}$, are associated with diabetes and neural disease, while its deletion results in overactivation of PERK leading to apoptosis. The Immediate Early Response 3 Interacting Protein 1 (IER3IP1) is another ER protein. Disruptions of *IER3IP1* lead to conditions related to WRS (Wek, 2018).

Initial studies have shown that some ISR kinases such as PKR, PERK, and GCN2, are implicated in tumors. However, understanding the role of the ISR remains difficult to explain. For example, loss of function mutations in the tumor repressor of phosphatase and tensin homolog, known as PTEN, and activation of MYC proto-oncogene protein results in increased protein synthesis. In this context, PERK maintains the integrity of the proteome, and therefore, promotes tumor progression. PERK or its downstream effector, ATF4, deletion in a mouse model of aggressive metastatic prostate cancer interferes with tumor progression. This indicates that cancer cells exploit the ISR signals to promote tumorigenesis. Although ISR is known for its cytoprotective functions, targeting ISR in different cancers may be a future direction (Costa-Mattioli & Walter, 2020).

In brief, I have highlighted the main regulators of eIF2α phosphorylation that are triggered by various stress cues. The importance of these regulators relies on maintaining proper expression to safeguard cells from apoptosis under various stress conditions. However, failure of these eIF2α kinases to develop an adaptive response to stress signals may lead to deleterious outcomes as reported by

diseases associated with disrupted ISR function. Interestingly, these kinases converge on eIF2α phosphorylation that inhibits global protein synthesis, including mRNA translation on the ER. I will introduce next ER functions in health and pathological conditions.

AN OVERVIEW OF THE ENDOPLASMIC RETICULUM AND ITS RESPONSE TO STRESS

The endoplasmic reticulum is an organelle found in all eukaryotic cells and initially discovered in the 19th century by Emilio Veratti. In 1952, this organelle was visualized under an electron microscope by Keith Porter and named as ER. The ER is constituted of tubules and sheets representing one domain of the ER. The tubules and stacked flat cisternae are interconnected and contiguous to the outer membrane of the nuclear envelope representing the other domain of ER. Since ER sheets are studded with ribosomes and polyribosomes, they are known as rough ER membrane where protein synthesis occurs. On the other hand, smooth ER membrane is characterized by less ribosomal density and represents tubules that connect between ER sheets, maintain ER curvature, and facilitate vesicle transport (Bagchi, 2020; Schwarz & Blower, 2016).

ER functions are not limited to protein synthesis

The ER is considered as the largest cellular organelle. In the ER multiple functions occur including protein synthesis, folding, and trafficking, lipid biogenesis, and Ca^{2+} regulation. The multi-functional ER requires a coordinated set of proteins that responds to homeostatic fluctuations in the intracellular environment (Schwarz & Blower, 2016).

Protein synthesis and folding

Initial studies have shown that mRNA translation begins in the cytosol. In 1981, the discovery of Signal Recognition Particles (SRP) revealed mRNA translation occurring on ER membranes and co-translational targeting to the ER (Reid & Nicchitta, 2015). In brief, SRP brings mRNA-ribosome complexes to a translocation channel in the ER. The attachment of these complexes to the ER membrane forms the rough ER membrane and allows the ribosomes to continue mRNA translation. Following the Signal Sequence Peptidase (SSP)-mediated cleavage of the signal peptide, the produced polypeptides are threaded via translocons that consist of several Sec proteins and form a channel through the bilayer lipid of the ER membrane.

Two major chaperone systems have been widely studied. The first system is lectin-like chaperones such as calnexin and calreticulin. They recognize unfolded nascent proteins with mono-glycosylated N-linked glycans (Ma & Hendershot, 2004). The second chaperone system is dependent on BiP, a heat-shock protein 70 kDa family member. The ER-resident chaperone BiP recognizes Hydrophobic Regions (HR) of unfolded proteins for protein folding. In addition, it prevents aggregation of intermediates and resolves misfolded proteins by trafficking to an ER-associated degradation system (ERAD) that eliminates misfolded or aggregated proteins via the proteosome (Bandla, Diaz, Nasheuer, & FitzGerald, 2019; Ruggiano, Foresti, & Carvalho, 2014). BiP consists of multiple signal sequences. The NTD contains sequences to direct the protein to the ER.

Also, the NTD contains the nucleotide-binding domain that binds ATP or Adenosine Diphosphates (ADP) in response to substrate binding or release, respectively. In addition, the nucleotide binding and catalysis are influenced by cation cofactors, such as Magnesium (Mg^{2+}), Ca^{2+} (Preissler et al., 2020), manganese, that act as cofactors and the status of the substrate binding domain within the CTD. Beside the CTD interaction with peptide substrates, it contains the KDEL sequence that functions to keep BiP retained within the ER (Bandla et al., 2019; Ma & Hendershot, 2004; Pobre, Poet, & Hendershot, 2019).

The emerging nascent polypeptides in the ER are properly folded and modified by ER-resident chaperones and folding enzymes in a complex process named as ER quality control. As nascent polypeptides enter the ER lumen and approximately reach 13 aa, they are modified with N-linked glycosylation by oligosaccharyltransferase. This enzyme recognizes Asparagine (Asn) residues within the Asn-X-Ser/Thr sequence and transfers two N-acetylglucosamine, nine mannose, and three molecules of glucose. Glucoses are trimmed by the enzymatic actions of glucosidase I and II leaving only one glucose that facilitates the binding of chaperones. Two motifs of thioredoxin are encoded by family members of Protein Disulfide Isomerase (PDI), specifically PDIA3, that catalyzes the formation of disulfide bond. Its inclusion with the complex appears to stabilize protein folding. However, when the last glucose molecule is removed from nascent folded proteins, chaperones cannot be bound, and the completely folded proteins are packaged and transported to Golgi. When protein folding is not complete, the UDP-

Glucose:Glycoprotein Glycosyltransferase (UGGT) re-glycosylates the partially unfolded proteins by transferring a glucose residue to the N-glycan. This will recruit chaperones again to the unfolded proteins. The process of protein folding can go through multiple cycles until the protein is fully folded and secreted or destined for degradation. Thus, the terminal residue of N-glycosylated proteins represents the key modification to which proteins can leave the ER or retained until they are completely folded (Braakman & Hebert, 2013; Breitling & Aebi, 2013; Ma & Hendershot, 2004).

Lipid biogenesis

Although the ER is the major site for protein production, it also produces the building blocks of membranous lipids such as Phosphatidylcholine (PC) and Phosphatidylethanolamine (PE) as well as sphingolipid structures. In addition, cholesterol and Triacyl Glycerides (TAG) are synthesized by ER-localized enzymes for energy storage. The ER is made up of functional domains where the smooth ER domain is considered the main site for lipid synthesis. The ER membrane is relatively thin because its lipid composition contains more PC and PE than sphingolipid and cholesterol. The most abundant membrane lipid is PC. It is synthesized by the enzyme of CTP:phosphocholine Cytidylyltransferase (CCTα) that can be a soluble protein or bound to membranes. In addition, CCTα is negatively regulated by the M domain, encoded in the CTD region of CCTα, that prevents access of cytidine diphosphate–choline to the catalytic site when it is in a soluble state. However, this auto-inhibition is reversed when it becomes a membrane-bound state. Therefore, membrane binding of CCTα, dictated by gaps

within lipid headgroups and their looser packing, represents the central regulator of PC synthesis (Jacquemyn, Cascalho, & Goodchild, 2017).

Although Phosphatidic Acid (PA) represents the branch point in the ER-localized Glycerophospholipid/Glycerolipid pathway for Phosphatidyl Inositol (PI), PC, or PE production, PA levels influence CCTα activity to upregulate membrane PC production. Therefore, it is tightly regulated. For example, lipin proteins have a phosphatase domain encoded in the CTD region that hydrolyzes the phosphate headgroup of PA to produce Diacyl Glycerol (DAG) and eventually form TAG for energy storage. Interestingly, lipin proteins are soluble and negatively regulated by phosphorylation. However, their NTD integrates into the ER membrane after sensing the increased levels of PA within the membrane. Similar to CCTα, the association of lipin proteins with the membrane is considered as the key regulator for TAG production (Jacquemyn et al., 2017).

Sterol Regulatory Element-Binding Proteins (SREBPs) are ER transmembrane proteins initially discovered as integral factors in cholesterol biosynthesis. SREBPs are encoded by two genes *Sterol Regulatory Element Binding Transcription Factor 1 and 2* (*SREBF1*) and (*SREBF2*). SREBP-1A and SREBP-1C are originated from different promoters of *SREBF1*, whereas the third SREBP2 is derived from *SREBF2* (Dorotea, Koya, & Ha, 2020). SREBP2 has a more specific role in cholesterol synthesis compared to SREBP1 isoforms. They predominantly upregulate fatty acid synthase, fatty acid elongase, and glyceraldehyde-3-phosphate O-acyltransferase enzymes to eventually promote

TAG synthesis. All SREBPs contain a cytosolic NTD that functions as a transcription factor that binds to sterol response elements. Under basal condition, the CTD of SREBPs is embedded within the ER membrane via interactions with both SREEBP-Cleavage Activating Proteins (SCAP) and Insulin-Induced Gene (INSIG). Upon low levels of cholesterol, SCAP undergoes a conformational change and consequently, dissociates from INSIG. As a result, SREBP/SCAP is budded from the ER to Golgi apparatus where the NTD of SREBP is liberated by proteolytic cleavage and translocated to the nucleus to activate gene expression such as 3-Hydroxy-3-Methylglutaryl-CoA Reductase that represents the rate limiting enzyme for cholesterol synthesis (Jacquemyn et al., 2017).

ER expansion has been noticed during ER stress, which I will explain later. The relationship between ER stress and lipid biosynthesis has been questioned. Previous studies have found that ER stress not only controls protein homeostasis, but also lipid biosynthesis. In fact, ER transmembrane proteins are sensitive to alterations in the ER membrane composition. Increased saturated lipids, for example, can activate PERK via an oligomerization process even in the absence of the luminal sensor for misfolded protein detection. Therefore, it can be concluded that proteomic defects and changes in lipid composition within the ER membrane can trigger ER stress (Jacquemyn et al., 2017).

Calcium storage

The ER is a major store of intracellular Ca^{2+}. Typically, the intracellular and extracellular Ca^{2+} concentration is approximately 800 μM and 2 mM, respectively.

The intracellular Ca^{2+} concentration is compartmentalized where the cytosolic concentration is around 100 μM, while the ER lumen contains more than eight-fold higher than the cytosolic Ca^{2+} concentration. The intracellular Ca^{2+} level is controlled through ER Ca^{2+} channels, ryanodine receptors and Inositol 1,4,5-Trisphosphate (IP3) receptors that release Ca^{2+} in response to low levels of cytosolic Ca^{2+} (Schwarz & Blower, 2016).

To release Ca^{2+} from ER stores, the Ca^{2+}-mediated phospholipase C activation leads to the cleavage of Phosphatidylinositol (4,5)-bisphosphate (PIP2) into DAG and IP3. Consequently, the binding of IP3 to its receptor allows a transient increase in the intracellular Ca^{2+} levels. Ca^{2+} influx across the plasma membrane may activate ryanodine receptors through a process known as Ca^{2+}-induced Ca^{2+} release due to increased cytosolic Ca^{2+} levels. In addition, ryanodine receptors can be activated by conformation changes in voltage-dependent Ca^{2+} channels such as dihydropyridine receptors in response to depolarization of transverse tubule membrane. The ER is equipped with Ca^{2+} pumps such as Sarcoendoplasmic Reticular Ca^{2+} Adenosine Triphosphatase (ATPases), known as SERCAs, that can return Ca^{2+} when it is leaked from ER stores or across the plasma membrane (Lemmens, Larsson, Berggren, & Islam, 2001; Schwarz & Blower, 2016).

Depletion of Ca^{2+} from ER stores activates Store Operated Ca^{2+} Entry (SOCE) through clustering of STIM1 proteins adjacent to the plasma membrane. The clustered STIM1 couples with Orai1 subunits forming Ca^{2+} Release-Activated

Channels (CRAC) to uptake extracellular Ca^{2+} and restores Ca^{2+} levels in the ER lumen. Despite SOCE and CRAC activation, being sensitive to the luminal Ca^{2+} concentration, they do not respond to the levels of cytosolic Ca^{2+} (Schwarz & Blower, 2016; Zomot, Achildiev Cohen, Dagan, Militsin, & Palty, 2021).

ER export of proteins and lipids

Cellular structure is maintained via the ER functions where proteins and lipids are manufactured and exported to other organelles and cellular membranes. Defects in ER export processes can lead to deleterious consequences including ER homeostasis disruption and other cellular functions. Although Coat Protein Complex II (COPII) budding vesicles represent the main ER secretory pathway, a non-vesicular pathway has been reported. For example, ER Membrane Contact Sites (MCS) facilitate non-vesicular routes of delivery because of the dynamic and extensive network of ER MCSs with other organelles. In addition, inhibition of the ER vesicular transport pathway did not affect the transfer of lipids, such as glycerophospholipids and sterols, to the plasma membrane. This emphasizes the importance of ER MCSs in shuttling lipids between compartments. An alternative of ER transport vesicles, named pre-chylomicron, in the intestine have been proposed to transfer large lipoprotein cargo from the ER (Almanza et al., 2019; Eden, 2016; Funato, Riezman, & Muniz, 2020).

COPII vesicular pathway

COPII vesicular trafficking constitutes the conserved delivery mechanism of ER-synthesized molecules to various organelles. Vesicles originate from the ER

membrane via polymerization of cytosolic COPII at the ER Exit Sites (ERES), are found in ER tubules and edges of ER sheets due to the presence of curvature-stabilizing reticulon proteins. At the ERES, Sec16 associates with Sec12, functions as a GEF protein, that recycles the Secretion Associated RAS-Related GTPase 1 (SAR1), a small GTPase Activating Protein (GAP), from the SAR1-GDP form to the SAR1-GTP form. In addition, two heterodimerized complexes of Sec23/24 and Sec13/31 constitute the conserved core machinery of COPII machinery. Vesicle budding is initiated by the activated SAR1 via recruitment of Sec23/24 complex to the ERES. The protein cargo is captured by Sec24 in the SAR1-GTP-Sec24/23 complex, representing the inner COPII layer. Meanwhile, the inner coat complex is recognized and bound by Sec13/31, forming the outer COPII layer. The binding of these two complexes deforms the ER membrane to form the budding vesicle. Following SAR1-GTP hydrolysis, the vesicles leave the ER membrane to fuse with the membrane of ER–Golgi intermediate compartment after the vesicular coat is released. Membrane bending is energy consuming, and its crowding cargo makes it difficult on the COPII transport machinery. Lysophospholipids, are the bioproduct of phospholipase hydrolysis of phospholipids and sphingolipids, have been proposed to facilitate membrane bending due to its structure that decreases membrane rigidity. Thus, lipid composition plays a role in vesicular trafficking (McCaughey & Stephens, 2018).

Ceramides with long acyl chains are believed to be mobilized through COPII vesicles to Golgi where they are converted to long acyl chain glucosylceramide.

This conversion is dependent on the ER biosynthesis of Glycosyl Phosphatidyl Inositol (GPI) anchors. These GPI anchors recruit a set of proteins, named GPI-Anchored Proteins (GPI-AP), to the ER membrane. The backbone of GPI consists of a phospholipid and glycan. In ER lumen, GPI-transamidase complex attaches GPI to nascent proteins containing a signal sequence in their CTD for GPI cleavage. Following the attachment of GPI to nascent proteins, the GPI anchor is remodeled by other enzymes. The remodeled GPI-APs, include a variety of proteins, such as receptors, adhesion molecules, and enzymes, are recognized by transmembrane p24 proteins. P24 proteins bridge between GPI-APS and the cargo binding Sec24C and COPII Coat Complex Component, Homolog D (Sec24D) to facilitate their ER export. In addition, sterol levels in the ER are tightly controlled via gene expressions for sterol synthesis, uptake, and other lipid components. Sterols have been proposed to be transported in non-vesicular routes. However, cholesterol in the ER binds to lipid-binding proteins, such as GPI-APs, the vesicular stomatitis virus glycoprotein and the scavenger receptor A, to be shuttled via ER-Golgi vesicular trafficking (Funato et al., 2020).

To maintain the ER function and ER membrane integrity, a retrograde transport of ER-resident proteins and lipids, respectively, is compensated from Golgi to the ER via Coat Protein Complex I (COPI) vesicles. ER-residents proteins contain ER retrieval signals at the CTD, such as the canonical KDEL motifs or the variant HDEL and RDEL motifs, captured by transmembrane proteins, recycled between ER and Golgi, and packaged into COPI vesicles. Although the molecular

basis driving the affinity between ER retrieval sequences and their receptors is less explored, mutational analysis of ER signal receptors has found that changing Aspartic Acid (Asp)-50 to Cysteine (Cys)-50 in the human KDEL receptor impairs affinity binding for various ER signals. Recently, Asp-50 and Glutamic acid (Glu)-117 residues of the KDEL human receptors serve as a gatekeeper, while tryptophan-120 has been found to explain the differential affinity of different ER signals including KDEL, HDEL and RDEL (Gerondopoulos et al., 2021).

Non-vesicular pathways

Non-vesicular lipid export has been reported to occur at ER MCSs and rely on active or passive transport along a concentration gradient. Ceramide, for example, represents a simple lipid delivery to the Golgi apparatus. Once it is delivered to Golgi, it is converted to glucosylceramide or sphingomyelin. Also, ceramides can be transported against a concentration gradient through the Ceramide Transfer Protein (CERT) for sphingomyelin synthesis. CERT contains an NTD of Pleckstrin Homology (PH), a domain with Two Phenylalanines in an Acidic Tract (FFAT) motif, and a START family domain that binds ceramide. The CERT-mediated ceramide delivery occurs within the membrane contacts sites of the ER and Trans-Golgi Network (TGN). CERT recruitment to the TGN is regulated by levels of Phosphatidylinositol 4-monophosphate (PI4P) synthesized by the TGN. Of note, PI4P is hydrolyzed into PI and phosphate by the ER-localized PI4P phosphatase, known as SAC1. The PI4P hydrolysis has been presumed to be the driving energy for the transfer of sterols to the TGN. Sterol transport to the TGN is

carried via Oxysterol Binding Proteins (OSBP). Like CERT, OSBPs contain a FFAT domain bound by ER Vesicle-Associated Membrane Protein-Associated Proteins (VAP). Meanwhile, the PH domain of OSBPs interacts with PI-Transfer Protein Membrane Associated (Nir) proteins such as the NTD of Nir2 that is capable of PI binding and localized in the vicinity of Golgi. Nir2 carries out the transfer of PI, after being hydrolyzed in the ER, back to the TGN for PI4P synthesis. This counter-exchange mechanism driven by interaction between OSBP and Nir2 proteins is evolutionarily conserved. Therefore, OSBPs not only bridges between the ER and TGN membranes, but also facilitates CERT-dependent ceramide transport through PI4P hydrolysis (Funato et al., 2020).

Non-vesicular transport of ER-synthesized lipids directly to the plasma membrane is mediated by proteins localized between the contact sites of the ER and the plasma membrane. Extended-Synaptotagmins (E-Syts) and TMEM24 are ER-plasma membrane localized proteins that contain a Synaptotagmin-Like Mitochondrial and Lipid-binding Protein (SMP) domain, which binds glycerophospholipids *in vitro*. E-Syts have been suggested to control the transfer of glycerophospholipids between these contact sites of ER and plasma membranes. Although TMEM24 contains a SMP domain, it preferentially transfers ER-synthesized PI to plasma membranes. Other lipid-binding proteins that do not contain the SMP domain have been documented in the ER-plasma membrane contact sites such as OSBPs-Related Proteins (ORP) and Nir proteins. Nir2 and Nir3 proteins maintain the ER-plasma membrane pool of PIP2 and PI4P. In

response to growth factor-stimulated the production of PA, Nir2 proteins are translocated to plasma membrane to pick up PA and deliver it to the ER for PI synthesis. On the other hand, ORP6 and ORP8 exchange between phosphatidylserines, supplied to the plasma membrane, and PI4P or PIP2, delivered to the ER (Funato et al., 2020).

The ER-endocytic pathway, facilitated by their MCSs, transfers sterols from ER to endosomes and lysosomes. This transfer is mediated by integral VAP-A proteins that bind phosphatidylinositol 3-monophosphate, an early endosomal lipid. In addition, VAP-A proteins bind Rab7, a small GAP protein involved in late endosomes, and thus, constitute the ER-endocytic pathway. ER-localized sterols are dependent on VAP-ORP1L interactions to reach multivesicular endosomes at the MCSs regulated by annexin A1 and its Ca^{2+}-dependent ligand, S100A11. ORP1L monitors the levels of sterols in late endosomes through its interaction with Rab7. In addition, ORP proteins including ORP1L, ORP6, and ORP8 have been involved in retrograde transport of sterols from different endosomal stages back to the ER. Other proteins have been reported to transport lipids across ER-endosome MCSs. For example, STARD3, a START-domain containing protein, acts as a sterol carrier from the ER to endosomes through its interaction with VAP proteins. Recently, the vacuolar protein sorting 13 has been implicated in the transport of glycerophospholipids at ER-endosome MCSs (Funato et al., 2020).

Perturbations of ER functions result in ER stress

Pathophysiological perturbations of ER functions

Several diseases, such as cancer, diabetes, neurodegenerative diseases, involve ER perturbations. Genetic instability and mutations in cancers are usually accompanied with ER stress response. In addition, the proliferative nature of cancer cells overloads ER with high protein production demands which can be exaggerated by the encoded mutations that may disrupt the folding process and augment ER stress levels as in melanoma. Microenvironment is one of the hallmarks of tumor cells. It is characterized by depletions of nutrients and oxygen in proliferating cells creating a known condition, microenvironmental stress. Microenvironment can activate multiple stress pathways because of the created hypoxia and starvation conditions. These conditions, particularly glucose starvation that blocks N-linked glycosylation important for protein folding, further increase perturbations to ER functions (Almanza et al., 2019; Oslowski & Urano, 2011). β-pancreatic cells respond to minimal changes in blood glucose levels to produce insulin. However, insulin production is impaired when it encodes the C96Y mutation and leads to its accumulation in the ER lumen in the Akita mouse. As a result, β cells die and the Akita mouse is considered as a model for Type 1 Diabetes (T1D) (Almanza et al., 2019). In human T1D, the insulin-producing β cells are thought to be destroyed via an autoimmune mechanism involving autoreactive T cells (Roep, Thomaidou, van Tienhoven, & Zaldumbide, 2021). However, there are several reports indicating ER stress association with T1D development (Eizirik, Pasquali, & Cnop, 2020; H. Lee et al., 2020; Ozcan et al., 2004). Recently, we

have shown that the low insulin-producing β cells in human islets of T1D subjects are likely due to their lost adaptation to chronic ER stress (C. W. Chen et al., 2022). Furthermore, neurogenerative diseases have also been linked to ER stress. For example, mutations in the ER vesicle-associated membrane protein-associated protein B represented in familial amyotrophic lateral sclerosis have been suggested to induce death of neuron motor due to altered ER stress response (Almanza et al., 2019).

External perturbations of ER functions

Chemical molecules, temperature, and Reactive Oxygen Species (ROS) can disrupt ER homeostasis leading to ER stress. Small molecules have been designed to induce ER stress and others to enhance ER proteostasis. Several pharmaceutical molecules have been widely used to induce ER stress through various mechanisms. 2-deoxyglucose or Tn, for example, inhibits N-linked glycosylation of proteins and thus affect protein maturation. In addition, Dithiothreitol (DTT) interferes with the formation of disulfide bonds. While Brefeldin A stalls ER-Golgi trafficking, Tg and Cyclopiazonic Acid (CPA) depletes ER Ca^{2+} stores via targeting SERCAs. The reduced Ca^{2+} concentration impairs ER functions (Almanza et al., 2019). On the other hand, 4-phenylbutyric acid has been proposed to decrease the accumulation of misfolded proteins in the luminal ER. Tauroursodeoxycholic acid, known as TUDCA, is another enhancer of ER homeostasis and derived from an endogenous bile acid. Although it alleviates ER stress in islet cells, its mechanism of action is still obscure. Body temperature of 36-37 Celsius Degree (°C) is critical for various cellular processes including protein

folding. Increased temperature during cell growth have been used to study thermotolerance through heat shock response and ER stress markers. Excessive temperature has been documented to distort the structures of ER and Golgi apparatus in a mechanism known as fragmentation. Conversely, hypothermia, 28° C, has been presented with low levels of ER stress in human stem cells (Almanza et al., 2019). The stress activation has been suggested to protect cells from severe stress that commits to cell death through a process known as ER hormesis (Mollereau, Manie, & Napoletano, 2014). Reactive oxygen species including free radicals, have been linked to ER stress even though the ER-mediated disulfide bond formation constitutes almost 25% of the cellular generated ROS. The oxidizing environment of the ER generates ROS through multiple signaling pathways involving glutathione/glutathione disulfide, Nicotinamide Adenine Dinucleotide Phosphate (NADPH) oxidase 4, NADPH-P450 reductase, Ca^{2+}, ER oxidoreductin 1 and PDI. The ROS accumulation is mitigated by increased mitochondrial respiration and biogenesis. If ROS accumulation surpasses the capacity of antioxidants, an oxidative stress develops and eventually disrupts ER proteostasis (Almanza et al., 2019).

ER stress activates the unfolded protein response

Folding and processing of native polypeptides, the primary function of the ER, are mediated by a cadre of ER-resident protein chaperones. ER dysfunction leads to an increase in misfolded proteins in the ER lumen, a condition known as ER stress (Adams, Canniff, Guay, Larsen, & Hebert, 2020). ER stress activates

ER-transmembrane proteins, including PERK, previously explained in the ISR section, Inositol-Regulated Enzyme 1-α (IRE1α), and Activating Transcriptional Factor 6-α (ATF6α). Together, these proteins sense the misfolded proteins in the ER and activate a protein quality control pathway known as the UPR. The UPR, in turn, reprograms gene expression at both transcriptional and translational levels to alleviate cell damage (Guan et al., 2017). The UPR is initiated with an acute phase involving reprogramming of translation, which severely attenuates global protein synthesis while promoting the translation of a select subset of pro-survival mRNA. Upon sustained stress, both transcriptional and translational reprogramming occurs to coordinate the adaptation to chronic ER stress conditions (Hetz & Papa, 2018). Although global translational inhibition during the acute phase of the UPR is partially restored in the late response, translational regulation remains a significant component of adaptation to chronic ER stress (Guan et al., 2017).

The conserved IRE1 pathway

IRE1 was first discovered in a yeast complementation study involved in the metabolism of inositol phospholipids. Following these studies, Peter Walter and Kazutoshi Mori have independently identified IRE1 as a UPR molecule involved in the signal transduction during the accumulation of misfolded proteins. In mammals two isoforms of IRE1 exist, IRE1α and Inositol-Regulated Enzyme 1-β (IRE1β), encoded by the *endoplasmic reticulum to nucleus signaling 1 and 2* genes, respectively. IRE1α expression is prevalent, whereas IRE1β expression is restricted to intestinal and pulmonary epithelia. IRE1α deletion in mice is

embryonic lethal compared to IRE1β-KO that develops colitis. Although both isoforms share a significant 39% sequence homology, IRE1β has been described to have weaker enzymatic activities (Almanza et al., 2019; Grey et al., 2020; Junjappa, Patil, Bhattarai, Kim, & Chae, 2018).

IRE1 is composed of three distinct domains. The NTD, localized in the ER lumen as an ER sensor to monitor the accumulation of unfolded proteins, a type I transmembrane domain, and the CTD. The CTD has a dual enzymatic activity represented by the kinase and Endoribonuclease (RNase) functions in the cytoplasm. In physiological conditions, IRE1 is rendered inactive due to the attachment of BiP, ER-resident chaperone, to the IRE1α-NTD. When misfolded proteins build up in the ER lumen, BiP dissociates and binds these faulty proteins because of its higher affinity toward them. The dissociation of BiP-NTD of IRE1α triggers IRE1α oligomerization in a face-to-face configuration and thus, allows trans-autophosphorylation of its cytosolic kinase domains. The phosphorylation of Ser-724, Ser-726 and Ser-729 encoded in the activation loop of cytosolic kinase causes conformation changes leading to the activation of RNase. In addition, these conformational changes recruit TRAF2 and thus, initiate c-Jun N-terminal kinase pathway signaling. Recently, there are a few reports showing direct binding of misfolded proteins to the luminal domain of IRE1α leads to its activation. In addition, aberrant membrane lipid composition, and disrupted cellular lipid homeostasis have been reported to activate IRE1α via its transmembrane domain (Almanza et al., 2019; Junjappa et al., 2018).

The active cytosolic RNase domain of IRE1, which is functionally homologous to RNase L, recognizes a conserved sequence, 5′-CUGCAG-3′, in the dual stem loops within the Coding Sequence (CDS) of *X-Box Binding Protein 1-Unspliced* (*XBP1u*) mRNA. Consequently, it catalyzes the removal of 26 Nucleotides (nt) from *XBP1*u mRNA in a spliceosome-independent manner. This cleavage gives rise to gives rise to 2′,3′-cyclic phosphate at 5′ exon and 5′-hydroxyl group (OH) at 3′ exons of *XBP1u* mRNA. These free ends are recognized by a cytoplasmic RNA ligase. Accumulating evidence show that both tRNA ligase, known as RTCB, and its co-factor archease are important for *XBP1u* splicing to form the *X-Box Binding Protein 1-Spliced* (*XBP1s*) mRNA (Almanza et al., 2019; Bashir et al., 2021).

XBP1 represents a member of the cAMP-Response Element-Binding (CREB)/ Activating Transcriptional Factor (ATF) family of transcription factors (S. M. Park, Kang, & So, 2021). The NTD of XBP1 containing a Basic Leucine Zipper Transcription Domain (bZIP) involves in DNA binding and dimerization. However, the CTD explains the functional difference between XBP1u and XBP1s based on the presence of a transcriptional activation domain. The XBP1u-CTD contributes to its short half-life because it contains a destabilizing-sequence, referred to as PEST sequence rich in Proline (Pro), Glu, Ser and Thr, that targets proteins for degradation via the proteosome-ubiquitin proteolysis (Almanza et al., 2019). In addition, the CTD of XBP1u contains HR, specifically HR2, encoding a translational arrest peptide 26 aa in length. HR2 has been proposed to cause a

ribosomal pausing on the *XBP1u* mRNA to enable SRP recognition. Interestingly, although the SRP recruitment of paused ribosome-nascent polypeptide-*XBP1u* mRNA complex to the ER membrane has not been well-documented, its membrane association is still controversial (Bashir et al., 2021; Shanmuganathan et al., 2019). As opposed to the canonical recognition of signal peptide sequence, XBP1u has been suggested to cytosolically interact with Sec61 and the ER membrane. In contrast, other studies have indicated the XBP1u is inserted into the membrane via the interaction of Sec61 translocon with a type II transmembrane domain within the HR of XBP1u. Consequently, the inserted transmembrane domain of XBP1u is subject to cleavage by SSP. In addition, the SSP contributes to the short half-life of XBP1u through interactions with ERAD components. For example, SSP interacts with the rhomboid pseudoprotease, known as Derlin1, and the E3 ubiquitin ligase that ubiquitinates XBP1u for efficient proteasomal degradation. Surprisingly, SSP-mediated cleavage of signal peptides is indispensable for Derlin1 function because of its recognition to the CTD of XBP1u, which presents in the ER lumen (Yucel et al., 2019). The functions of XBP1u have been proposed to downregulate the response to ER stress through heterodimerization with stress transcription factors such as XBP1s. In addition, XBP1u has been reported as a dominant-negative domain of p53/p21 in T-Helper cells to regulate cell proliferation. Deletion of XBP1u-HR2 negatively affects its own mRNA recruitment to the ER membrane for efficient splicing (Bashir et al., 2021; Yucel et al., 2019).

IRE1-mediated splicing of *XBP1u* mRNA introduces a frameshift resulting in a larger protein of XBP1s. The *XBP1u* mRNA encodes 276 aa, while *XBP1s* mRNA encodes the larger protein with 371 aa in mice. Following *XBP1s* mRNA translation, XBP1s proteins translocate to the nucleus where they bind to specific sequences such as the 5′-CCACG-3′ section of ER Stress Response Elements (ERSE) including ERSE-I and ERSE-II. In addition, XBP1s preferentially associates with the UPR element that encodes the complementary sequence of ERSE-I, 5′-CGTGG-3′. XBP1s binding to these elements upregulate UPR gene expression depending on the stimuli as well as cell types. Several studies have indicated that XBP1s is involved in many cellular processes during physiological and pathological conditions. For instance, XBP1s plays an important role in ER stress response including the secretory function, but also contributes to inflammatory response, carbohydrate metabolism and lipid homeostasis. The key roles of XBP1s in cellular functions and metabolic pathways are mediated through transcriptional induction of numerous target genes. A recent review has listed the transcriptional regulations by XBP1s in each cell to highlight the functional importance of XBP1s (S. M. Park et al., 2021). In response to ER stress, XBP1s activates the transcription of ER chaperones, co-chaperones, translocation proteins, other components involved in ERAD and ER-Golgi transport. For examples, XBP1s induces the expression of BiP, an ER chaperone, folding enzymes such as PDI-related protein 5, and co-chaperones that are members of DnaJ Heat Shock Protein 40 (HSP40) family including ERdj4 and $p58^{IPK}$. Other

components involved in ER stress have been dependent on XBP1s such ribosome-associated membrane protein 4, and ER Degradation-Enhancing α-Mannosidase-Like Proteins (EDEM) (Junjappa et al., 2018). Similar to IRE1α KO mice, XBP1-KO is embryonic lethal in mice due to liver hypoplasia and apoptosis (Bommiasamy & Popko, 2011). Furthermore, the reported cell-specific deletions of XBP1 demonstrate deleterious outcomes. In lymphoid precursors, XBP1-KO interferes with the maturation of B cells to plasma cells, whereases XBP1 deletion in intestine confers inflammatory bowel disease. Additionally, neuron-specific XBP1 deletion exhibits resistance to leptin and subsequently obesity (Duwaerts et al., 2021).

Recently, studies focusing on other functions of IRE1 besides *XBP1u* splicing have been reported. During stress conditions, IRE1 has been recognized to cleave other mRNAs than *XBP1u* mRNA after being co-translationally delivered to the ER membrane. This ER stress-dependent mechanism is referred to Regulated IRE1-Dependent Decay (RIDD) that was initially noticed in Drosophila S2 cells and later in yeasts and mammals. Both isoforms of IRE1 exhibits RIDD, but RIDD activity of IRE1β is stronger. Interestingly, most mRNAs targeted by RIDD encodes signal peptides and transmembrane domains that consume ER folding machinery during misfolded protein conditions. Thus, RIDD may decrease the ER load and participate in alleviation of ER stress. Deletion of sequences encoding signal peptides allows mRNA to escape degradation by RIDD. However, there are a few mRNAs, such as *PlexinA*, that encodes a transmembrane protein

which associates with the ER membrane. *PlexinA* mRNA is resistant to RIDD activity even during ER stress. On the other hand, a *small ubiquitin-like modifier 3* mRNA has been characterized as a RIDD target due to the presence of an *XBP1u*-like stem loop. A comprehensive list of RIDD targets seems a challenging task due to the UPR-mediated transcriptional changes and mRNA isoforms present in each system (Bashir et al., 2021)**.** To date, 37 mRNAs, including the *Biogenesis of Lysosomal Organelles Complex 1 Subunit 1* (*BLOS1*), have been listed and confirmed as canonical RIDD targets. These RIDD substrates share two criteria: the conserved consensus conserved sequence, 5′-CUGCAG-3′ and the predicted structure of *XBP1*u-like stem loop (Maurel, Chevet, Tavernier, & Gerlo, 2014). Genetic manipulation and distortion of the loop structure within RIDD targets can protect them from RIDD degradation. RIDD mainly targets ER-localized mRNAs that account for 64%, compared to other cellular localizations. RIDD activity vary depends on the ER stress inducers as well as cell types. For example, the reduced expression of *BLOS1* mRNA in DTT-treated cells is higher than Tg-treated cells. In addition, the levels of degraded *BLOS1* mRNA are different between human embryonic kidney 293 and human hepatoblastoma cell lines (Bashir et al., 2021). RIDD is positively regulated by ER stress-mediated translation inhibition. For example, PERK knockdown protects some RIDD targets, including *BLOS1* mRNA, from degradation. Thus, the mRNA translational status is the key to control RIDD where translational attenuation may give IRE1-RNase accessibility to the ribosome-dissociated mRNA to perform RIDD degradation (Bashir et al., 2021).

Although active PERK has been shown to positively influence RIDD activity, a recent report antagonizes the positive regulation of PERK on RIDD. Ashkenazi and co-workers have shown that PERK dephosphorylates Ser residues of the activation loop of IRE1, under unsolved ER stress. This dephosphorylation is exerted via the phosphatase of RNA polymerase II-associated protein 2. As a result, RIDD activity was diminished (T. K. Chang et al., 2018). The differences in RIDD regulations mediated by PERK could be explained by the strength and duration of the applied ER stress inducers.

ATF6 pathway

ATF6 is a type II transmembrane protein inserted into the ER membrane and a member of the UPR sensors. ATF6 contains a cytosolic bZIP transcription factor and transactivation domain followed by a 20-aa transmembrane domain. The NTD of ATF6 is exposed to the cytosol, while its CTD region is inserted into the ER lumen. Two isoforms of ATF6 have been expressed in mammals: ATF6α with 670 aa and Activating Transcriptional Factor 6-β (ATF6β) with 703 aa. Although ATF6 isoforms share similar structures, the transcriptional activity of ATF6α is more potent than ATF6β (Almanza et al., 2019; Hillary & FitzGerald, 2018). Combined deletion of these isoforms in mice leads to embryonic lethality, while neither ATF6α-KO nor ATF6β-KO causes this effect. The ER stress-sensitive Mouse Embryonic Fibroblasts (MEF cells) derived from ATF6α-KO, but not ATF6β-KO, imply that ATF6α is a critical regulator during the UPR (Yamamoto et al., 2007).

In contrast to the other UPR sensors, ATF6α represents a type II 90 kDa ER-resident transmembrane protein. In response to ER stress, BiP-disassociated ATF6 is exported to Golgi where it is subject to a sequential cleavage by Golgi-resident proteases; site-1 protease and site-2 protease, respectively. Digestion of transmembrane anchor together with the luminal domain liberates the NTD of 50 kDa cytosolic transcription factor. The active truncated ATF6 protein, the NTD of ATF6, migrates to the nucleus and binds ERSE-I and ERSE-II to induce the UPR adaptive genes. Since ATF6 shares XBP1s binding sites, ERSE-I and ERSE-II, they often share targets. The cytoprotective role of ATF6 has been shown through an upregulation of the UPR target genes such as *XBP1* and *BiP* to restore ER proteostasis. Other ER targets induced by ATF6 include *EDEM-1* and *PDIA6*. The repertoire of ATF6 targets is extended through interaction with other transcription factors such as CREB, cAMP-Response Element-Binding Protein 3 (CREB3)-like 3, SREBP-2, XBP1, components of nuclear transcription factor complex, and serum response factor. In addition to ATF6, other ER-resident transmembrane proteins have been documented. These alternative members of the ATF6 family include Luman, CREB3-like 1, also known as OASIS, CREB3-like 2, CREB3-like 3 and CREB, and their functions are still under investigations (Almanza et al., 2019; Hillary & FitzGerald, 2018).

In short, the nature of the ER structure and its interactions with other cellular organelles subject ER functions to numerous internal and external signals. Perturbations of ER functions result in ER stress that is sensed by PERK, IRE1α,

and ATF6α. Consequently, they activate the well-known UPR adaptive programs primarily defined by an early translational control. In prolonged stress, the UPR integrates transcriptional and translational controls to establish an adaptive UPR. Therefore, the stress response mechanisms including transcriptional and post-transcriptional mechanisms are integrated to influence the mRNA life cycle and consequently maximize the stress response to cope with ER stress. These mechanisms will be discussed below to indicate how they are regulated to maintain proper gene expression to restore ER homeostasis.

OVERVIEW OF TRANSCRIPTIONAL CONTROL

Eukaryotic transcription transfers the genetic information encoded in DNA molecules into RNA molecules, subsequently translated into proteins. Eukaryotic transcription is mediated by three RNA Polymerase (Pol) machineries; RNA Pol I is involved in the synthesis of Ribosomal RNAs (rRNA) that is matured into 28S, 18S, and 5.8S rRNA. However, 5S rRNA is synthesized by Pol III that also produces tRNAs. RNA Pol II manufactures mRNA and non-coding RNAs such as Long Non-Coding RNA (lncRNA), Enhancer RNAs (eRNA) and small RNA species including MicroRNA (miRNA), Small Nuclear RNA (snRNA), and small nucleolar RNA. Transcription is tightly regulated and varies among cells due to various internal or external signals (Proudfoot, 2016; Wissink, Vihervaara, Tippens, & Lis, 2019).

Transcriptional regulation

The process of transcription can be divided into the assembly of pre-initiation complex to initiate transcription, promoter-proximal pausing, processive Pol II elongation, and finally termination coupled to pre-mRNA processing. During transcription initiation, two regulatory elements, including promoters and enhancers, are bound by transcription factors, including activators and repressors, to define a gene activity and its transcription frequency. The binding of transcription cofactors increases chromatin accessibility. The core initiation regions of promoters and enhancers are recognized by general transcriptional factors including TFIIB, TFIID, TFIIE, TFIIF, and TFIIH. When they combine with Pol II, the pre-initiation complex is formed and considered as the first step in transcription

initiation that is regulated by transcription factors and chromatin structures. Other regulatory components of transcription include the CTD of RNA Polymerase II (Pol II-CTD) containing repeats of heptad consensus sequence (Tyrosine-Ser-Pro-Thr-Ser-Pro-Ser). Phosphorylation of Pol II-CTD has been reported to control Pol II activity during transcriptional stages. When Pol II-CTD is phosphorylated on Ser-5 and Ser-7 and the double-stranded DNA is unwound by the general TFIIH containing a Cyclin-Dependent Kinase (CDK)-7 subunit, Pol II initiates transcription of a target gene from a distinct transcription start site. Following transcription initiation and synthesis of 20-60 nt downstream of the transcription start site, Pol II pauses at the promoter-proximal pausing site. As a product of core initiation sites, enhancer transcripts tend to be short and unstable, whereas the protein-coding transcripts, known as pre-mRNAs, are long and more stable due to their binding to U1 Small Nuclear Ribonucleoprotein (snRNP). Although the functional link between enhancers and promoters is less explained, a recent report has suggested the amount of eRNAs correlates with the functional capacity of the enhancer (Rambout & Maquat, 2020; Wissink et al., 2019).

Pol II stalling serves as a quality control checkpoint and rate-limiting step in transcription. The pol II pausing is regulated by Negative Elongation Factors (NELF) and DRB Sensitivity-Inducing Factors (DSIF) that act to stabilize the Pol II pausing. In contrast, the Positive Transcription Elongation Factor B (P-TEFb) complex, containing a CDK-9 subunit, release the paused Pol II by phosphorylation of NELF, DSIF and Pol II-CTD on Ser-2 residue. With increased Ser-2 and decreased Ser-5 phosphorylation of Pol II-CTD, Pol II engages in a processive

elongation under the control of elongation factors such as the CDK-12 subunit. In addition to the promoter-proximal pausing, Pol II transiently pauses at stable first nucleosomes, relieved by P-TEFb, serving as feedback to the promoter-proximal pausing, co-transcriptional splicing, and early Pol II termination. Pausing at the stable first nucleosomes has been proposed to enforce the promoter-proximal pausing by increased NELF recruitment or cause early termination if Pol II encounters CpG islands, a genomic region with large CpG dinucleotide repeats, prior to the nucleosomes. The early termination is based on the failure of U1 snRNP to recognize the 5′ Splice Site (5′-SS) of the first intron (Rambout & Maquat, 2020; Wissink et al., 2019).

As Pol II passes through the Polyadenylation Signal (PAS), the pre-mRNA is cleaved and polyadenylated mediated by the phosphorylated Ser-2 residue of Pol II-CTD that has been reported to interact with the Cleavage and Polyadenylation Complex (CPAC). Further elongation of Pol II results in degraded transcripts mediated by the nuclear 5′–3′ exoribonuclease 2, XRN2, due to lack of 5′–capped transcripts. To destabilize the elongating Pol II and facilitate its termination, the recruited CPAC and other chromatin features including heterochromatin and R-loops, which results from hybridization of nascent transcripts to antisense strand of DNA outside the elongation complex, have been proposed to recycle Pol II for another round of transcription unless it is ubiquitinated and degraded due to transcriptional arrest induced by DNA damage (Proudfoot, 2016; Wissink et al., 2019).

Co-transcriptional processes

During transcription, pre-mRNA undergoes maturation in a three-step process, known as co-transcriptional processes. The pre-mRNA processing involves 5′-capping, intron splicing and 3′-polyadenylation. These processes add another layer of gene expression regulation (Figure 1.2). For example, transcript isoforms, produced due to alternative splicing and polyadenylation, and RNA modifications such as methylations have been reported to affect post-transcriptional mechanisms such as mRNA translation and stability (Wissink et al., 2019).

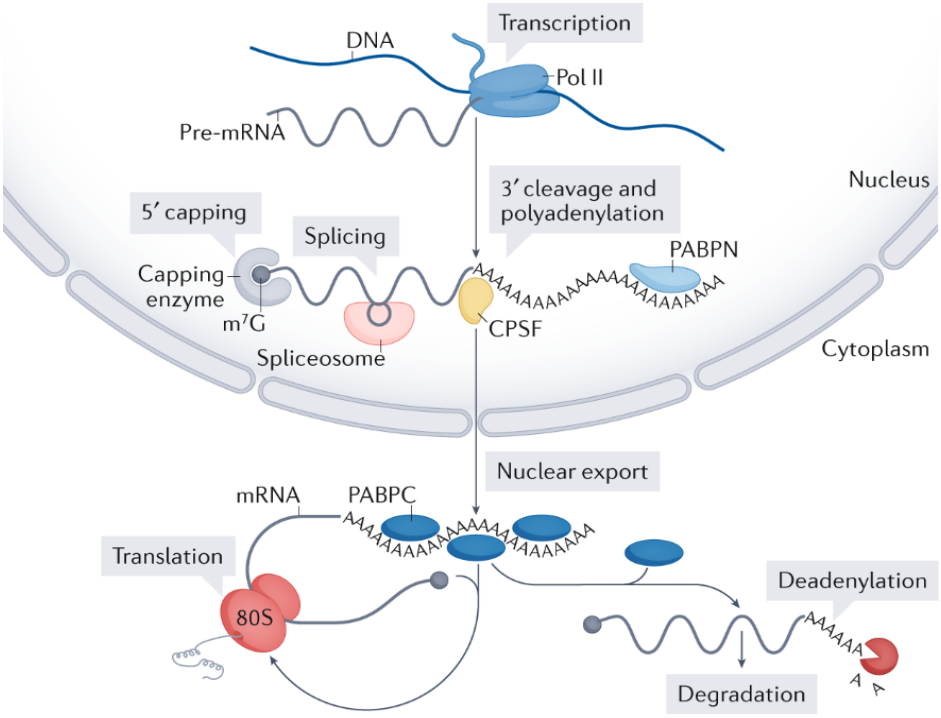

Figure 1. 2. Overview of mRNA biogenesis.
Pol II drives the synthesis of nascent RNAs, pre-mRNAs, that are simultaneously subject to canonical processing of 5′-7-Methylguanosine (m^7G) by the capping enzyme, intron splicing mediated by the spliceosome, and 3′-end cleavage and polyadenylation controlled by the Cleavage and Polyadenylation Specificity Factor (CPSF) and Nuclear Poly(A)-Binding Proteins (PABPN). Matured mRNA is

exported to the cytoplasm. mRNA translation by ribosomes is enhanced by the Cytoplasmic Poly(A)-Binding Proteins (PABPC), while poly(A) tail removal influence mRNA stability and leads to degradation. Reprinted with permission from Springer Nature, the publisher of (Passmore & Coller, 2022).

mRNA capping

The 5′-end of pre-mRNA is capped constituting the first step in pre-mRNA maturation. Pre-mRNA capping is essential for cell viability and occurs shortly after transcriptional initiation. In mammals, the capping enzyme consists of a single protein containing triphosphatase and guanylyl-transferase domains. The capping enzyme has been reported to associate with Pol II-CTD phosphorylated on Ser-5, whereas truncated Pol II domains promote mRNA degradation due to failed 5′-pre-mRNA capping. During transcription initiation, the emerging nascent transcript contains a triphosphate at the 5′-pre-mRNA. The γ-phosphate of the first nucleotide at the 5′-pre-mRNA is removed by the triphosphatase forming a diphosphate-terminated pre-mRNA. Next, the guanylyl-transferase domain attacks the α-phosphate of GTP releasing a Guanosine Monophosphate (GMP) that is covalently linked to the diphosphate-terminated pre-mRNA forming the cap structure. As a final reaction in the capping process, the N-7 position of Guanosine (G) cap is methylated by the RNA guanine-7 methyltransferase. This cap structure represents the minimal cap structure, Cap-0, recognized by binding proteins such as the eukaryotic Translation Initiation Factor 4 E (eIF4E). In addition to the 7-Methylguanosine (m^7G) cap, the nucleoside-2′-*O*-methyltransferases have been found to methylate the ribose O-2 position of the first and second nucleotides of nascent RNAs, representing Cap-1 and Cap-2, respectively. Other nucleotide

modifications have been documented such as N-6 Methylation of Adenosine (m^6A) of the first nucleotide of nascent RNAs in Hela cells indicating different regulations of mRNA. In addition, the cap structure is important for the innate immune response to viral infections. During viral infections, Pattern Recognition Receptors (PRR) can distinguish between endogenous and invading viral cap structures and stimulate inflammatory response through IFN expression. Retinoic acid inducible 1 and DEAD-Box Helicase (DDX)-58 are examples of PRRs that bind dsRNAs with aberrant cap structure with 5′-triphosphate or diphosphate structures or those lacking the O-2 methylation of the first nucleotide. Recently, nicotinamide adenine dinucleotide cap, a different cap structure, have been identified and targeted by Non-Canonical Decapping Exoribonuclease (DXO) (Decroly, Ferron, Lescar, & Canard, 2011; Galloway & Cowling, 2019; Kiledjian, 2018; Martinez-Rucobo et al., 2015).

The m^7G cap is targeted by nuclear and cytoplasmic binding proteins. In the nucleus, two conserved Nuclear Cap-Binding Proteins, (NCBP1) and (NCBP2), forming a Cap-Binding Protein Complex (CBP). The recruitment of CBP complex to the mRNA cap is facilitated via NELF in which NCBP1 has been documented to bind the 5′-cap, while NCBP2 interacts with other proteins involved in pre-mRNA maturation steps, and nuclear exit. In addition, the CBP complex has been proposed to remain associated with mRNA post a few rounds of translation. In the cytoplasm, mRNA cap is bound to the cytoplasmic cap-binding complex, known as eukaryotic Translation Initiation Factor 4 F (eIF4F) consisting of multiple translation factors, explained in the below section of translation. Interestingly, both CBP and

eIF4F complexes exhibit a strong affinity to the cap-0 when the first nucleotide is a purine and less affinity toward other caps especially when its first nucleotide is methylated at the ribose O-2 position. This implies the effect of cap structures on mRNA translation. In addition to CBP and eIF4F, La-Related Protein (LARP)-1 has been identified as a cap binding protein that binds to mRNAs containing the 5′-terminal oligo pyrimidine, known as TOP motifs. TOP motif-containing mRNAs encode for ribosomal proteins and translational elongation factors. These mRNAs are involved in growth-dependent translational control. The LARP1 binding to the capped mRNA has been suggested to influence mRNA stability and translation. Under the activation of Mammalian Target of Rapamycin (mTOR), LARP1 is phosphorylated and released from 5′-mRNA caps, containing a Cytosine (C) in the first nucleotide, to allow mRNA translation initiation (Galloway & Cowling, 2019; Rambout & Maquat, 2020; Wende, Friedhoff, & Strasser, 2019).

mRNA splicing

Removal of non-coding introns, a mechanism known as splicing, is another step in the maturation of pre-mRNA and mediated by the large spliceosome complex. The assembly of the spliceosome on pre-mRNA occurs as a few nucleotides emerge from Pol II exit channel. The spliceosome activity is influenced by the speed of and CTD phosphorylation status of elongating Pol II, chromatin structures, and pre-mRNA processing such as the 5′-end capping (Carrocci & Neugebauer, 2019; Herzel, Ottoz, Alpert, & Neugebauer, 2017).

Intron splicing is carried out by the spliceosome composed of five Uridine (U)-rich snRNAs associated with specific proteins to form snRNPs, named U1, U2,

U4, U5, and U6. Among these protein complexes is Nineteen Complex (NTC), Nineteen-Related Proteins (NTR), retention and splicing complex and other non-snRNP proteins that assist the spliceosome assembly and activity. Interesting, the splicing activity itself is cost-effective, while the spliceosome assembly and its intrinsic reorganization are energetically expensive due to its reassembly at every intron in the genome. Efficient splicing reactions depend on recognition of three conserved elements within introns of pre-mRNA. Two splice sites define the intron boundaries and encode the dinucleotides of GU for a 5′-SS, and AG for a 3′ Splice Site (3′-SS). The third element represents the Branchpoint Sequence (BPS), encompasses 18-49 nt located upstream of the 3′-SS. In higher eukaryotes, a polypyrimidine tract downstream of the BPS helps in recognition of the 3′-SS during the spliceosome assembly. Splicing includes a two-stepwise transesterification reaction to remove a single intron: the first reaction involves the nucleophilic attack of the BPS adenosine, mediated by 2′-OH, on the first exon-intron boundary, containing 5′-SS. This cleavage generates a 3′-free OH of the first exon and 2′-5′ phosphodiester bond, a lariat intron intermediate. The second transesterification involves the attack of first exon 3′-OH to the phosphodiester backbone connecting the 5′- second exon to the 3′-intron, representing the 3′-SS, leading to ligation of exons and release of lariat (Carrocci & Neugebauer, 2019; Herzel et al., 2017).

The molecular steps of spliceosome assembly have been well studied and divided into sub-complexes sequentially involved in the identification of 5′-SS, BPS and 3′-SS of an intron, spliceosome maturation and activation followed by splicing catalysis. In the beginning, the 5′-SS of an intron is exposed in Pol II-synthesized

pre-mRNA and base paired with U1 snRNA to form the Early complex (E complex). Meanwhile, U2 Auxiliary Factor 65 kDa ($U2AF^{65}$, also known as U2AF2) is the larger subunit of U2AF that recognizes the polypyrimidine tract, while the essential splicing factor, U2AF 35 kDa ($U2AF^{35}$), represents the smaller subunit and specifically recognizes the 3′-SS of an intron. In addition, $U2AF^{65}$ has been documented to bind Pol II during early transcriptional stages. U2AF associates with the Splicing Factor 1 (SF1) that binds to the BPS. Next, the branchpoint binding protein, SF1, is replaced with U2 snRNP, recruited by $U2AF^{65}$, that also contacts with the 3′-SS of an intron. Consequently, the E complex is transformed into the assembled spliceosome, known as the A complex. Upon recruitment of the trimeric complex of U4, base paired with U6 snRNA forming a snRNP complex, and U5 snRNPs, the pre-B complex is formed. The pre-B complex undergoes conformational rearrangements including the 5′-SS base-paired with U6 snRNA instead of U1 snRNA and subsequent release of U1 snRNP from the B complex. However, the exchange of U4 snRNA with U2 snRNA leads to formation of the U2-U6 active site. In addition to the release of U4 snRNA, the recruitment of protein complexes such as NTC and NTR, the B complex is labeled as the B^{act} complex (matured spliceosome). Although the catalytic center is formed in the B^{act} complex, it has been shown to be obstructed by U2 snRNP components, especially the Splicing Factor 3 (SF3) b. To activate the spliceosome complex, the Prp2 ATPase transforms the catalytically inactive B^{act} complex into an active B* complex by exposing the BPS upon the release of U2 snRNP components, SF3a and SF3b. Bringing the U2-U6 duplex together with U2-BPS represents the first

transesterification reaction, and extensively remodels the spliceosome forming the C complex (activated spliceosome I). Following the first reaction, the 5′-exon is base paired with U5 snRNA, while U5 snRNP-related Prp8 has been shown to contact sequences located downstream of the BPS, nearby the 3′-SS. Meanwhile, the U6 snRNA maintains its interaction with the branched 5′-SS, and the U2 snRNA stabilizes the lariat intron. Upon the catalysis of first splicing reaction, other splicing factors such as Prp16 facilitate the second transesterification reaction catalyzed by the C* complex (activated spliceosome II). The exons are ligated, and the lariat intron is released from the P complex (post-catalytic spliceosome). The P complex dissociates from mRNA leading to the spliceosome disassembly (Carrocci & Neugebauer, 2019; Herzel et al., 2017; Ujvari & Luse, 2004).

Numerous studies have shown that intron splicing simultaneously occurs during transcription in multiple organisms and this coupling is required for accurate gene expression. Although a slow transcriptional rate, referred to transcriptional pausing, has been previously considered as an essential element for efficient splicing, the presence of rapid spliced products compared to the rate of elongating Pol II excludes the requirement of transcriptional pausing for splicing. Interestingly, the fast and slow elongating pol II confer changes in splicing events, while dysregulated splicing leads to accumulation of Pol II over introns indicative of transcriptional pausing. These data reflect the extensive regulations of transcription and splicing machineries. Like the capping enzyme, the Ser-5 phosphorylation of Pol II-CTD stimulates the pre-mRNA splicing as indicated by immunoprecipitation of Ser-5 antibody with splicing reaction intermediates as well

as splicing factors alongside Pol II. *In vitro*, pre-mRNA produced by Pol II is efficiently spliced compared to that produced by a CTD-deficient polymerase. Furthermore, the CBP complex, involved in pre-mRNA capping, has been shown to promote nascent RNA splicing via recruiting U1 snRNP to the 5′-SS and stabilizing it to facilitate the formation of E complex. Another study indicates the role of CBP complex in stabilizing the recruited trimeric complex of U4, U5, and U6 snRNPs. Together, these data emphasize the role of the CBP complex in co-transcriptional processes. Finally, chromatin structures have been suggested to impact the splicing efficiency. For example, earlier experiments of integrated adenoviral sequences at various genomic locations yielded changes in the outcomes of splicing. Interestingly, nucleosomes have been frequently found at exons where the rate of elongating Pol II is slower than introns. As a result, nucleosomes have been thought to act as chromatin marks for exons and transient Pol II pausing site. Regardless of nucleosome positions, modifications of histone proteins have been linked to increased gene outputs dependent on splicing efficiency. Tri-Methylation of Histone 3 on the Lysine (Lys)-4 (H3K4me3), for example, is peaked at the first 5′-SS of genes due to gene architecture, represents the organization of exons and introns within a gene. Once the gene architecture is manipulated, the chromatin marks including H3K4me3 are rearranged. Therefore, this may explain the disrupted splicing in the previous genome-editing experiments or decreased gene outputs due to loss of uncharacterized interactions between splicing components and histone modifying enzymes. In agreement with this notion, the inhibition of histone deacetylase, a histone modifying enzyme, resulted

in global alternative splicing. Despite the evidence of chromatin influence on splicing and its natural localization in close proximity to spliceosome and elongating Pol II, the molecular linkage between chromatin, transcription rate and the spliceosome is difficult to establish unless new tools are developed to underpin their regulatory networks (Carrocci & Neugebauer, 2019; Herzel et al., 2017).

Alternative splicing can result into production of different protein-coding mRNAs. It includes, but is not limited to exon skipping or inclusion, intron retention, and alternative splice sites. Although alternative splicing is regulated by many RBPs, a comprehensive list of factors regulating splicing is still under exploration (Ule & Blencowe, 2019). These RBPs are dysregulated during cellular stress and consequently result in alternative splicing (Krebs, Groenendyk, & Michalak, 2011). In addition, many signaling networks have been reported to regulate alternative splicing in specific cell types or conditions (Ule & Blencowe, 2019). For example, elongation factor for Pol II 2 is induced in response to ER stress and leads to RNA splicing patterns in antibody-secreting cells (Carew, Nelson, Liang, Smith, & Milcarek, 2018). In addition, nucleotide deprivation induces a transcriptional elongation factor, called Hexamethylene-Bis-Acetamide-Inducible Protein (HEXIM1) in vascular smooth muscle cells. In melanoma, HEXIM1 acts as a tumor suppressor because it inhibits the kinase activity of P-TEFb complex (Michels & Bensaude, 2018; Tan et al., 2016).

mRNA cleavage and polyadenylation

RNA cleavage and polyadenylation constitute the 3′-end processing of nascent RNAs that happen simultaneously with elongating Pol II. The 3′-end

processing has been suggested to terminate transcription. Upon recognition of the PAS, the multi-subunit complex of 3′-end processing machinery cleaves and adds Adenosines (A) to the 3′-end of pre-mRNA that has been suggested to promote mRNA translation and stability. The selection of PAS occurs simultaneously during transcription and defines the 3′-end of the mRNA. Failure to recognize the correct PAS can affect gene expression and lead to deleterious effects involved in many diseases (Kumar, Clerici, Muckenfuss, Passmore, & Jinek, 2019).

The CPAC contains three enzymatic activities including endonuclease, Poly(A) Polymerase (PAP) and phosphatase. Most components of CPAC have been initially discovered via cell fractionation and affinity purification experiments in yeast. In humans, more than eighty proteins have been associated with the complex of pre-mRNA 3′-end processing. However, many of these proteins are functionally uncharacterized (Kumar et al., 2019). To date, the human CPAC is composed of many proteins including the Cleavage and Polyadenylation Specificity Factor (CPSF), Cleavage Stimulation Factor (CstF), Cleavage Factors I (CF I) and II (CF II), and PAP. These complexes represent the core of pre-mRNA 3′-end processing (Di Giammartino, Nishida, & Manley, 2011; Kumar et al., 2019). CPSF binds to the highly conserved PAS, encoding AAUAAA or close variants, and dictates the pre-mRNA cleavage at 10-30 nt downstream of the PAS. Meanwhile, UGUA-containing or U-rich sequence upstream of the PAS is bound by CF I, while U- or GU-rich elements downstream of the PAS is recognized by CstF. These RNA-protein interactions have been considered as a quality control checkpoint for a correct usage of the pre-mRNA cleavage site and subsequent

efficient cleavage (Kumar et al., 2019). As a result of the pre-mRNA cleavage, PAP adds A′s up to 250 nt in which the first 11-14 A′s enable the binding of Nuclear Poly(A) Binding Proteins (PABPN). PABPN binding has been suggested to transform PAP activity from the distributive mode to the processive synthesis of poly(A) tail. Although all RNA species produced by Pol II are subject to 3′-end processing, some mRNAs encode poly(A) limiting elements that restrict their poly(A) tail length to as low as 20 nt, while others such as histone mRNAs lack poly(A) tails and having stem-loop structures at their 3′-ends, instead (Nicholson & Pasquinelli, 2019).

Early studies of poly(A) tails have found a positive correlation between long poly(A) tails and translation efficiency. During oocyte maturation, the short poly(A) tails of maternal mRNA are re-elongated by non-canonical PAPs, present in the cytoplasm, in a mechanism known as cytoplasmic polyadenylation. Like maternal mRNA, some dendritic transcripts are stored in a translationally repressed state with short poly(A) tails in synapses. Upon synaptic stimulations, these mRNA are actively translated due to their increased poly(A) tails. These reports indicate the role of mRNA poly(A) tail length in enhancing mRNA translation. Although the poly(A) tails positively regulate mRNA translation, the synergetic connection between mRNA poly(A) tails and translation is still debatable. In addition, poly(A) tails have been shown to influence translation initiation and its interactions with translation factors, such as the eukaryotic Translation Initiation Factor 4 G (eIF4G), at the 5′-capped mRNA have led to the proposed model of a closed loop. The Cytoplasmic Poly(A)-Binding Proteins (PABPC) have been suggested to play a

significant role in translation regulation between embryonic and somatic cells (Nicholson & Pasquinelli, 2019).

In addition to the role of poly(A) tails in mRNA translation and stability, mRNA poly(A) tails have been suggested to facilitate mRNA export to the cytoplasm. In the cytoplasm, the ploy(A) tails are covered with the available PABPC proteins. The transition between nuclear and cytoplasmic proteins associated with newly synthesized mRNA such as PABPN and PABPC is not fully understood. Although transitions between PABPN and PABPC have been interpreted as a consequence of the first round of mRNA translation, the absence of repeated footprints of PABPN compared to the repeating PABPC footprints, 20-30 nt, argue against that notion. Based on the PABPC interactions, PABPC may have a dual role involved in mRNA translation and stability. For example, PABPC has been shown to interact with translation factors such eIF4G and the eukaryotic Release Factor 3 (eRF3). Despite the fact that poly(A) tails protect mRNA from degradation by exonucleases, PABPC has been recently found to interact with components recruiting deadenylases and LARP proteins that modulate mRNA translation and stability (Nicholson & Pasquinelli, 2019).

Recent advanced technologies have overcome the difficulty in sequencing the poly(A) tail due to its nature of homopolymers and illustrated the potential regulation of poly(A) tail length in condition- or cell-specific contexts. For example, a poly(A) tail length comparison among different species, including human, mouse, *Drosophila melanogaster* and *Caenorhabditis elegans*, has set the median tail length within the range of 50-100 nt, less than the expected poly(A) tail length

in mammals. However, the yeast median poly(A) tail length was lower around 30 nt due to the initial yeast poly(A) tail length estimated to be around 90 nt. In addition, some stable mRNA such as β-actin mRNA, previously thought to have long poly(A) tails, tend to have short poly(A) tails. This finding contradicts the traditional thought of correlating the long poly(A) tail to increased mRNA stability. Surprisingly, a genome-wide study has concluded that highly expressed and well-translated genes are associated with short poly(A) tails, while less abundant and poor translated genes are associated with long poly(A) tails. Furthermore, the analysis of poly(A) tail length has shown a phasing distribution explained by the footprint of PABPC where the absence of PABPC exposes A′s for removal by deadenylases. This phasing pattern is exclusively for polyadenylated mRNA, especially highly expressed and well translated mRNA, but not other polyadenylated RNA species such as lncRNA. In contrast, increased poly(A) tails of transcripts by cytoplasmic polyadenylation during specific conditions, such as synaptic plasticity, oocyte maturation and developmental stages, positively correlate with translation efficiency (Nicholson & Pasquinelli, 2019; Passmore & Coller, 2022).

Like alternative splicing, Alternative Polyadenylation (APA) results from different usage of multiple PAS locations encoded in the genome. Consequently, APA results in isoforms with different proteins or 3′-Untranslated Regions (UTR) depending on the location of PAS. In addition, APA is an essential process in mammalian development and considered as a prevalent mechanism where almost 80% of elongating Pol II can undergo APA. APA has been documented to alter the

mRNA fate including mRNA translation, stability, or localization. In cancer, signaling networks are dysregulated and have been suggested to increase APA. For example, the synthesis of oncogenic mRNA with short a 3′-UTR due to APA escapes tumor suppressive regulations by limiting regulatory sites for factors such as miRNA. Furthermore, the length of the 3′-UTR has been reported to regulate protein expression and mRNA localizations. For instance, brain and bone marrow have long 3′-UTR transcripts, while others such as testis and blood have the opposite. In contrast to the long 3′-UTR, the short 3′-UTR mRNA tend to be highly translated. Recently, the APA-mediated short 3′-UTR was found to be regulated by DNA methylation that interferes with elongating Pol II leading to the choice of proximal PAS. Similarly, cellular stress conditions have been linked to APA. Stress leads to widespread shortening of transcripts. An example of APA with a functional significance is the ER co-chaperon $p58^{IPK}$. The $p58^{IPK}$ has two isoforms different in size and stability during differentiation of syncytiotrophoblast, a secretory cell producing hormones critical during pregnancy (Cheng et al., 2020; Di Giammartino et al., 2011; Nanavaty et al., 2020).

mRNA export

The nuclear envelope ensures the separation between transcription and translation processes. After mRNA processing, only export-competent, mature Messenger Ribonucleoproteins (mRNPs) are translocated to the cytoplasm via the macromolecular assembly forming nuclear pores. Nuclear pores penetrate the nuclear envelope and selectively facilitate the movement of large molecules, more than 40 kDa, between nuclear and cytoplasmic compartments in an energy-

dependent manner. Defects in mRNA processing or nuclear export may lead to the development of diseases (M. Stewart, 2019).

The Nuclear Pore Complex (NPC) is conserved and consists of several copies of thirty different proteins. The cylindrical skeleton of NPC is made by the structured domains of Nucleoporins (NUP), while their unfolded regions protrude to the central channel to ensure selectivity of macromolecular transport. These unfolded regions are rich in hydrophobic residues such as phenylalanine and Glycine (Gly) and referred to as FG-NUPs. FG-NUPs mediate a transport barrier that can be overcome by factors bound to large molecules, known as carriers. Interactions of carriers with FG-NUPs allow passive movements through the NPC channel. However, energy is required to drive the movement directionality. In addition to the attached cargos, carriers are bound by the RAS-Related Nuclear Proteins (Ran) to mediate transport of cargos. Generally, carriers import molecules to the nucleus are known as importin, while those export molecules to the cytoplasm are referred as exportin. For example, karyopherin β–family carriers, such as importin-β, attach to cytoplasmic proteins as cargos for the nuclear delivery and associate with Ran-GTP to release the cargo into the nucleus. Upon return to the cytoplasm, the carrier-Ran-GTP is dissociated by GTP hydrolysis mediated by Ran-GAP proteins, resulting in Ran-GDP. The Ran-GDP is associated with Nuclear Transport Factor 2 (NTF2) as a carrier to be delivered back to the nucleus where is recycled into RNA-GTP by the regulator of chromosome condensation 1, which acts as a Ran GEF protein. Similarly, the transport of nuclear cargos, such as proteins and small RNAs, to the cytoplasm

requires β-karyopherins, such as Chromosomal Maintenance 1 (CRM1), known as exportin 1. The carrier-cargo complex is bound to RNA-GTP that is hydrolyzed upon the cytoplasmic delivery of cargo. The remaining complex is recycled back to the nucleus where it is recharged with GTP to start a new cycle (M. Stewart, 2019).

The nuclear export of mRNA is conserved in eukaryotes despite some small RNAs such as viral RNA uses a member of karyopherin β–family such as CRM1. In mRNA nuclear export, the carriers are not karyopherin β members and ATP is the source of energy that is hydrolyzed by DEAD-box helicases. The mammalian complex of Nuclear RNA Export Factor 1 (NXF1): Nuclear Transport Factor 2 Like Export Factor 1 (NXT1), also referred as transporter associated with antigen processing: p15 protein, binds nonspecifically to mRNA in a combination with other factors and acts as a general export factor of mRNPs through the NPC channel. In the nucleus, the NXF1:NXT1 complex is bound to mRNA via proteins such as DDX39b, also known as UAP56. In contrast, DDX19 facilitates the disassembly of complexes when they reach the cytoplasmic face of the NPC. Additional proteins involved in both processes of mRNA transport include Transcription/Export (TREX) complex subunits, including Aly/REF Export Factor (ALYREF), in the nucleus and GLE1 RNA Export Mediator (GLE1) and NUP42 in the cytoplasm. Interestingly, mRNA export through NPC channels is rapid compared to the duration of assembly, possibly by Translocated Promoter Region (TRP) proteins, or disassembly of transported mRNPs and that may serve as a quality checkpoint (M. Stewart, 2019).

The NTD of NXF1 contains a RNA-Binding Domain (RBD) followed by a leucine-rich repeat domain, NTF2-like domain, that binds polyadenylated mRNA and FG-NUPs, respectively, while the ubiquitin-associated CTD together with the heterodimeric NTF2 binds to FG-NUPs (M. Stewart, 2019; Viphakone et al., 2012). The activity of a cytoplasmic helicase enhanced by GLE1 and NUP42 removes mRNP-associated factors such as the yeast Nab2, involved in coordination of mRNA processing steps and regulating the length of poly(A) tails. To recycle the NXF1:NXT1 complex for another export, DDX19 and GLE1 dissociate the complex from mammalian transcripts. Upon completion of mRNA maturation in the nucleus, transcripts are linked to the NXF1:NXT1 complex via ALYREF, acts as an RNA adaptor, that has been proposed to be removed from the complex before export by other TREX subunits especially DDX39b. Other proteins rich in Ser and arginine such as nucleolar protein 3 have been reported to function as RNA adaptors in yeast (M. Stewart, 2019).

The TREX complex is a conserved multi-subunit complex involved in coordination between nuclear steps of mRNA maturation and mRNA export. It consists of THO complex (THOC), the helicase DDX39B (Sub2, the yeast homolog), and an RNA export adapter such as ALYREF. The THOC contains six subunits, THOC1-3 and THOC5-7 (Puhringer et al., 2020). The mammalian TREX is primarily involved in the nuclear splicing by binding to Exon-Junction Complex (EJC) encompassing 20 nt upstream the 5′-ligated exons. Toward later stages of mRNA processing, the TREX complex contributes to the formation of export-competent mRNPs. However, there are some exceptions such as viral mRNAs

that encode Constitutive Transport Element (CTE) that enables unspliced mRNA to bypass the default pathway of formation export-competent mRNPs. In addition, CTE mRNA have higher affinity for binding to the NXF1:NXT1 complex in the absence of RNA adaptors such as ALYREF. Little is known how the TREX complex integrates signals to selectively export a fully processed mRNA. The current view of mRNA export is mediated by ATP-dependent helicases that remodel mRNA structure that becomes accessible for direct binding by the NXF1:NXT1 complex or through RNA adaptors such as ALYREF (M. Stewart, 2019).

Finally, the TRP and TREX-2 complex subunits involve in mRNA export, where their loss mimics the observed phenotypes upon loss of major mRNA export factors such as NXF1 (Aksenova et al., 2020). The TREX-2 members include the core Germinal Center-Associated Nuclear Protein (GANP), serving as scaffolding protein for other subunits within the complex and have been proposed to function as chaperones to condense mRNPs for export (M. Stewart, 2019). Also, GANP has been reported to interact with FG-NUPs and facilitate mRNA transport in response to environmental changes (Aksenova et al., 2020).

OVERVIEW OF TRANSLATIONAL CONTROL

Upon mRNA maturation and nuclear export, cytoplasmic mRNAs are recruited to ribosomes to produce proteins and subsequently maintain gene expression. mRNA translation has been well studied and is mediated by the canonical cap-dependent translation mechanism. However, alternative translation mechanisms have evolved for when the cap-dependent translation is suppressed

under cellular challenging environments. In general, mRNA translation is a stepwise process that involves sequential stages including translation initiation, elongation, termination, and recycling (Kwan & Thompson, 2019). In a simple version of a translation cycle, eukaryotic translation initiation begins by the assembly of TC. After the TC associates with the small ribosomal subunit, 40S, in combination with other translation factors, 43S PIC is formed and associated with the 5′-capped mRNA. The 43S complex begins scanning the 5′-UTR in search for the start codon, typically AUG, Recognition of the initiation codon leads to GTP hydrolysis in the active TC allowing joining the larger subunit of ribosome, 60S, to form a component ribosome, 80S (Figure 1.3) (Costa-Mattioli & Walter, 2020). Consequently, translation elongation starts by a processive 80S ribosome that decodes mRNA sequence in three-nucleotide fashion synthesizing a polypeptide. Next, translation termination happens when the translating ribosome encounters a termination codon followed by the release of elongated polypeptide from the ribosome. Finally, the ribosomal subunits are dissociated from mRNA to be recycled (Sonneveld, Verhagen, & Tanenbaum, 2020).

Translation initiation

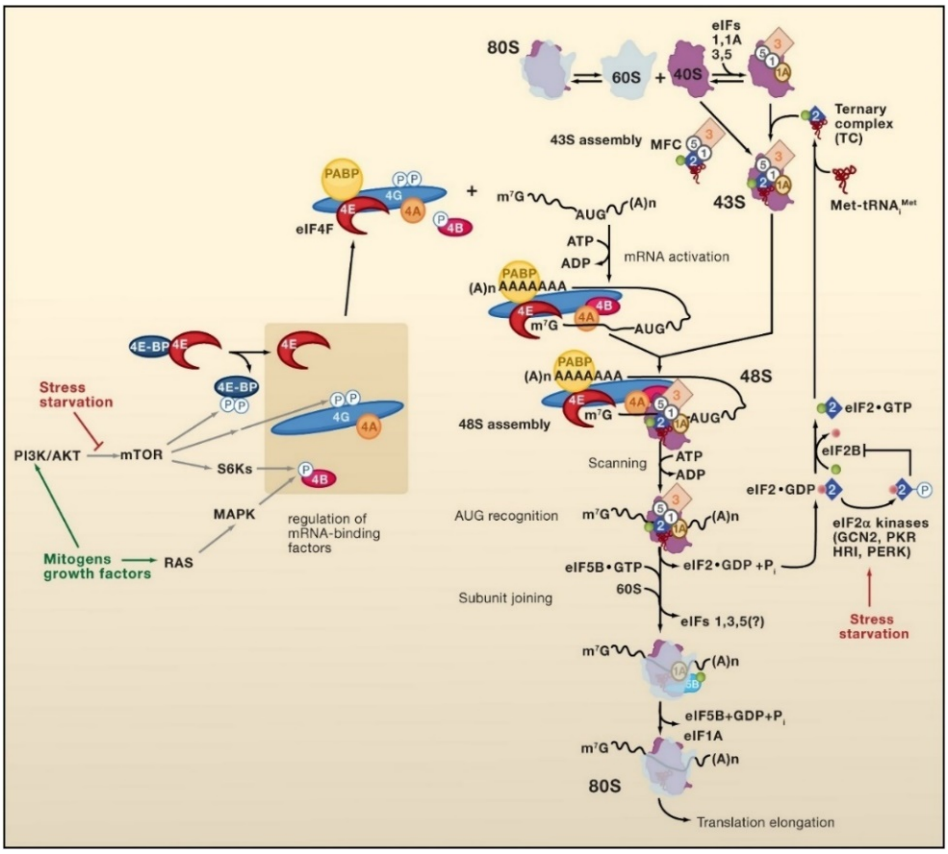

Figure 1. 3. Overview of mRNA translation initiation.
Translation factors, eIF1, eIF1A, and eIF3 promotes the assembly of 43S PIC along with eIF5 and the active ternary complex (eIF2-GTP-tRNAi). The cap-binding complex eIF4F (eIF4E-eIF4G-eIF4A) binds to 5′-mRNA for mRNA activation, while PABPC binds to poly(A) tail. mRNA circulation is proposed by interaction between the cap-binding complex and PABP. The PIC scans for AUG codon in ATP-dependent manner. Upon recognition, eIF2-GTP is hydrolyzed followed by the release of some translation factors from the complex. The 60S subunit joining is facilitated by the hydrolysis of eukaryotic Translation Initiation Factor 5 B (eIF5B)-GTP and the release of eIF5B-GDP together with eIF1A forms the 80S initiation complex to begin the elongation step. Following stress conditions, eIF2α phosphorylation, eIF4E sequestration by eIF4E-Binding Protein (4E-BP) reduce the ternary complex. 4E-BP phosphorylation by mTOR allows the assembly of eIF4F. Also, mTOR or its downstream effectors, the 70-kDa Ribosomal Protein S6 Kinase (S6K), regulate the phosphorylation of eIF4G and eIF4B. These phosphorylation events are also induced by mitogens and growth factor stimulation that activates mTOR via Phosphoinositide 3-Kinase (PI3K)-Akt pathway or RAS/mitogen-activated protein kinase signaling. Reprinted with permission from Elsevier, the publisher of (Sonenberg & Hinnebusch, 2009).

The translation initiation process involves the assembly of TC, mRNA recruitment to the assembled 43S PIC, and ribosomal scanning of 5′-capped mRNA followed by recognition of a start codon. First, the TC is assembled. GTP binds eIF2 and the eIF2-GTP complex is associated with an $tRNAi^{Met}$ to form the active TC (Costa-Mattioli & Walter, 2020). tRNAi is conserved across species and unique from other elongator tRNAs. $tRNAi^{Met}$ exhibits a greater binding affinity toward eIF2-GTP complex than eIF2-GDP complex. The increased affinity is due to the direct sensing of L-Methionine (Met) by eIF2-GTP in part, and the stimulatory role of conserved nucleotides in the tRNAi acceptor stem, A1:U72 bp (Hinnebusch & Lorsch, 2012). In addition to the base pairs within the acceptor stem, tRNAi contains unique nucleotides compared to elongator tRNAs in the anticodon stem, G31:C39 bp, and the T-loop such A54 and A60 (Kolitz & Lorsch, 2010). The second component of the TC is the eIF2 that is composed of α, β, and γ subunits. eIF2α has been shown to interact with the acceptor stem of $tRNAi^{Met}$, while eIF2β has been proposed to mediate connection between translation factors such as eIF1 and eIF1A and $tRNAi^{Met}$ on a 40S ribosomal subunit. On the other hand, the subunit of eIF2γ provides a platform to which other eIF2 subunits bind. eIF2γ associates with $tRNAi^{Met}$ in a GTP-dependent manner. eIF2γ contains a GTP-Binding Domain (G domain) that binds GTP, constituting the third component of the TC, and allows interactions with translational GAPs and GEFs such as eIF5 and eIF2B, respectively. The stable TC-eIF5 complex has been suggested to be recruited upon binding of ribosomal 40S subunit to eIF1, eIF1A, and eIF3 or bound by eIF1 and eIF3 before recruitment to ribosomal 40S subunit (Alone & Dever,

2006; Jennings, Kershaw, Adomavicius, & Pavitt, 2017; Kershaw et al., 2021; Merrick & Pavitt, 2018).

Following the assembly of the 43S PIC, mRNA is recruited via several translation factors such as eukaryotic Translation Initiation Factor 4 A (eIF4A), 4 B (eIF4B), eIF4E, and eIF4G, collectively known as the eIF4F complex, that recognizes capped mRNA at the 5′-ends. eIF4E is a cap-binding protein and is regulated by the inhibitory eIF4E-Binding Proteins (4E-BP) that sequester eIF4E from eIF4G binding. In addition, eIF4G acts as a scaffolding protein linking 5′- and 3′-ends of an mRNA by additional interactions with other factors and mRNA elements such as poly(A) tails (Koromilas, 2019; Merrick & Pavitt, 2018). These eIF4G interactions have been thought to create a closed loop-like structure proposed to enhance mRNA translation and mediated by eIF3 (Wolf, Lin, Duan, & Cheng, 2020). Furthermore, eIF4A is an RNA helicase that belongs to the DDX family. eIF4A unwinds RNA duplexes and linearizes mRNA secondary structures in an ATP-dependent manner. The relative weak activity of eIF4A helicase has been shown to be stimulated in the presence of mRNA and eIF4B. The mammalian eIF4B is an RNA-binding protein due to the RBD domain that is absent in yeasts. The eIF4A cofactor, eIF4B, has a stimulatory effect on translation especially for mRNA with long or extensively structured 5′-UTRs. eIF4B has been thought to mediate mRNA recruitment to the 43S PIC via interactions with eIF3. The mammalian eIF3 complex is large and includes thirteen subunits that interreact with mRNA and other translation factors such as eIF4F, believed to mediate mRNA recruitment. Therefore, eIF3 is not only essential for the 43S PIC assembly, but

also plays a major role in mRNA recruitment (Merrick & Pavitt, 2018; Sen, Zhou, Harris, Ingolia, & Hinnebusch, 2016; Wolf et al., 2020).

Pioneering studies of Kozak indicate the requirement of ATP hydrolysis, mediated by eIF4F, to fuel the 43S PIC in search for the start codon. As the 43S PIC scans the 5′-UTR of an attached mRNA, the 48S PIC is formed when the first start codon is selected within a preferred sequence context called the Kozak consensus sequence. The optimal Kozak sequence, CRCCAUGG, involves an AUG codon surrounded by specific nucleotides including a purine nucleotide (A or G), designated by “R”, 3 nt upstream of the AUG and the G nucleotide just after AUG (Acevedo, Hoermann, Schlimbach, & Teleman, 2018; Merrick & Pavitt, 2018). The AUG codon has been proposed to be impeded by eIF1 that occupies the region around the Ribosomal Peptidyl tRNA-Site (P-Site). Upon eIF1 relocation and recognition of the AUG codon by $tRNAi^{Met}$, the scanning PIC adapts a closed conformation mediated by changes in the PIC associated factors leading to the release of eIF1, eIF2-GDP, and eIF5. For example, eIF1A stabilizes the codon-anticodon interactions and contacts the NTD of eIF5 that catalyzes the hydrolysis of GTP, associated with the TC. Because the low affinity of eIF2-GDP for $tRNAi^{Met}$, eIF5 and eIF2 have been proposed to be eliminated together from the 48S PIC (Merrick & Pavitt, 2018).

Binding of small and large subunits to each other requires the eukaryotic Translation Initiation Factor 5 B (eIF5B)-mediated GTP hydrolysis. Recent 48S structures have inferred that the release of factors, including eIF2, is a prerequisite for eIF5B-GTP binding. Upon the ribosomal subunit joining, eIFB5-GTP interacts

with the ribosomal 40S subunit forcing the $tRNAi^{Met}$ to acquire the P/I configuration. Regaining the $tRNAi^{Met}$ position at the P-Site requires GTP hydrolysis, followed by the release of eIF5B-GDP and eIF4A from the 80S ribosome. Interestingly, the 80S ribosome is partially or completely excluded from eIF3 indicative of uncharacterized mechanisms of eIF3 release (Merrick & Pavitt, 2018).

Translation initiation regulation by stress signaling

Two pathways, ISR and mTOR, regulate the process of translation initiation. Upon cellular exposure to stresses, these pathways are extensively communicated to determine the cell fate in specific contexts (Koromilas, 2019; G. Y. Liu & Sabatini, 2020). First, ISR activation induces eIF2α-P that decreases the GEF activity of eIF2B. eIF2B consists of two copies of five, α-ε, subunits in which α, β, and δ subunits sense eIF2α-P and γ and ε subunits activate eIF2. Recently, eIF2B has been found to compete with $tRNAi^{Met}$ for eIF2-GTP binding leading to TC destabilization unless the TC is bound by eIF5. Therefore, eIF5 functions as a GAP representing the other TC regulator. In addition, the TC-eIF5 complex is dissociated upon eIF2α-P and consequently, the TC becomes unstable by eIF2B (Costa-Mattioli & Walter, 2020; Jennings et al., 2017; Kershaw et al., 2021; Merrick & Pavitt, 2018).

On the other hand, the mTOR pathway, a member of the Phosphoinositide 3-Kinase (PI3K)-related family, regulates 4E-BP that competes with eIF4G for eIF4E binding. The 4E-BP is negatively regulated by mTOR phosphorylation to permit the eIF4E binding to the m^7G cap and thus, promote cap-dependent translation (Koromilas, 2019; G. Y. Liu & Sabatini, 2020). Upon cellular stress,

eIF2α-P has been suggested to decrease the mTOR activity. In addition, ATF4-upregulated 4E-BP1 expression antagonizes cap-dependent translation promoted by activated mTOR Complex 1 (mTORC1). In acute ER stress, ATF4 upregulates amino acid transporter genes to maintain mTORC1 activation. However, mTORC1 activity is lowered under chronic ER stress and mRNA translation switches to an eIF3-dependent mechanism to avoid ER dysfunction (Koromilas, 2019).

Alternative mechanisms of translation to cope with cellular stress

As a consequent of limited availability of the active TC by eIF2α-P, alternative translation mechanisms have been suggested for a subset of mRNAs. For example, leaky scanning has been documented when the first AUG codon is skipped due to the absence of an optimal Kozak AUG context. Leaky scanning has been used to regulate mRNA expression as shown by bypassing the initiation at inhibitory Upstream Open Reading Frames (uORF) in some transcripts during stress conditions (Merrick & Pavitt, 2018; Wek, 2018). In addition to leaky scanning, many other alternative translation mechanisms have been described including internal ribosomal entry site, ribosomal shuttling, and translation initiation of short 5′-UTRs (Kwan & Thompson, 2019; Merrick & Pavitt, 2018). These mechanisms may explain how other initiation codons, such as CUG or ACG, have been reported in reading frames of cellular and viral mRNAs (Starck & Shastri, 2016).

In stress conditions, the well-studied mechanism of alternative translation was the uORF. uORFs are defined as sequences encoding minimally 3 codons, in

which the last is the termination codon, and located upstream or partially overlapped with the main CDS of a gene. There are many factors influencing the roles of uORFs in translation such as uORF numbers, their length, sequence context, and distance to the CDS and start codon. Although uORF-regulated translation is documented under ISR activation, some stress specific mRNAs are devoid of uORFs (H. H. Chen & Tarn, 2019; Guan et al., 2017; Wek, 2018).

The uORF-mediated translation was first noticed in yeast encoding GCN4, a stress transcriptional factor, followed by the metazoan ATF4, an ortholog of GCN4. These mRNA have been characterized to involve uORFs in their translation mechanisms. Both *ATF4* and *GCN4* mRNA encode inhibitory uORFs that has been suggested to inhibit downstream translation of their CDS in physiological conditions of high levels of the active TC. When the TC is scarce due to activated ISR, some ribosomes have been hypothesized to scan through the inhibitory uORFs due to their delayed acquisition of the TC, and instead they initiate at the main CDS of *ATF4* and *GCN4* mRNAs. This uORF-mediated translation has been expanded to other mRNAs involved in ISR. These mRNAs include *ATF5*, *CHOP*, *GADD34*, glutamyl-prolyl tRNA synthetase, and oligophrenin 1. The stress-induced transcripts containing uORFs are preferentially translated during ISR. Now, emerging questions have been addressed toward the selectivity of these uORF-mediated translation mechanisms because of the prevalence of uORFs in the human genome. In addition, regulatory features of stress mRNAs such as secondary structures and cis-regulating elements are less explored (H. H. Chen & Tarn, 2019; Costa-Mattioli & Walter, 2020).

Translation elongation

The translation elongation mechanism is conserved and well-studied in prokaryotic cells consuming up to 50% of cellular energy. Compared to translation initiation, translation elongation requires fewer canonical elongation translation factors such as the eukaryotic Translation Elongation Factor 1 A, (eEF1A) and 2 (eEF2), which act as GAP proteins (Dever, Dinman, & Green, 2018; Hu, Dourado, Schubert, & Lercher, 2020). Additional eukaryotic factors have been reported to affect the rate of translation elongation including the eukaryotic Translation Initiation Factor 5 A (eIF5A) and eukaryotic Translation Elongation Factor 1 B (eEF1B) (Xu, Liu, & Song, 2021). Generally, the translating ribosomes have binding sites for tRNAs referred as an A-Site, P-Site, and the Ribosomal Deacylated tRNA Exit-Site (E-Site). In the cycle of translation elongation, charged tRNA is delivered to the ribosomal A-Site and interreacts with mRNA codon. Upon correct base pairing between mRNA and the amino-acylated tRNA, a peptide link is formed by the Peptidyl Transferase Center (PTC) of ribosome. As a result, tRNA is deacylated and translocated as the ribosome moves to release uncharged tRNA for another round of translation elongation (Sonneveld et al., 2020).

Following translation initiation, the 80S ribosome is formed and secured $tRNAi^{Met}$ base paring with the start codon in the P-Site. The conserved and essential eIF5A has been originally found as an initiation factor important for the first peptide bond formation as shown by early studies of Met-Puromycin (Puro) dipeptide. Since Puro is a weak substrate due to its misplacement in the PTC, eIF5A-mediated Puro addition into a nascent peptide uncovers its stimulatory role

in translation elongation especially for poor substrates. However, *in vitro* studies showed the efficient synthesis of different dipeptides even in the absence of eIF5A minimizing its importance. In contrast, *in vivo* depletion of eIF5A results in impaired translation initiation, elongation, and termination. In addition, the modification of a conserved Lys, hypusine, in eIF5A is critical for stalled ribosomes by stretches of Pro, a poor substrate. Although eIF5A was discovered over 40 years ago, the broader role of its function is still under investigation (Dever et al., 2018; Schuller, Wu, Dever, Buskirk, & Green, 2017; Xu et al., 2021).

Once the $tRNAi^{Met}$ binds the P-Site, the next mRNA codon occupies an empty A-Site. eEF1A binds GTP and the charged tRNA to form a trimeric complex that supplies the ribosomal A-Site. In humans, there are two homologs of eEF1A, the ubiquitously expressed eEF1A1, and eEF1A2 expressed in specific tissues such as skeletal muscle, cardiomyocytes and neurons during adult-life. Upon delivery of charged tRNA, tRNA binding to the A-Site is stabilized by hydrogen bonds mediated by the conserved bases, including A1824 and A1825, of the 18S rRNA Helix (H44) that interact with the minor groove of codon-anticodon helix. When these bases are flipped out of H44, it stabilizes Watson-Crick base-pairing in the first two positions of the codon, while the third position is left for wobble interactions because the genetic code is degenerate. In addition to its interaction with codon-anticodon helix, G626 in rabbit ribosomes has been suggested to lock the helix in the decoding center of ribosome. After mRNA decoding, the stimulatory interaction of the Sarcin-Ricin Loop (SRL) of 28S rRNA with the GTPase domain of eEF1A triggers GTP hydrolysis of charged tRNA-eEF1A-GTP complex leading

to binding of the amino-acylated tRNA in the A-Site and subsequent release eEF21A-GDP. To recharge eEF1A with GTP, eEF1B functions as a GEF protein to maintain subsequent rounds of tRNA delivery and translation elongation. As a consequent step in translation elongation, the PTC contains conserved rRNA elements in the large ribosomal subunit that rapidly catalyzes peptide bond formation by favorably positioning amino-acylated and peptidyl tRNAs for catalysis. In addition, the binding of eIF5A to the E-Site interreacts with the acceptor stem of peptidyl tRNAs to establish a stimulatory peptidyl transfer. The formation of peptide linkage is initiated by the nucleophilic attack of the α-amino group of the accommodated charged tRNA in the A-Site on the carbonyl group of peptidyl tRNA in the P-Site. Consequently, tRNAs are displaced among the ribosome sites in three states due to tRNA binding and subunit rotation as indicated by Cryogenic Electron Microscopy (Cryo-EM) images. In unrotated complexes, tRNA becomes deacylated in the P-Site, the transferred peptidyl-tRNA in the A-Site becomes longer due to the formed peptide bond. In the second state known as “rotated 1-complexes”, the deacylated tRNA harbors a P/E hybrid state where anticodon stem interacts with the P-Site, while the acceptor arm present in the E-Site. Meanwhile, the extended peptidyl-tRNA is still secured in the A-Site. In the third state “rotated 2-complexes”, the peptidyl-tRNA is changed to the A/P hybrid state where anticodon stem interacts with the A-Site, while the acceptor arm present in the P-Site. During the third state, no change is observed in the P/E hybrid state of the deacylated tRNA (Dever et al., 2018; Xu et al., 2021).

Following peptidyl transfer and peptide bond formation, eEF2 mediated GTP hydrolysis triggers deacylated and peptidyl-tRNA translocations to the E-Site and the P-Site, respectively. eEF2 has been shown to occupy the A-Site in structural studies of bacterial translation system. The location of eEF2 binding is proposed to disrupt the interaction of ribosomal decoding nucleotides in the H44 with the codon-anticodon helix allowing the tRNA translocation and release of eEF2-GDP the post-translocated ribosomes. After translocation, the release of deacylated tRNAs from the E-Site was proposed to be coupled with recruitment of charged tRNA in complex with eEF1A-GTP in eukaryotic and bacterial systems. However, this coupling was not strict in bacterial systems, while a single study concluded that a slow release of the deacylated tRNA from the E-Site in human ribosome was independent of charged tRNA binding in the A-Site. Therefore, further studies will highlight important factors controlling the release of deacylated tRNA from the E-Site (Dever et al., 2018; Xu et al., 2021).

eEF2 has a unique modification in eukaryotes and archaea where a Histidine (His) residue is converted to diphthamide. This modification is a substrate for ADP-ribosylation by bacterial toxins such as diphtheria, exotoxin A or cholera toxins that inactivate the eEF2 translocase function, and therefore block global protein synthesis leading to cell death (Susorov et al., 2018). Interestingly, mice lacking this eEF2 modification suffer from developmental defects and die before birth. In addition, eEF2 is downregulated by the eEF2 Kinase (eEF2K). the eEF2K phosphorylates eEF2 on Thr-56 and inhibits translation elongation due to impaired ribosomal binding. In contrast, mTORC1 stimulation inactivates eEF2K by ser-366

phosphorylation mediated by mTORC1 downstream kinase, S6K. In cancer, hyperactivation of mTORC1 and dysregulated kinases have been reported to target eEF2K for inhibitory phosphorylation. Other regulations of eEF2K include eEF2K phosphorylation by the adenosine monophosphate-activated protein kinase in response to low levels of available ATP as a source of energy (R. Liu & Proud, 2016).

Finally, co-translational folding has been shown to promote translation elongation by ribosome associated chaperones such as HSP70s and co-chaperones such as the conserved heteromeric HSP40-HSP70. Chaperones directly bind to nascent peptides as they emerge from the ribosomal peptide tunnel. These chaperones have been reported to bind nascent peptides of around 50 residues in length as shown by crosslinking data *in vivo*. Interestingly, a global translation elongation pause has been reported in misfolding conditions where the nascent peptides reach 65 aa. This highlights the importance of chaperones in translation elongation (Y. Chen, Tsai, Li, & Gao, 2022; Shalgi et al., 2013).

Translation Termination

Translation termination is the last step in the translation cycle. In the translation termination step, two translation factors known as eukaryotic Release Factor 1 (eRF1) and eukaryotic Release Factor 3 (eRF3) are required. These factors play a major role in terminating mRNA translation. Translation termination occurs when the elongating ribosomes find a stop codon in the A-Site. After translation termination, ribosomes are dissociated from mRNA by the conserved

and essential ATP-Binding Cassette Subfamily E Member 1 (ABCE1) for ribosomal recycling (Hellen, 2018; Nurenberg-Goloub et al., 2020).

The release factors, eRF1 and eRF3, combine with GTP to form a trimeric complex. The NTD of eRF1 decodes mRNA sequence in the A-Site containing stop codons, while the middle domain of eRF1 has a conserved an apical Gly-Gly-Glutamine (Gln) motif involved in release of nascent peptides at the P-Site. The CTD of eRF1 influences stop codon specificity and interreacts with ABCE1 and eRF3. The binding of eRF1 to eRF3 stabilizes eRF3-GTP binding. In contrast to eRF1, eRF3 is encoded by two genes producing eRF3a and eRF3b. eRF3a is ubiquitously expressed, while eRF3b is prevalent in brain tissues. The eRF3 is composed of the NTD that is not involved in translation termination. In addition to its binding to eRF1, eRF3 interreacts with PABPC and the UPF3b, a non-sense mediated decay regulator. In addition, eRF3 has a canonical G domain, two β-barrel domains, homologous to translational GAP proteins, and CTD containing Hbs1, a translational GTPase known as a ribosomal rescue factor (Hellen, 2018). In all GAP proteins, G domains are conserved and act as molecular switch transitioning between the active bound complex containing GTP and the inactive bound complex containing GDP. The G domains are composed of five motifs. G1-G5. G1 motif, known as P-loop, stabilizes α and β phosphates of GTP, while G2 and G3 motifs known as switch I and switch II, respectively, interact with the γ-phosphate. These interactions are mediated by conserved residues of G1-Ser and G3-Thr residues that coordinate the binding of β and γ phosphates of GTP and

Mg^{2+}, an essential cofactor to maintain binding with GTP and GDP. Consequently, GTP binding by G2 and G3 motifs induces conformational changes of the complex leading to the exposure of catalytic residues Ser or His of G3 motif that coordinate the water molecule to mediate GTP hydrolysis. Meanwhile, G4 and G5 motifs contact the guanine base and are important for GTP binding and specificity (Maracci & Rodnina, 2016).

The activation of eRF3 GTPase is mechanistically different from the elongation translation, eEF1A, that achieves its activation by a domain closure in the 40S ribosomal subunit due to binding of charged tRNA to the A-Site codon. In translation termination, GTP hydrolysis mediated by eRF3 is activated by the middle and CTD of eRF1 and depends on the ribosome. In addition, recognition of stop codons by eRF1 has been suggested to enhance eRF3-mediated GTP hydrolysis (Hellen, 2018).

The canonical stop codons include UAA, UAG and UGA. However, some of these codons are reassigned as sense versus stop codons in some organisms such as ciliate protists, green algae, and diplomonads. In some cases of ciliate protists, all three codons are sense codons and reassigned as stop codon if it is near to the 3′-ends of mRNA. The reassignment of stop codon depends on eRF1 based on its mutational analysis and Cryo-EM studies that have shed light into conserved motifs in the NTD of eRF1. In addition to the position of stop codon within mRNA, the surrounding sequence has been shown to enhance the termination efficiency. For example, stop codons enhancing translation termination

has been reported if a purine is in the 4+ position. If the 4+ position contains a pyrimidine, the purine at the 5+ position has been reported to efficiently terminate translation (Hellen, 2018).

In termination complexes, the SRL of the large ribosomal subunit has been identified as a requirement for the activation of eRF3. Since the mechanism of 40S domain closure is absent in eRF3 activation, the middle domain of eRF1 attached to the eRF3-switch I and II is dissociated and removed allowing GTP hydrolysis. The middle domain of eRF1 dissociation has been proposed as a consequence of its interactions with helix 14 of 18S rRNA and helix 5 of 18S rRNA with eRF3. Together, these interactions emphasize the role of eRF1 in regulating eRF3 GTPase activity (Hellen, 2018). Following GTP hydrolysis, eRF3-GDP remains associated with ribosome for a long time and eRF1 undergoes conformational changes. For example, the connection of eRF1 CTD with 40S ribosome is disrupted, while new interactions with ribosome have been established such as interactions of ribosomal protein UL11 that impair termination upon yeast UL11 deletions. In addition, the eRF1-Gly-Gly-Gln motif accommodates the ribosomal PTC in an extended conformation inhibited by eRF3-GTP binding. The eRF1-Gly-Gly-Gln motif interacts with the CCA end of the peptidyl-tRNA in the P-Site where the conserved Gln residue of eRF1 coordinates the attack of catalytic water to the ester bond linking the nascent peptide with the peptidyl-tRNA resulting in the release of a newly synthesized peptide. Furthermore, eRF1 has been shown to induce peptide release in an eRF3-indepedent mechanism. However, eRF3-eRF1 interaction has been documented to accelerate the peptide release. After the

release of the nascent peptide, ABCE1 binds the ribosomal inter-subunit and uses cycles of ATP hydrolysis to dissociate vacant 80S and stalled ribosomes after they are recognized by ribosomal rescue factors such as Hbs1. Recycling of ribosomal subunit depends on the binding of eRF1 to the A-Site. Therefore, eRF1 is not only responsible for translation termination, but also for ribosomal recycling. After the ribosomal 60S subunit is dissociated, tRNA and mRNA are still associated with the ribosomal 40S subunit. To release uncharged tRNA and mRNA, eIF1, eIF1A, and eIF3 have been reported to facilitate their release from the ribosomal subunit. Since eIF1 and eIF1A bind close to the P-Site, eIF1 recognizes non-initiator tRNAs and destabilizes its binding in the P-Site with the other translation factors. Once tRNA is released from the P-Site, mRNA is consequently released from the ribosomal subunit. Additional factors have been reported to induce mRNA/tRNA release after the dissociation of ribosomal subunits. For example, eIF2D, previously known as ligatin, and the Density Regulated Re-Initiation and Release Factor (DENR) interfere with the codon-anticodon interaction leading to the release of deacylated tRNAs and subsequently mRNA (Hellen, 2018).

mRNA SURVEILLANCE MECHANISMS

Nonsense-Mediated mRNA Decay (NMD)

It is a conserved mRNA quality control that recognizes NMD-activation features such as Premature-Stop Codons (PSC) during mRNA translation and dictates the degradation of aberrant mRNAs. Originally, NMD was discovered in the human blood disorder of β-thalassemia. Several studies have linked NMD to cellular responses, induced by physiological and external stimuli, driving changes

in gene expression. However, NMD has been believed to be repressed in ER stress to stabilize the stress-specific mRNAs, especially those containing uORFs because they are potential targets of NMD. The NMD regulators include UPF1, UPF2, and UPF3 that together coordinate the degradation of NMD substrates via different reported mechanisms such as deadenylation or deadenylation-independent decapping. Interestingly, UPF1 is an essential factor in the NMD pathway. In NMD pathway, UPF1 is an ATP-dependent helicase and interacts with mRNA containing a PSC that recruits the translation termination complex. The UPF1 activity is enhanced by interactions with UPF2 and UPF3. The mammalian isoforms of UPF3, UPF3a and UPF3b, have differential contributions to NMD determined by the high affinity of UPF3 for UPF2 binding. Previously, UPF1 was thought to be recruited for damaged mRNA. However, UPF1 has been found to promiscuously bind mRNA through the termination complex regardless of their PSC content. Therefore, two updated models have been proposed to select NMD targets including 3′-UTR EJC-dependent NMD and 3′-UTR EJC-independent NMD, known as long 3′-UTR-mediated NMD. In addition to the EJC complex involved in splicing, it associates with NMD components such as UPF3 and is removed by translating ribosomes. Once the first round of translation terminates and ribosomes are dissociated, these proteins are still associated with 3′-UTR of translated mRNA. If PSC is more than 50-55 nt upstream of the bound EJC, UPF3 binds with UPF2 to recruit UPF1 and other proteins such as the NMD-Associated Factors (SMGs). For example, NMD-associated PI3K related kinase, known as SMG1, phosphorylates UPF1 to activate the NMD pathway. The phosphorylated

UPF1 recruit components of endonucleases such as SMG5 and deadenylases such as Carbon Catabolite Repression 4 (CCR4)-Negative on TATA (NOT), known as CCR4-NOT complex, via interactions with SMG7, and thus create substrates for 5′ to 3′ or 3′ to 5′ exonucleolytic degradations. After mRNA degradation, UPF1 dephosphorylation is mediated by the protein phosphatase 2A recruited by the SMG5−SMG7 bound to UPF1. On the other hand, long 3′-UTR-mediated NMD lacks EJC and is less understood mechanistically. The long 3′-UTR-mediated NMD commonly targets mRNA that do not have PSC and instead have very long 3′-UTR estimated to be more than 1 kilobase (Heck & Wilusz, 2018; Kurosaki, Popp, & Maquat, 2019).

No-Go mRNA Decay (NGD)

The NGD is a translational quality control that releases stalled ribosomes from aberrant mRNAs. For example, ribosomal stalling due to improper translation termination has been reported to be released through the action of Ski proteins, specifically Ski7, that recruits the Exosome (EXO) to degrade the mRNA. Although the faulty transcripts are destined for degradation by NGD machinery, the RNase responsible for the mRNA cleavage remains elusive. The NGD machinery includes ribosomal rescue factors, Hbs1 and its binding partner Dom34, components of the EXO-Ski complex, and ABCE1 to dissociate ribosomal subunits. Additional factors like strong hairpins or other RNA structures, defective ribosomes, and stretches of positively charged amino acid can impede translating ribosomes (Heck & Wilusz, 2018; Parker, 2012).

Non-Stop mRNA Decay (NSD)

Premature transcriptional termination and polyadenylation results in transcripts with accumulated ribosomes at the 3′-UTR that trigger NSD. Similar to NGD, the importance of this surveillance mechanism ensures ribosome recycling among transcripts instead of being trapped on faulty mRNAs. The accumulation of ribosomes because they decode the poly(A) tracts into positively charged Lys residues that have been found to strongly interact with negatively charged resides in the ribosomal peptide tunnel channel leading to ribosomal stalling. These stalled ribosomes are primarily sensed by associated Ski7 proteins to activate the NSD. However, the Hbs1-Dom34 complex has been reported to compensate for the absence of Ski7 proteins in yeast. Since ribosomes interact with Ski7 and the Hbs1-Dom34 complex, a new hypothesis has been proposed for the competitive mechanism mediated by Ski7 and the Hbs1-Dom34 complex to activate NSD (Heck & Wilusz, 2018).

mRNA DEGRADATION

mRNA decay is an essential process to modulate gene expression. Although global mRNA changes have been originally attributed to transcriptional regulations, mRNA decay has been reconsidered to significantly contribute to a changed transcriptome. An outstanding deficit in the field of mRNA turnover is how RNA decay plays a role in reprogramming or shaping gene expression during cellular exposure to environmental insults. Furthermore, mRNA degradation is linked to other mechanisms, such as translation, complicating interpretations of its role (Chavez, Garcia-Martinez, Delgado-Ramos, & Perez-Ortin, 2016; C. A. Chen

& Shyu, 2017; Garneau, Wilusz, & Wilusz, 2007). mRNA decay can be achieved by three main routes including endo-nucleolytic cleavage, 5′ to 3′ or 3′ to 5′ exonucleolytic decay. Other pathways of RNA decay have been found in yeast. For example, the vacuolar endonuclease RNase in Yeast 1 and the mitochondrial nuclease, known as Rny1 and Nuc1, respectively, are released to the cytosol upon stress conditions. They have been suggested to target mRNA for degradation (Buttner et al., 2007; Parker, 2012; Thompson & Parker, 2009). In the cytoplasm, mRNA turnover sequentially begins with deadenylation and decapping followed by either 5′ to 3′ or 3′ to 5′ degradation (Heck & Wilusz, 2018).

mRNA deadenylation

mRNA deadenylation is a process to shorten the poly(A) tail via multi-subunit deadenylase complexes including CCR4-NOT complexes and Poly(A)-Specific Ribonuclease Subunit 2 and 3 (Pan2)-(Pan3) complexes. In addition, a third deadenylase complex, known as Poly(A)-Specific Ribonuclease (PARN) has been discovered. However, PARN is not conserved in all eukaryotes and its orthologs have been found in vertebrates. Some studies have indicated the involvement of PARN in maturation and stability of some RNAs such as rRNA and miRNA. Other deadenylases including ANGEL1, ANGEL2, and the circadian rhythm–associated Nocturnin enzyme have been reported and suggested to target the poly(A) tails of specific mRNAs (Buschauer et al., 2020; Heck & Wilusz, 2018; Passmore & Coller, 2022).

The CCR4-NOT complex is considered as the predominant deadenylase in the cytoplasm and consists of seven subunits. Two subunits of CCR4-NOT complex have poly(A)-specific exonuclease activities including the yeast Ccr4, represented by the mammalian isozymes of CNOT6 or CNOT6L, and CCR4-Associated Factor 1 (Caf1), also known as the mammalian CNOT7 or CNOT8. In yeast, Ccr4 depletion impairs deadenylation rate more than Caf1 deletions. Although Ccr4 and Caf1 share similar enzymatic activities, they differ in their nuclease structure in which Ccr4 contains the endonuclease-exonuclease-phosphatase and Caf1 represents an RNase D fold. The yeast Not1 subunit is essential for Ccr4 assembly and cell viability. The mammalian CNOT2 and CNOT3 subunits interact with decapping factors, while CNOT9 subunit facilitates the CCR4-NOT complex to mRNA due to its interactions with RNA and RBPs. The last subunit is CNOT4 that contains an E3 ubiquitin ligase to direct degradation of ribosomal proteins and maybe other proteins (Heck & Wilusz, 2018; Webster et al., 2018).

Another enzyme regulating the poly(A) tail length is the conserved Pan2-Pan3 complex. In this complex, Pan2 contains DEDD motif/RNaseD-type exonuclease selective for polyadenylated RNA, while the homodimer of Pan3 functions as a scaffold for the Pan2 subunit. In addition, the NTD of Pan3 specifically binds A′s and its PABP-Interacting Motif 2 (PAM2) binds poly(A) tails via PABPC that has been shown to stimulate deadenylation. Additional interactions with RBPs have been documented by other regions of the Pan2-Pan3 complex.

For example, Pan2-Pan3 interactions with GW182 protein of RNA-Induced Silencing Complex (RISC) facilitates the Pan2-Pan3 recruitment to specific mRNA. Pan2 and Pan3 gene deletions did not affect cell viability in yeast and deadenylation process due to functional redundancy between CCR4-NOT and Pan2-Pan3 complexes. Interestingly, individual gene deletion of Pan2 or Pan3 resulted in longer poly(A) tails (Heck & Wilusz, 2018; Passmore & Coller, 2022).

Recent studies have explained the mechanistic function of CCR4-NOT and Pan2-Pan3 complexes on PABPC-coated poly(A) tails. These complexes function in a biphasic model that starts with the action of Pan2-Pan3 to remove naked A′s at the distal parts of poly(A) tails. Next, the CCR4-NOT complex removes A′s proximal to the 3′-UTR explained by the accumulation of tails with 20-40 nt in the absence of CCR4. Similarly, the presence of two exonucleases within the CCR4-NOT complex has been questioned for their roles on poly(A) tails. In yeast, the Poly(A)-Binding Protein (PAB1) can protect the poly(A) tails from Caf1 activity that removes unprotected A′s, whereas it fails to block CCR4-NOT activity. In addition, Caf1 activity was more dependent on translation than Ccr4. In the absence of the poly(A) binding protein, the Ccr4-Caf1 complex exhibited slower rates of deadenylation indicative of a PAB1 role in recruitment of the Ccr4-Caf1 complex (Nicholson & Pasquinelli, 2019; Passmore & Coller, 2022).

The deadenylation rate is major determinant of transcript half-life and varies among transcripts up to 1000-fold. Since these deadenylases cannot distinguish between poly(A) tails once they are recruited, two factors have been proposed to control the rate of deadenylation. First, RBPs, usually bound to the 3′-UTR

sequence, facilitate the recruitment of deadenylase complexes. Second, codon optimality that controls the rate of translation elongation. A recent study concludes that the translational rate accounts for 55% of the variation in mRNA half-life compared to the 5.5% of 3′-UTR motifs. In addition, specific mRNA sequences at the 3′-UTR are recognized by RBPs that recruit deadenylases via regions of IDR. For example, AU-rich and Pumilio-response elements are recognized by RBPs such as Tristetraprolin (TTP) and Pumilio/PFB (PUF) proteins, respectively. The list of RNA-deadenylase adaptor is growing and includes GW182 protein of RISC, nanos, roquin and YTHDF2. However, the tethering process mediated RBPs has been shown to be regulated and subsequently influence the deadenylation of target mRNAs. During inflammatory response, TTP is phosphorylated and dissociated from CCR4-NOT complex leading to enhanced mRNA stability. Another example of RNA regulation can be explained by the differential affinities of RBPs to bind RNAs (Passmore & Coller, 2022).

Other factors affecting the deadenylation rate are mRNA sequence and structure, PABPC interactions with deadenylase complexes, and heterogenous poly(A) tails. For example, histone mRNAs have a stem-loop structure at the 3′-UTR and that impedes access of deadenylases. Inclusion of poly(U) is another example that prevents deadenylation by base pairing with mRNA poly(A) tails and blocking PABPC binding sites. In addition, isoforms produced due to APA contain variations in their final nucleotides defining the 3′-ends and subsequently result in differential half-lives ($t_{1/2}$). Together, these mRNA sequences and structures may decrease the rate of deadenylation via deadenylase recruitment-dependent

manner. Recruitment of deadenylases is well explained by PAM2 motifs that directly interact with the mademoiselle domain of PABPC and found in some RNA adaptors (Passmore & Coller, 2022). For instance, Transducer of ERB-B2 Receptor Tyrosine Kinase 1 (TOB 1) and 2 (TOB 2) proteins are encoded by paralogous genes involved in anti-proliferative functions. TOB-2 has been shown to promote deadenylation of cell cycle-related transcripts by TOB phosphorylation at IDR region that contains two PAM2 motifs interacting with PABPC (C. A. Chen, Strouz, Huang, & Shyu, 2020). In contrast, LARP proteins such as LARP1 and LARP4, contain PAM2 motifs to stabilize PABPC1 binding to poly(A) tails. Other proteins containing PAM2 motifs include eRF3, PABPC-interacting protein 1 and 2 that contribute to translation and dynamic poly(A) tail length. Finally, heterogenous poly(A) tails disrupt the helical conformation caused by A′s specifically preferred by the CCR4-NOT deadenylases. For example, the addition of G′s to poly(A) tails has been found in long poly(A) tails and can delay the action of CCR4-NOT complex *in vitro*. However, poly(A) tails containing U′s are found in short poly(A) tails, fewer than 25 nucelotides, and represent a signal for mRNA decay. The last modification is C-containing poly(A) tails that are the least frequent modification and less characterized (Nicholson & Pasquinelli, 2019). In addition, Pan2-Pan3 activity has been shown to be less if it encounters non-A nucleotides such as C′s. The addition of non-A′s has been noticed in viral mRNA poly(A) tails to avoid the host deadenylation machinery (Passmore & Coller, 2022).

Finally, mRNA translation has been long thought to modulate poly(A) tail length. Several studies have shown that inhibited translation initiation negatively

affects long-lived transcripts. In addition, the translation elongation rate has been indexed by codon optimality where high optimal codons confer faster elongating ribosomes, while low optimal codons result in slower elongating ribosomes. The codon optimality is based on the balance between the availability of charged tRNA in the cytoplasm and tRNA demands by translating ribosomes (Presnyak et al., 2015). Moreover, the translation elongation rate has been inversely correlated with mRNA deadenylation and decapping. For instance, Caf1-deficient cells greatly decreased the deadenylation of mRNAs with low optimal codons suggesting that low optimal genes have less bound PAB1 and Caf1 targets low-translated mRNA than high-translated mRNA (Nicholson & Pasquinelli, 2019; Passmore & Coller, 2022). However, the slow elongating ribosomes and subsequent faster deadenylation and decapping cannot be exclusively explained by variability in tRNA concentration since other factors such as tRNA charging, RNA modifications, mRNA structure, and availability of amino acid, may be involved (Passmore & Coller, 2022). In addition, not4 and not5 have been proposed to signal slow elongating ribosomes to deadenylation and decapping complex. For example, not4 monoubiquitinates the upregulated ribosomal protein eS7 during the UPR, while not5 has been shown to bind empty A-Site and E-Site in translating ribosomes of transcripts characterized with non-optimal codons. Perturbations of not5 binding to ribosomal E-Site and eS7 mono-ubiquitination result in stabilized transcripts and block association of the decapping activator yeast Dhh1, DDX6 in mammals (Matsuki et al., 2020; Passmore & Coller, 2022).

mRNA decapping

The m^7G cap at the 5′-ends of mRNAs is known for its mRNA protection against the 5′ to 3′ degradation and its stimulation for mRNA translation. mRNA decapping is an integral process in the mRNA decay pathway and can be initiated independent of mRNA deadenylation. mRNA caps are mainly removed by the complex of Decapping Protein 1 (DCP1) and 2 (DCP2). Additional proteins, such as a few Nudix Hydrolases (NUDIX) and DXO, have shown decapping activity on a subset of mRNAs, including those with different cap structures. Decapping enzymes break the triphosphate bridge, while DXO cleaves between the first and second nucleotides (Galloway & Cowling, 2019; Heck & Wilusz, 2018; Parker, 2012).

DCP2 is a well-characterized decapping enzyme and belongs to the NUDIX family that has pyrophosphatase function. The DCP2 associates with other decapping cofactors for optimal substrate recognition and catalytic function. An efficient decapping complex includes cofactors such as DCP1, the Sm-Like (LSM) 1-7 complex, PAT1 homolog 1 Processing Body mRNA Decay Factor (PATL1), the RNA helicase DDX6, LSM14A mRNA Processing Body Assembly Factor (LSM 14), and a subset of Enhancer of mRNA Decapping Proteins (EDC). For example, the DCP2-DCP1 complex has a low affinity to mRNA but hydrolyzes the mRNA cap. Recruitment of the DCP2-DCP1 complex is enhanced by the interaction between PATL1 and the heptameric LSM 1-7 complex, recognizes deadenylated mRNA. The assembly and activation of the decapping complex is mediated by

EDC1, EDC2, EDC3 and LSM 14 that function as scaffolding proteins, while DDX6 has been shown to enhance the assembly of the DCP2-DCP1 complex by remodeling target mRNAs. Recently, another factor, the non-annotated 7 kDa microprotein NoBody, has been suggested to contribute to mRNA decay based on its association with the DCP2-DCP1 complex (Heck & Wilusz, 2018; Parker, 2012).

Furthermore, several studies have reported interactions between deadenylation and decapping complexes through ribosomes. Accumulating evidence shows that efficient mRNA decapping is dependent on some subunits of the CCR4-NOT complex such as Not1 and Not5. Thus, mRNA deadenylation proceeds decapping and that maybe serves as a major checkpoint for mRNA integrity. Not1 has been shown to mediate the interaction between the CCR4-NOT complex and the decapping helicase Dhh1/the mammalian DDX6 (Passmore & Coller, 2022). Also, Dhh1 has been documented to physically interact with ribosomes, especially on mRNA encoding suboptimal codons (Radhakrishnan et al., 2016). Interestingly, mRNA with non-optimal content is associated with ribosomes targeted by Not5 that senses vacant ribosomal A-Site and E-Site and Not5 binding to the latter serves as a prerequisite for Dhh1 binding to ribosomes (Buschauer et al., 2020; Passmore & Coller, 2022).

mRNA decay

Following mRNA decapping, the cytoplasmic 5′ to 3′ degradation of mRNA is activated by the Cytoplasmic 5′-3′ Exoribonuclease 1 (XRN1). XRN1 is conserved and preferentially attached to monophosphates at the 5′-ends of mRNA.

Although the highly processive XRN1 enzyme lacks a helicase, extensive secondary structures such as the viral three helix junction knot-like structures and increased cellular levels of adenosine 3′, 5′ bisphosphate can stall the enzyme and thus, affect gene expression homeostasis. XRN1 repression is accompanied by defects in mRNA decapping as well as deadenylation (Heck & Wilusz, 2018; Parker, 2012). On the contrary, 3′ to 5′ degradation is activated following mRNA deadenylation and mediated by the EXO complex including its cofactors. The cytoplasmic EXO is composed of ten proteins in which nine subunits form the inactive EXO-9 complex that requires the DIS3 homolog, EXO endoribonuclease and 3′-5′ exoribonuclease (RRP44) subunit for the activation of EXO-10 complex. In addition, the EXO is associated with additional cofactors such as Ski proteins to efficiently degrade cytoplasmic mRNA. For example, Ski2 functions as a helicase to unwind the EXO-targeted mRNA, whereas the Ski7 has been reported to recruit the EXO. The EXO degrades mRNA from 3′ to 5′ until it reaches close to the cap that is removed by the scavenger decapping enzyme together with the fragile His triad diadenosine triphosphtase. In addition to 3′ to 5′ degradation mediated by the EXO, other RNAs including mRNA and non-coding RNA can be degraded in a 3′ to 5′ direction by the cytoplasmic and EXO-independent DIS3-Like 3′-5′ Exoribonuclease 2 (DIS3L2). DIS3L2 is conserved and targets short mRNA with poly(U) tails added by terminal uridylyl transferase 4 or 7, non-canonical PAPs (Heck & Wilusz, 2018; Parker, 2012).

Finally, the endo-nucleolytic cleavage creates free ends, either 5′-monophophsates or 3′-OH, contributing to mRNA decay by the exonucleolytic pathways. For example, RNA interference has been documented to provide substrates to exoribonucleases. The RISC-mediated endo-nucleolytic cleavage of mRNA is well characterized and has been reported to recruit the cytoplasmic EXO. Because several endoribonucleases significantly modulate the mRNA fate, they are under tight regulations as explained by the cellular production of Cys-rich ribonuclease inhibitor (Heck & Wilusz, 2018; Parker, 2012). For example, mRNA stability has been influenced by a few major endoribonucleases such as MCP-1-induced protein 1/Regnase 1, Heat-Responsive Protein 12 (HRSP12), IRE-1 and RNase L. First, the Regnase 1 is implicated in the inflammatory response to pathogenic infections and regulated by an inhibitory phosphorylation. The phosphorylation of Regnase 1 is mediated by the inhibitor of transcription factor NF-κB kinase during inflammation. In addition to its role in the immune response, the Regnase 1 regulates mRNA decay of transcripts related to iron homeostasis and fat storage and accumulation (Heck & Wilusz, 2018). Secondly, the HRSP12 is an endoribonuclease along with the Y-box-binding protein 1, Pro-rich nuclear receptor coregulatory protein 2, UPF1 and DCP1A that have been identified as factors of the Glucocorticoid Receptor-Mediated Decay (GMD). GMD targets a wide range of transcripts involved in

various cellular processes (O. H. Park et al., 2016). The last two endoribonucleases, IRE-1 and RNase L, function under stress conditions. In ER

stress, the IRE-1 containing endoribonuclease is involved in RIDD as described previously. On the other hand, RNase L is induced in response to viral infections. Together, these endoribonucleases target specific mRNA and thus, reshape gene expression (Heck & Wilusz, 2018).

In conclusion, ER stress causes eIF2α phosphorylation that reprograms gene expression to tolerate the stress conditions. Thus, mRNA life cycle is tightly regulated via mechanisms including transcription, translation, and eventually degradation. Under ER stress conditions, these mechanisms are reprogrammed to boost an adaptive response and avoid cell death. In ER stress, the acute response may represent the anticipation of recovery before commitment to the chronic adaptive response that survives the persistent ER stress for prolonged periods. My thesis will use the ER stress-induced *XBP1* gene, as a model to illustrate a new mechanism of adaptation to acute and chronic ER stress, via the length of polyadenylation.

CHAPTER 2: BIPHASIC REGULATION OF POLY(A) TAIL LENGTH AND HALF-LIFE OF *XBP1* TRANSCRIPTS DURING THE UNFOLDED PROTEIN RESPONSE

Gene expression is reprogrammed to adapt to cellular stresses. During ER stress, the UPR is not limited to protein misfolding, but extends to and intertwines with other regulation programs. The UPR coordinates gene expression in a temporal fashion to avoid short term and expanded deleterious effects (Arensdorf, Diedrichs, & Rutkowski, 2013; Gonen, Sabath, Burge, & Shalgi, 2019; Guan et al., 2017; Hetz, Chevet, & Oakes, 2015). For example, several studies highlight the modulation of mRNA stability upon ER stress (Kawai, Fan, Mazan-Mamczarz, & Gorospe, 2004; Majumder et al., 2012; Rutkowski et al., 2006; Woo et al., 2018). The molecular mechanisms of ER stress-induced differential mRNA stability, however, remain elusive. Because we have previously reported that *XBP1s* mRNA is transiently stabilized during the acute phase of the UPR (Majumder et al., 2012), I sought to investigate the temporal regulation of *XBP1* mRNA during the acute and chronic phases of the UPR in mammalian cells.

Dynamic regulation of *XBP1* expression during the UPR

To study the temporal regulation of *XBP1* expression, I confirmed the previously reported *XBP1* expression in my experimental system, WT MEF cells treated with Tg for up to 24 hours (h). Upon Tg treatment, temporal changes of protein expression were observed for phosphorylated eIF2α and ATF4 as early as

1 h after Tg treatment (Figure 2.1A) (Dorrbaum, Alvarez-Castelao, Nassim-Assir, Langer, & Schuman, 2020; Rothenberg et al., 2018). Notably, the accumulation of XBP1s and BiP proteins (Gonen et al., 2019; Majumder et al., 2012) was delayed for 3 h and 6 h after Tg treatment, respectively (Figure 2.1A). This delay of XBP1s protein expression may be explained by a documented transient ribosomal pausing at the Asn-256 codon or the low basal level of *XBP1* mRNA in cells (Gonen et al., 2019; Ingolia, Lareau, & Weissman, 2011; Yan, Hoek, Vale, & Tanenbaum, 2016). In contrast, splicing of *XBP1u* mRNA was observed to occur rapidly within 1 h after Tg treatment in MEF cells (Figure 2.1B) (Rutkowski et al., 2006; Tam, Koong, & Niwa, 2014).

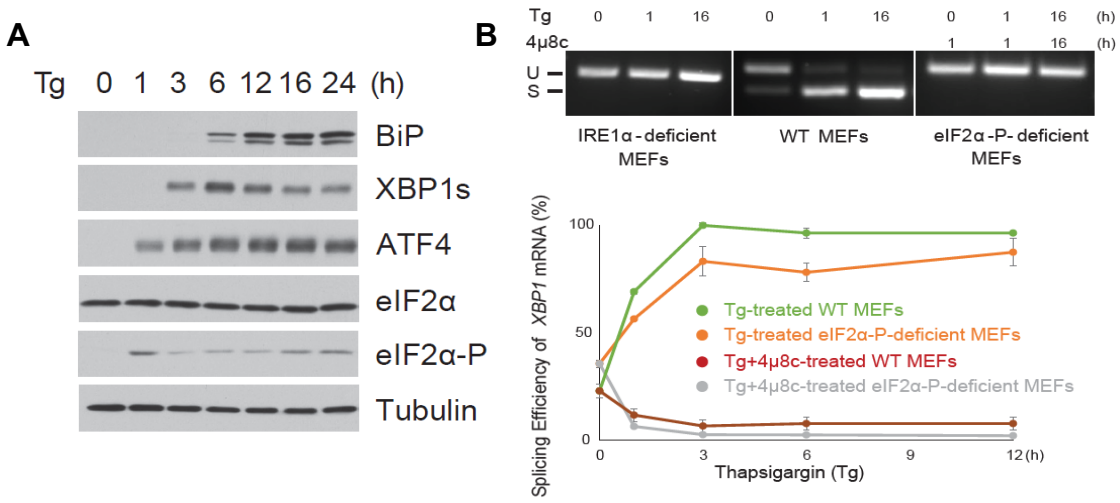

Figure 2. 1. ER stress-induced temporal regulation of *XBP1* mRNA splicing and translation.
(A) Western blot analysis of ER stress markers, including XBP1s protein, in MEF cells treated with Tg (400 nM) for the indicated time. **(B)** (top) Reverse Transcription-Polymerase Chain Reaction (RT-PCR) analysis of *XBP1* mRNA splicing in IRE1α-deficient and WT MEF cells, treated with Tg for 0, 1, and 16 h, or eIF2α-P-deficient MEF cells treated with Tg and the IRE1α Inhibitor (4μ8C) together for the indicated time (U; *XBP1u*, and S; *XBP1s*). (bottom) Splicing efficiency of *XBP1* mRNA in the indicated cell treatments evaluated by Reverse Transcription-quantitative Polymerase Chain Reaction (RT-qPCR) analysis.

To recapitulate previous studies on *XBP1* gene expression (Majumder et al., 2012; C. Stewart et al., 2017), *XBP1s* mRNA was gradually increased and stabilized during the acute UPR, during the first 3 h of Tg treatment, in MEF cells. On the contrary, *XBP1s* mRNA stability and steady state levels were decreased during the chronic phase of the UPR, represented by 6 h and beyond of Tg treatment (Figure 2.2A). While many studies have focused on *XBP1s* mRNA, little is known about regulation of *XBP1u* mRNA. To evaluate *XBP1u* mRNA, a pharmacological inhibitor of IRE1α, 4μ8C, was applied in MEF cells during the UPR to block splicing and caused an accumulation of the unspliced *XBP1* transcript (Cross et al., 2012). To ensure inhibition of *XBP1* mRNA splicing, various 4μ8C concentrations were tested in MEF cells treated together with Tg for 3 h, at the time point corresponding to the highest level of *XBP1* expression. Inhibition of *XBP1* mRNA splicing occurred for concentrations of 4μ8C, in the range of 25-100μM, with 50μM of 4μ8C being selected for further analysis (Figure 2.2B). Similar to *XBP1s* mRNA, *XBP1u* mRNA was observed in cells to be transiently stabilized during the acute UPR in MEF cells. Notably, levels of *XBP1u* mRNA showed an increase during the acute phase of UPR (Figure 2.2C).

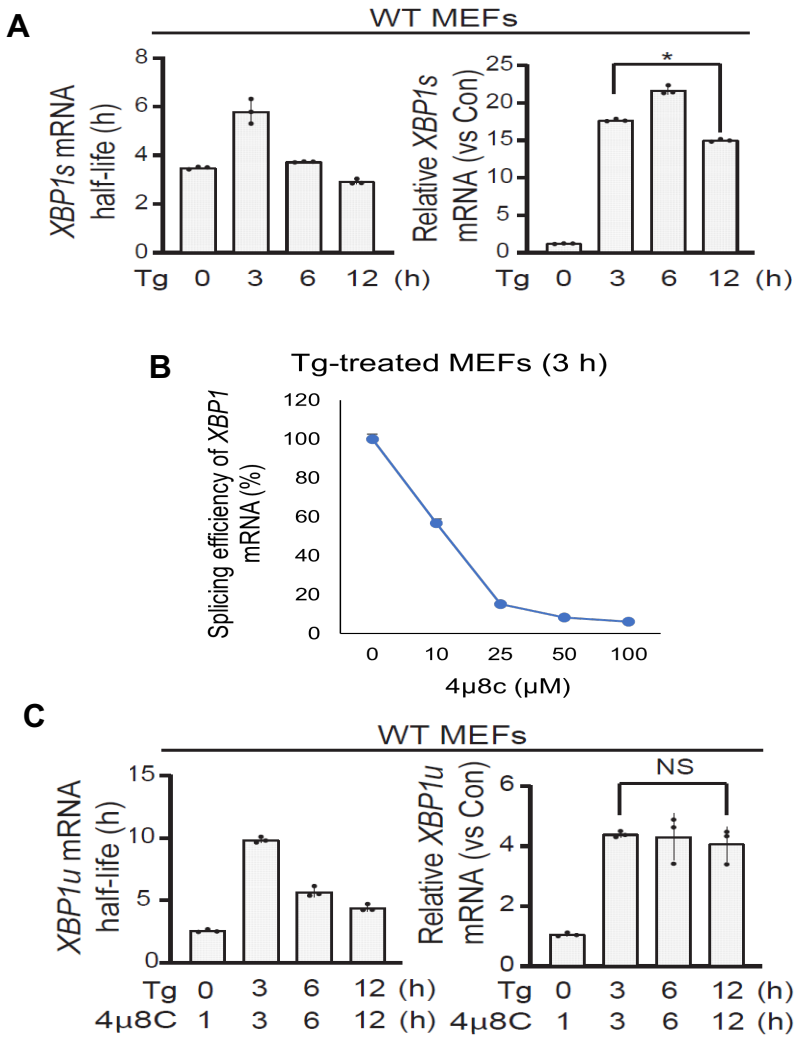

Figure 2. 2 Temporal regulation of *XBP1* mRNA stability and steady state levels during the UPR.
(A) (Left) *XBP1s* mRNA half-life was determined by treating MEF cells with Tg for the indicated time (0, 3, 6 and 12 h). following Tg treatment, actinomycin D was added to inhibit transcription for 0, 0.5, 1, 2, 3, and 4 h, and *XBP1s* mRNA decay rate was calculated. (Right) *XBP1s* mRNA steady state level was quantified by RT-qPCR at the indicated time. **(B)** Splicing efficiency of *XBP1u* mRNA in Tg-treated MEF cells in the presence of indicated concentrations of the IRE1α inhibitor, 4μ8C, for 3 h was determined by RT-qPCR analysis. **(C)** *XBP1u* mRNA half-life and steady state level were assessed as in A, except that MEF cells were treated with Tg in the presence of 4μ8C (50 μM), for the indicated time. In the absence of Tg treatment (the control condition), MEF cells were treated with only 4μ8C for 1 h. Asterisks (*) indicate statistical significance of replicates with $P < 0.00005$, while (NS) indicates non-significance.

To confirm regulation of *XBP1u* mRNA during the UPR and exclude any off targets of 4μ8C (C. Stewart et al., 2017), IRE1α-deficient MEF cells lacking IRE1α splicing activity were tested (K. Lee et al., 2002). First, the persistent expression of *XBP1u* mRNA was confirmed in IRE1α-deficient MEF cells, even during the UPR (Figure 2.1B). In collaboration with Dr. Guan, the regulation of *XBP1u* mRNA stability was observed to be indistinguishable from that observed for 4μ8C-treated MEF cells. Similarly, during the acute UPR, *XBP1u* mRNA was transiently stabilized, and its level gradually increased, while during the chronic UPR, *XBP1u* transcripts were destabilized and significantly decreased in levels (Figure 2.3A). Similar to *XBP1s* mRNA (Guan et al., 2017; Majumder et al., 2012), translation of *XBP1u* mRNA was repressed under the acute UPR and de-repressed under the chronic UPR in IRE1α-deficient MEF cells as monitored for polysome association of *XBP1u* transcripts (Figure 2.3B). As anticipated, translation of *ATF4* mRNA increased during the acute phase of UPR and remained high during the chronic phase, thereby confirming the experimental system (Figure 2.1A and Figure 2.3C). These data support regulation of *XBP1u* mRNA stability and translation during the UPR and demonstrate that it is similar to regulation of *XBP1s* mRNA. For the remaining of the thesis, we will use the term *XBP1* to describe common regulation of the *XBP1u* and *XBP1s* mRNA. In specific experimental settings that we study *XBP1u* or *XBP1s* mRNA regulation, we will use the appropriate term.

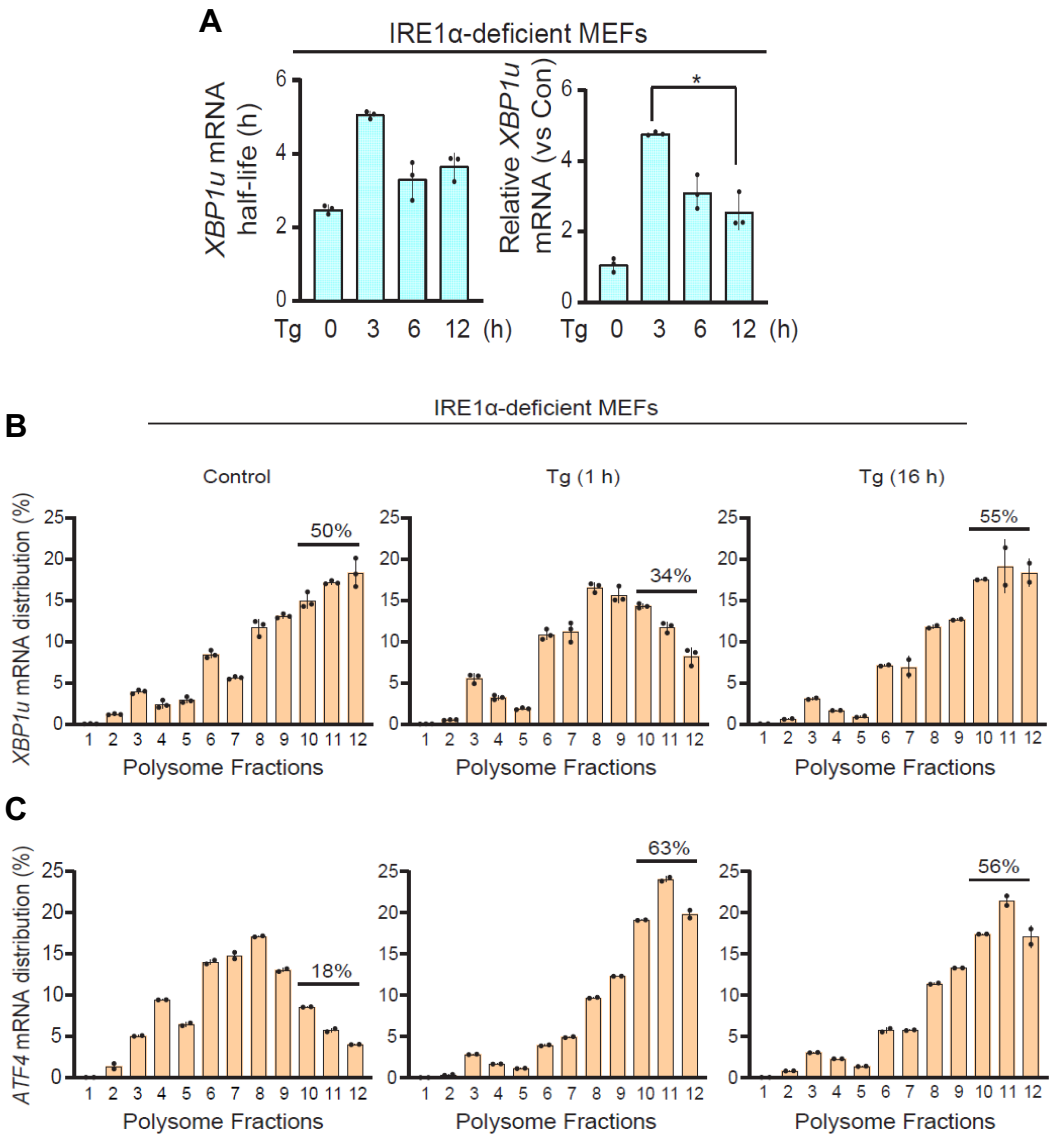

Figure 2. 3. Temporal regulation of *XBP1u* mRNA stability, steady state levels, and translation in IRE1α-deficient MEF cells during the UPR.
(A) (Left) Half-life of the *XBP1u* mRNA was determined by treating IRE1α-deficient MEF cells with Tg for the indicated time (0, 3, 6 and 12 h) followed by actinomycin D-mediated transcriptional shut off for 0, 0.5, 1, 2, 3, and 4 h. *XBP1u* mRNA decay rate was calculated. (Right) *XBP1u* mRNA steady state levels were quantified by RT-qPCR. **(B-C)** Polysome profile distribution of *XBP1u* and *ATF4* mRNA in IRE1α-deficient MEF cells treated with Tg for 0, 1, and 16 h in cell extracts analyzed by sucrose gradient ultracentrifugation. The enrichment of these mRNA in the last 3 fractions of each condition was quantified. Asterisks (*) indicate statistical significance of replicates with $P < 0.05$.

To further understand the *XBP1* regulation, *XBP1u* mRNA was monitored in MEF cells expressing a mutant eIF2α, unable to be phosphorylated at Ser-51 during the UPR. These cells, referred to as eIF2α-P-deficient MEF cells, are deficient at attenuating translation initiation in response to ER stress (Figure 2.4A). Notably, *XBP1u* mRNA splicing was not affected in these cells upon Tg treatment unless cells were also treated with the IRE1α inhibitor, 4μ8C (Figure 2.1B). With the help of Dr. Guan, treating cells with the 4μ8C together with Tg revealed that despite an increase in the steady state level of *XBP1u* mRNA during the acute phase of UPR, the half-life of *XBP1u* transcripts was unchanged in these cells (Figure 2.4B). Increased levels of the *XBP1u* mRNA in eIF2α-P-deficient cells was therefore not due to increased mRNA stability and was likely a consequence of transcriptional activation of the *XBP1* gene. Based on these observations, stabilization of the *XBP1* mRNA during the acute UPR phase is not obligatorily coupled to transcriptional induction of the *XBP1* gene expression, as previously suggested (Figure 2.4B) (Slobodin et al., 2020). Importantly, translation of *XBP1u* mRNA was not inhibited during the acute UPR phase in eIF2α-P-deficient MEF cells, as expected (Figure 2.4C). Together, these data indicate that *XBP1s* and *XBP1u* mRNA are subject to similar regulation at the level of transcript stability during the UPR in an eIF2α phosphorylation-dependent manner.

A

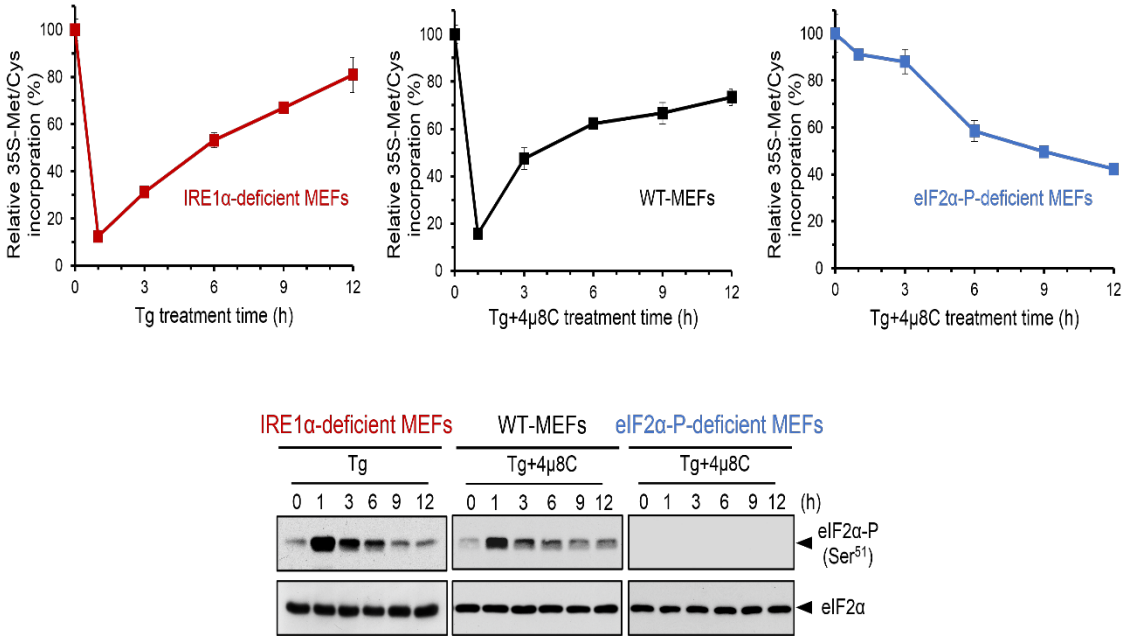
Relative 35S-Met/Cys incorporation (%)
IRE1α-deficient MEFs
Tg treatment time (h)
WT-MEFs
Tg+4μ8C treatment time (h)
eIF2α-P-deficient MEFs
Tg+4μ8C treatment time (h)
IRE1α-deficient MEFs
WT-MEFs
eIF2α-P-deficient MEFs
Tg
Tg+4μ8C
Tg+4μ8C
0 1 3 6 9 12 (h)
eIF2α-P (Ser51)
eIF2α

B

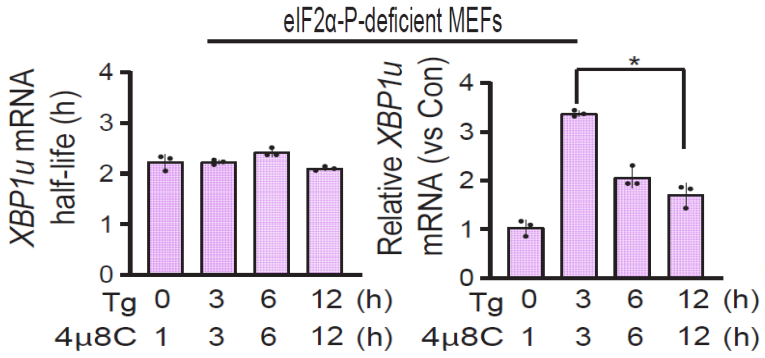
eIF2α-P-deficient MEFs
XBP1u mRNA half-life (h)
Relative XBP1u mRNA (vs Con)
*
Tg 0 3 6 12 (h)
4μ8C 1 3 6 12 (h)
Tg 0 3 6 12 (h)
4μ8C 1 3 6 12 (h)

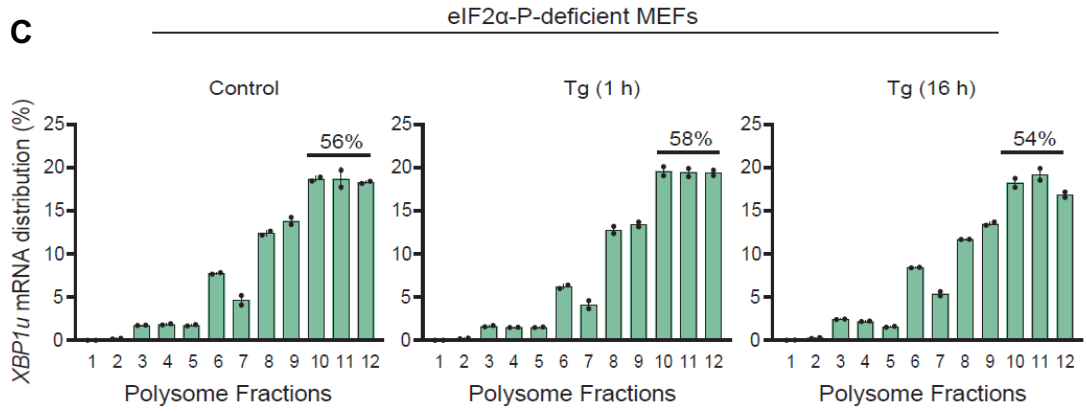

Figure 2. 4 Temporal regulation of *XBP1u* mRNA stability, steady state levels, and translation in eIF2α-P-deficient MEF cells during the UPR.
(A) (Top) Protein synthesis was measured by [^{35}S]-Met/Cys metabolic labeling in (Left) IRE1α-deficient MEF cells treated with Tg for up to 12 h, (Middle) WT MEF cells, or (Right) eIF2α-P-deficient MEF cells treated with Tg together with 4μ8C for up to 12 h. Western blot analysis of total eIF2α or its phosphorylated form on Ser-51 (eIF2α-P) in (Left) IRE1α-deficient MEF cells, (Middle) WT MEF cells, or (Right) eIF2α-P-deficient MEF cells treated with Tg for the indicated durations. **(B)** Half-life and steady state levels of the *XBP1u* mRNA in eIF2α-P-deficient MEF cells in the presence of 4μ8C as described in Figure 2.2C. **(C)** Distribution of *XBP1u* mRNA by polysome analysis of eIF2α-P-deficient MEF cells treated with Tg for 0, 1, and 16 h in the presence of 4μ8C. *XBP1u* mRNA levels in the last 3 fractions of each condition were quantified. Asterisks (*) indicate statistical significance of replicates with $P < 0.005$.

XBP1 mRNA stability is determined by *XBP1* mRNA translational status

To address whether translational reprogramming mediated by eIF2α phosphorylation during the acute UPR contributes to the observed increased stability of *XBP1u* mRNA, I worked under the supervision and guidance of Dr. Guan to evaluate bulk mRNA translation in IRE1α-deficient, WT and eIF2α-P-deficient MEF cells. As anticipated, the phosphorylation of eIF2α upon Tg treatment in IRE1α-deficient MEF cells or the combined treatment of Tg and 4μ8C in WT-MEF cells led to a significant reduction protein synthesis that was partially

restored during the chronic phase of the UPR (Figure 2.4A). Importantly, eIF2α-P-deficient MEF cells demonstrated no significant decrease in protein synthesis during the acute phase of UPR, as expected (Figure 2.4A) (Guan et al., 2014). In light of the observation that *XBP1u* mRNA was not stabilized in eIF2α-P-deficient MEF cells during the UPR, I investigated whether translational repression mediated by eIF2α-P is required for the increased stability of the *XBP1* mRNA during the acute phase of the stress response. In the absence of Tg-stimulated UPR, eIF2α-P-deficient MEF cells were treated with 4μ8C in the presence or absence of 5 micrograms (μg) of Puro, an inhibitor of translational elongation, and protein synthesis was monitored by metabolic labeling. As expected, eIF2α-P-deficient MEF cells treated with Puro for 1 h exhibited a dramatic decrease in protein synthesis compared to control cells (treated with only 4μ8C, Figure 2.5). Measurement of *XBP1u* mRNA half-life in eIF2α-P-deficient MEF cells treated with Dimethyl Sulfoxide (DMSO) or 4μ8C alone revealed similar half-lives under both conditions. In contrast, eIF2α-P-deficient MEF cells treated with both 4μ8C and Puro for 1 h resulted in an increase in the half-life of *XBP1u* mRNA, as a consequence of Puro-mediated translation inhibition (Figure 2.5). To confirm the stability of *XBP1u* mRNA under conditions of translation inhibition, harringtonine, an attenuator of translation initiation, was tested. Interestingly, *XBP1u* mRNA half-life was stabilized in these cells and was increased further in harringtonine-treated eIF2α-P-deficient MEF cells for 1 h compared to Puro treatment (Figure 2.5).

These data demonstrate that *XBP1* mRNA half-life is tightly correlated with the translation status of *XBP1* transcripts in cells during the UPR.

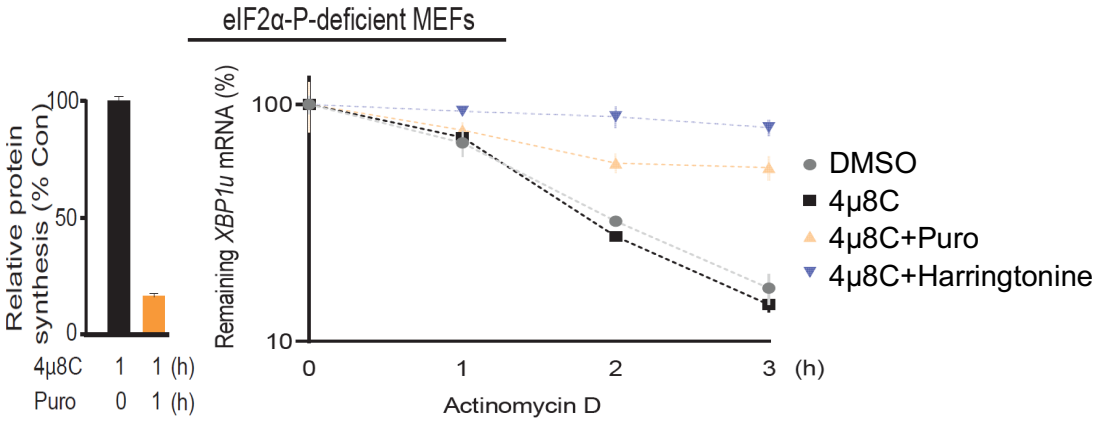

Figure 2. 5. Translational repression mediated by eIF2α phosphorylation is linked to *XBP1u* mRNA stability.
(Left) Protein synthesis as measured by [^{35}S]-Met/Cys metabolic labeling in eIF2α-P-deficient MEF cells in the presence of 4μ8C alone or together with 5 μg Puro for 1 h. (Right) Half-life of the *XBP1u* mRNA in eIF2α-P-deficient MEF cells treated with DMSO or 4μ8C alone as controls for 1 h. In addition, *XBP1u* mRNA stability was measured in eIF2α-P-deficient MEF cells treated with 4μ8C together with either Puro or 2 μg/mL harringtonine for 1 h. Following the indicated treatments, actinomycin D was added to inhibit transcription for 0, 1, 2, and 3 h, and *XBP1u* mRNA decay rate was calculated ($t_{1/2}$ = DMSO: 1.4 +/- 0.2 h; 4μ8C: 1.2 +/- 0.2 h; 4μ8C + Puro: 3.5 +/-0.5 h; 4μ8C + Harringtonine 9.9 +/- 0.9 h).

Temporal regulation of *XBP1* mRNA poly(A) tails during the UPR

To determine the poly(A) tail length of *XBP1* mRNA under conditions that induce the UPR, a PCR-based poly(A) tailing assay was employed (Patil, Bakthavachalu, & Schoenberg, 2014). Using this assay, the poly(A) tail length of *XBP1* mRNA was found to be dynamic during the UPR with long poly(A) tails being observed during the acute UPR and short poly(A) tails during both control conditions and during the chronic UPR (0 h or 6 h and beyond of Tg treatment,

respectively, Figure 2.6). In control cells (treated with DMSO instead of Tg, called Tg0), *XBP1* mRNA poly(A) tail length was short (~30 nt), likely due to deadenylation that would in turn, contribute to the instability of *XBP1* mRNA in these cells. Compared to the control condition, two populations of *XBP1* mRNA were observed in Tg treatment for 1 h; one with relatively long (~170 nt) poly(A) tails and the other with short (~30 nt) poly(A) tails. Notably, during the acute phase of the UPR (Tg-treated MEF cells for 3 h) the poly(A) tail of *XBP1* mRNA was predominantly long. Under extended Tg treatment, the length of *XBP1* mRNA poly(A) tails progressively shortened (see Tg-treated MEF cells for 6 h) and further decreased during the 16 h Tg treatment such that the length it was comparable to that observed in control cells (Figure 2.6). On the contrary, the poly(A) tail length of the stable Glyceraldehyde 3-Phosphatase Dehydrogenase *(GAPDH)* mRNA demonstrated little change between the control and acute UPR, poly(A) tails were relatively long. Interestingly, under chronic UPR conditions *GAPDH* mRNA poly(A) tail length gradually decreased in size, comparable to what was observed for *XBP1* mRNA poly(A) tail (Figure 2.6).

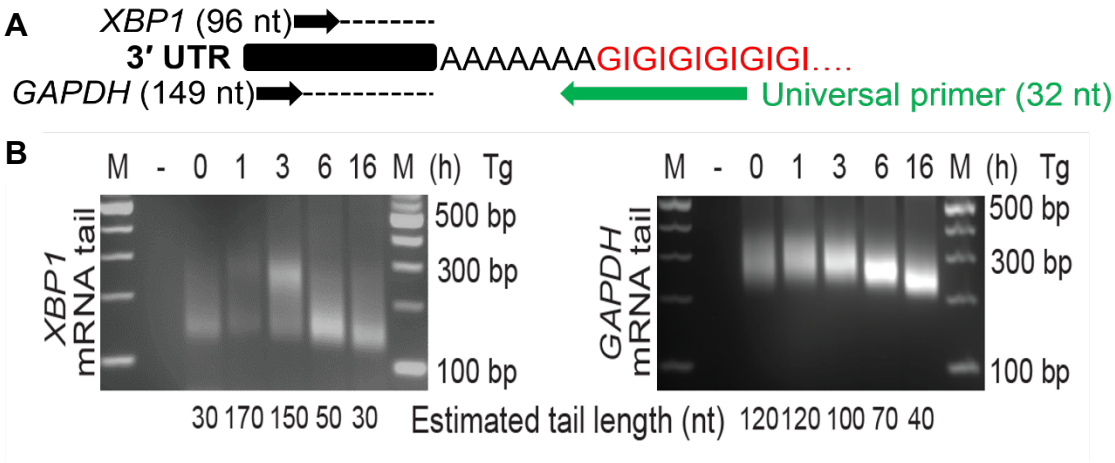

Figure 2. 6. Measurement of poly(A) tail length for XBP1 and GAPDH mRNAs during the UPR.
(A) Schematic of the PCR-based poly(A) tailing assay for *XBP1* and *GAPDH* mRNAs. The 3′-end of total RNA is extended with GMP/inosine monophosphate nucelotides by PAP to generate a Guanosine/Inosine Oligo Tail (GI-Oligo Tail) connected to the poly(A) tail. Following RNA isolation and RT using a poly(C) primer, a gene specific and universal primer are used for complementary DNA (cDNA) amplification of target mRNA. **(B)** PCR-based poly(A) tailing assay in MEF cells treated with Tg for the indicated durations. Estimated poly(A) tail length of *XBP1* (Left) and *GAPDH* (Right) mRNA are estimated based on the length difference between 3′-end and tail-PCR reactions. As a negative control (-), reactions were performed on cDNA derived from RNA not extended with a GI-Oligo Tail. M indicates 100 base-pair DNA ladder.

To quantify *XBP1* mRNA harboring different long poly(A) tail lengths during each phase of the UPR, two different approaches were employed. First, in collaboration with Dr. Zagore, total RNA from untreated WT, or Tg-treated MEF cells (for 3 h; acute UPR or 16 h; chronic UPR) was isolated and mixed with biotinylated oligo(dT) beads. The bound, polyadenylated mRNA was then eluted from the beads using decreasing salt concentrations in the elution buffer to fractionate mRNA based on their poly(A) tail length. High salt buffers elute mRNA with short poly(A) tails and low salt buffers elute mRNA species with long poly(A)

tails (Meijer & de Moor, 2011). Bulk poly(A) tail length distribution during the two phases of the UPR did not reveal any significant difference in mRNA poly(A) tail length for total mRNA as compared to untreated cells (Total lanes, Figure 2.7A). In contrast to bulk poly(A) tail length, a dramatic increase in mRNA with long poly(A) tails in cells treated with Tg for 3 h, which decreased by the 16 h timepoint (Figure 2.7A).

To identify populations of *XBP1* mRNA harboring different poly(A) tail lengths, the poly(A) tail length was measured from RNA isolated from the various fractions eluted from the oligo(dT) beads using the PCR-based poly(A) tailing assay. Notably, increased levels of *XBP1* mRNA harboring long poly(A) tails were observed during the acute UPR phase compared to the chronic phase of the UPR or untreated control cells (Figure 2.7B). In contrast, *GAPDH* mRNA harboring long poly(A) tails was found enriched in untreated cells and levels of these populations decreased as cells progressed to the chronic phase of the UPR (Figure 2.7B).

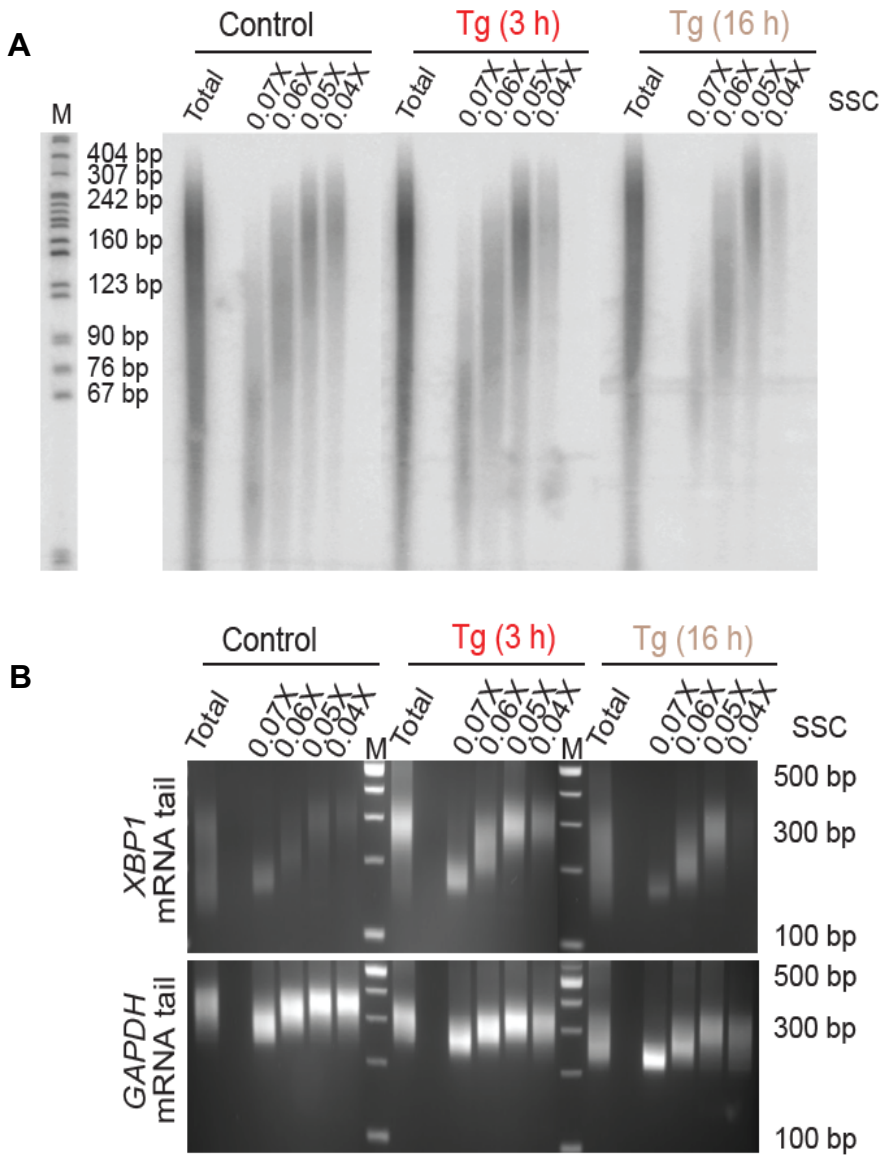

Figure 2. 7. Global poly(A) tail length does not increase during the acute UPR. **(A)** RNA fractionation based on the poly(A) tail length (long poly(A) tailed mRNAs were eluted in low salt buffers, i.e., 0.05X and 0.04X saline-sodium citrate (SSC) fractions, and short poly(A) tailed mRNAs were eluted in high salt buffers, i.e., 0.06X and 0.07X SSC fractions) in WT MEF cells treated with Tg for the indicated time (DMSO; Control, Tg for 3 h; acute UPR, and Tg for 16 h; chronic UPR). **(B)** The poly(A) tail length of *XBP1* and *GAPDH* mRNAs was estimated using the PCR-based poly(A) tailing assay on samples from **A**. M indicates 100 base-pair DNA ladder.

In a second approach, Reverse Transcription-quantitative Polymerase Chain Reaction (RT-qPCR) analysis was performed for both *XBP1* and *GAPDH* mRNAs in fractions eluted from the oligo (dT) beads shown in Figure 2.7A. During the acute UPR, *XBP1* mRNA harboring long poly(A) tails was at its highest level compared to untreated control cells (Figure 2.8, 0.04X fraction). In contrast, during the chronic UPR, *XBP1* mRNA was found to harbor shorter poly(A) tails (Figure 2.8, 0.06X fraction). Notably, both *XBP1* and *GAPDH* mRNAs displayed a reduction in poly(A) tail length during the chronic UPR [Figure 2.8, compare *XBP1* Tg (16h) 0.06X fraction to *GAPDH* Tg (16h) 0.06X fraction], suggesting a general mechanism of post-transcriptional regulation as cells adapt to chronic ER stress. Together, these data demonstrate temporal changes in *XBP1* mRNA poly(A) tail length during the UPR and provide a possible mechanism for regulation of *XBP1* gene expression during stress.

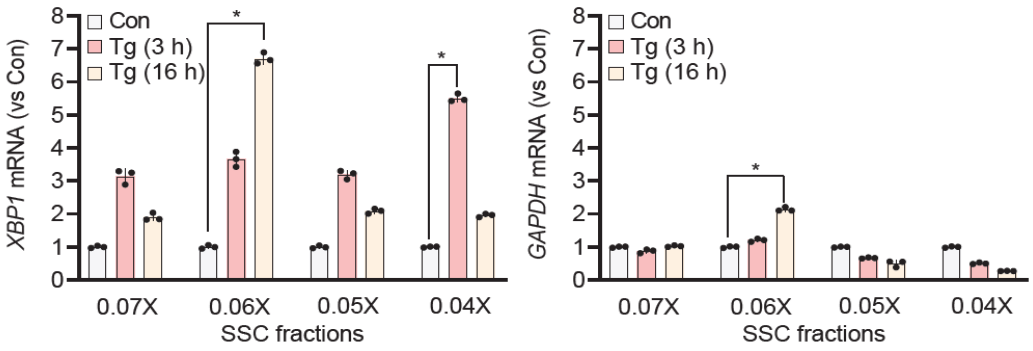

Figure 2. 8. Poly(A) tail fractionation of *XBP1* and *GAPDH* mRNAs during the UPR. RNA fractionation based on the poly(A) tail length in MEF cells treated with Tg for the indicated time (DMSO; Con, Tg for 3 h; acute UPR, and Tg for 16 h; chronic UPR). The levels of fractionated *XBP1* (Left) and *GAPDH* (Right) mRNAs were determined by RT-qPCR for each eluted fraction and compared to Con (i.e., DMSO-treated cells) in each fraction. Asterisks (*) indicate statistical significance of replicates with $P < 0.0005$.

To evaluate whether other ER stress conditions will recapitulate the dynamic poly(A) tail length changes caused by the acute and chronic UPR phases, additional stress agents known to elicit the UPR in WT MEF cells were tested. Cyclopiazonic acid, a well-known competitive inhibitor of the SERCA pump that leads to ER Ca^{2+} depletion and thus causes the UPR, was evaluated. Notably, CPA can be washed from cells compared to Tg, which is irreversible (Guan et al., 2017; Moncoq, Trieber, & Young, 2007). Activation of UPR by *XBP1* mRNA splicing in MEF cells treated with CPA for 3 h was confirmed (Figure 2.10D) and the impact of CPA treatment on cell viability of MEF cells was tested. WT MEF cells were treated with DMSO, CPA for 3 h, or CPA (for 3 h) followed by 24 h recovery and cell viability measured. Interestingly, cell viability of MEF cells treated with either DMSO or CPA for 3 h was equivalent but reduced as compared to CPA-treated MEF cells after CPA was washed from these cells (Figure 2.9A). To evaluate the length of *XBP1* and *GAPDH* mRNAs poly(A) tails under CPA-induced UPR conditions, WT MEF cells were treated with CPA for up to 16 h and PCR-based poly(A) tailing assay was performed. As anticipated, similar patterns for changes in poly(A) tail length for *XBP1* and *GAPDH* mRNAs were observed in CPA-treated MEF cells compared to those in Tg-treated MEF cells. Specifically, a transient accumulation of *XBP1* mRNA with long poly(A) tails was observed in CPA-treated MEF cells for 3 h, while short poly(A) tailed *XBP1* and *GAPDH* mRNAs were dominant during the chronic UPR (compare Figure 2.6 with Figure 2.9B). These data indicate that regulation of poly(A) tail length is a common mechanism to regulate *XBP1* mRNA during UPR.

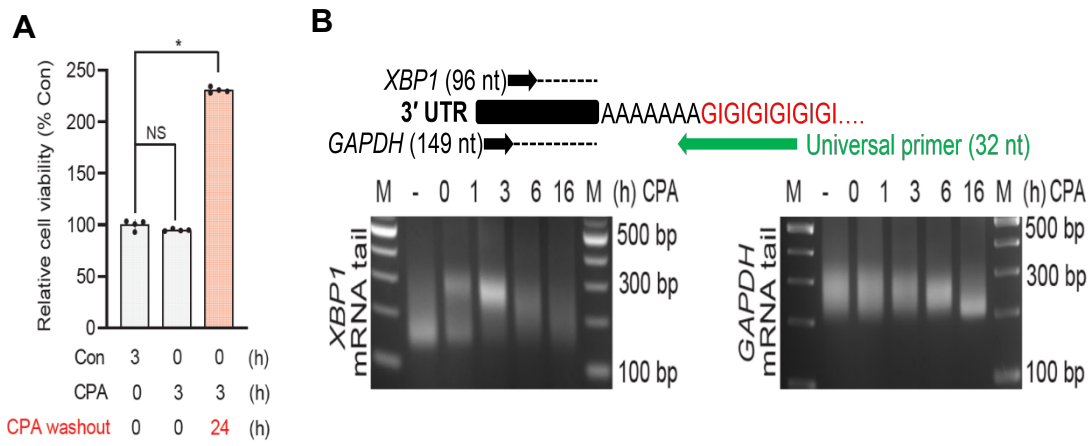

Figure 2. 9. The effect of CPA on cell viability and mRNA poly(A) tail length in WT MEF cells.
(A) MEF cells were treated with DMSO (Con) or CPA for 3 h (acute UPR) and cell viability was measured. Following CPA treatment, cells were allowed to recover in fresh media in the absence of CPA for 24 h (i.e., CPA washout). **(B)** MEF cells were treated with CPA for the indicated time and the poly(A) tail length of *XBP1* and *GAPDH* mRNAs was measured. Asterisks (*) indicate statistical significance of replicates with $P < 0.0000005$, while (NS) indicates non-significance. M indicates 100 base-pair DNA ladder.

Increased poly(A) tail length of *XBP1* mRNA is independent of increased *XBP1* mRNA stability during the acute UPR

To delineate the correlation between mRNA half-life and poly(A) tail length for *XBP1* mRNA, cordycepin, an analog of adenosine that blocks the synthesis of poly(A) tails on mRNA, was evaluated to investigate impact of poly(A) tails on *XBP1* mRNA stability during the acute UPR (Kondrashov et al., 2012). First, to determine whether *XBP1* expression impacted by cordycepin treatment during the acute UPR, WT MEF cells were treated with CPA in the presence or absence of cordycepin for 3 h. Generally, cordycepin treatment was observed to negatively influence *XBP1* expression, perhaps due to the high levels of AU-rich motifs in the

3′-UTR of *XBP1* mRNA. Specifically, cordycepin-treated MEF cells led to a decrease in *XBP1* mRNA expression and attenuated the induction of *XBP1* mRNA during the acute UPR (Figure 2.10A). Under these conditions, accumulation of long poly(A) tails on *XBP1* mRNA also decreased during the acute UPR (Figure 2.10B). Interestingly, treating MEF cells with the transcriptional inhibitor actinomycin D or 5,6-Dichloro-1-Beta-D-Ribofuranosylbenzimidazole (DRB) caused a further decrease in the steady state level of *XBP1* mRNA (Figure 2.10C). Under these conditions of transcription inhibition, decreased *XBP1* expression was also shown through diminished expression of *XBP1u* mRNA (Figure 2.10D) and an absence of long poly(A) tails on *XBP1* mRNA during the acute UPR (Figure 2.10B). In contrast, the length of *GAPDH* mRNA poly(A) tails did not show dramatic changes, with subtle changes of poly(A) tail length likely due to the gene's transcriptional status (Figure 2.10B). Together, these data suggest that inhibition of transcription abolishes the synthesis of long poly(A) tails of *XBP1* mRNA observed during the acute UPR.

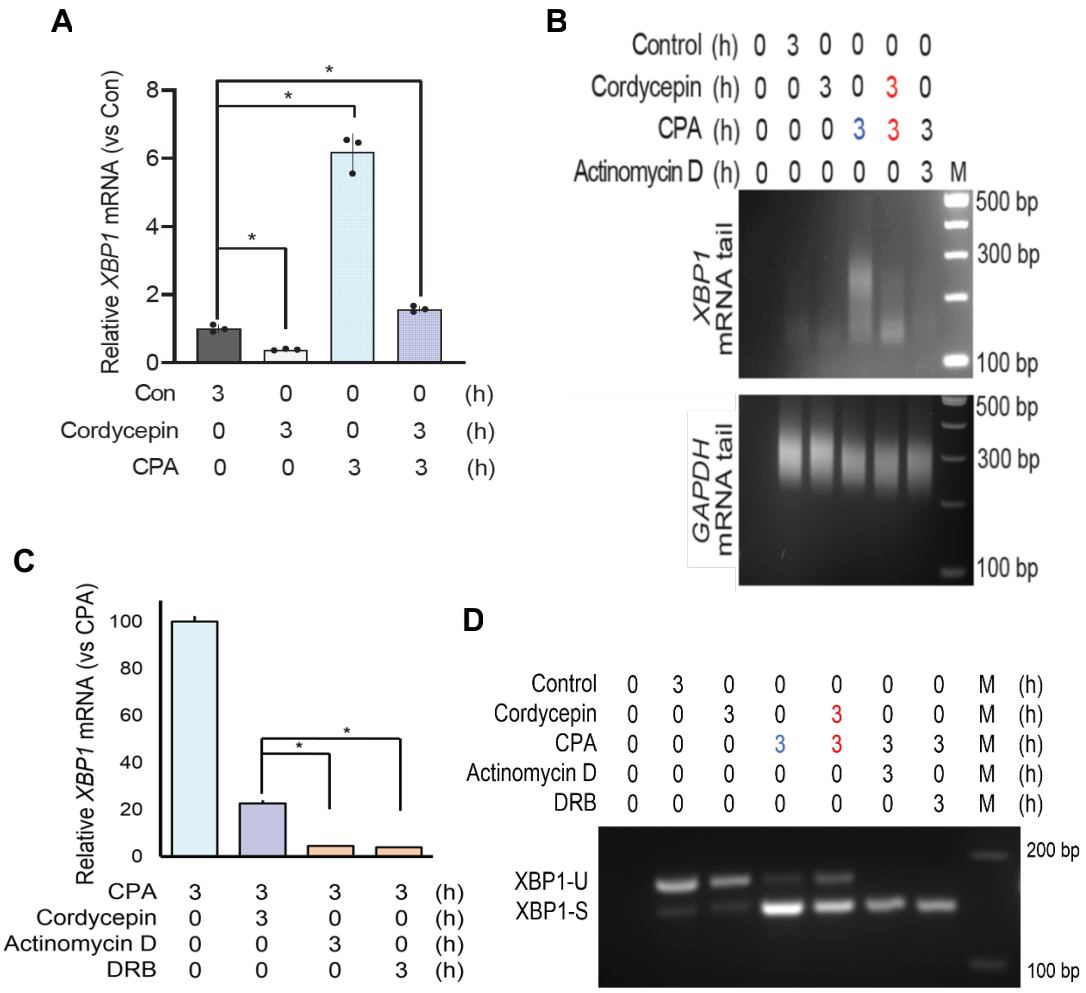

Figure 2. 10. Cordycepin treatment decreases *XBP1* mRNA poly(A) tail length and steady state level in WT MEF cells during the acute UPR.
(A) RT-qPCR analysis of *XBP1* mRNA steady state levels in MEF cells treated with DMSO (Con), CPA, cordycepin, or combined treatment of CPA and cordycepin (for 3 h). **(B)** Poly(A) tail length of *XBP1* and *GAPDH* mRNAs in MEF cells treated with DMSO (Con), CPA, cordycepin, or combined treatment of CPA with either cordycepin or actinomycin D (for 3 h). **(C)** RT-qPCR analysis of *XBP1* mRNA steady state levels in MEF cells treated with CPA, or combined treatment of CPA with cordycepin, actinomycin D or DRB (for 3 h). **(D)** *XBP1* mRNA spliced in the indicated cell treatments was demonstrated by RT-PCR analysis. Asterisks (*) indicate statistical significance of replicates with $P < 0.005$, S; *XBP1s* mRNA and U; *XBP1u* mRNA. M indicates 100 base-pair DNA ladder.

To investigate whether long poly(A) tails on *XBP1* mRNA contribute to the observed long half-life of the transcript during the acute UPR, WT MEF cells were treated with CPA in the presence or absence of cordycepin and the half-life of *XBP1* transcripts measured. The stability of *XBP1* mRNA upon cordycepin treatment together with CPA for 3 h was found to be greater as compared to the stability of *XBP1* mRNA upon CPA-treatment alone (Figure 2.11A). Notably, cordycepin treatment in the absence of ER stress had no significant effect on *XBP1* mRNA half-life (Figure 2.11A). Similarly, MEF cells were treated with Tg in the presence or absence of cordycepin and *XBP1* mRNA half-life was measured. Cordycepin treatment led to an increase in *XBP1* mRNA stability compared to cells treated with Tg alone (i.e., in the absence of cordycepin) (Figure 2.11B). Together, these data suggest that the accumulation of *XBP1* mRNA with long poly(A) tails does not necessary contribute to the observed increase in *XBP1* mRNA stability during the acute UPR, and the increased stability of *XBP1* mRNA during the acute UPR may reflect the metabolism of the population of short poly(A) tailed *XBP1* mRNA present at pre-stress conditions.

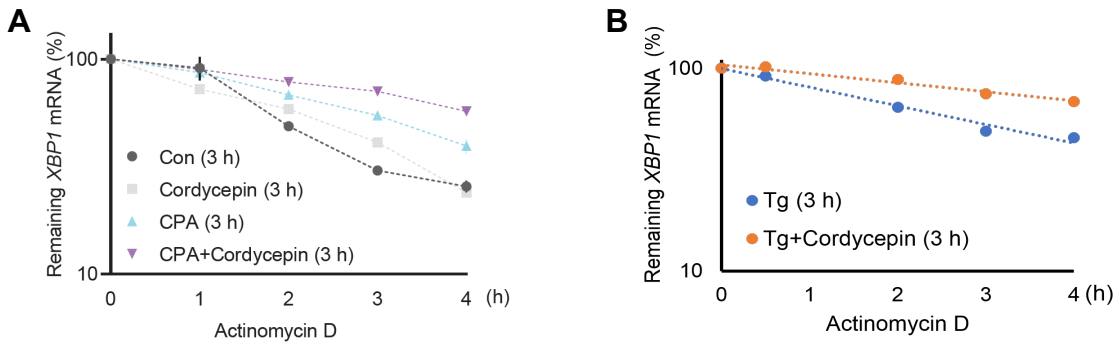

Figure 2. 11. Cordycepin treatment increases *XBP1* mRNA stability under the acute UPR in WT MEF cells.
(A) MEF cells were treated with DMSO (Con), CPA, cordycepin, or combined treatment of CPA and cordycepin for 3 h followed by actinomycin D treatment for the indicated durations. The half-life of *XBP1* mRNA was calculated as $t_{1/2}$ = Con: 2 +/- 0.3 h, cordycepin: 2.3 +/- 0.2 h, CPA: 3.5 +/- 0.3 h, and CPA+cordycepin: 5.3 +/- 0.1 h. **(B)** MEF cells were treated with Tg in the presence or absence of cordycepin for 3 h followed by actinomycin D treatment for the indicated durations. The half-life of *XBP1* mRNA was calculated as $t_{1/2}$ = Tg: 3.5 +/- 0.2 h, and Tg+cordycepin: 6.9 +/- 0.7 h.

In summary, this work investigated *XBP1* mRNA steady state levels and stability as a model to understand temporal gene regulation during the acute and chronic UPR phases in mammalian cells. Upon ER stress, the two mRNA isoforms of *XBP1* gene, *XBP1u* and *XBP1s* transcripts, are subjected to the same biphasic regulation during the UPR. Specifically, *XBP1* gene expression was upregulated during the acute phase of the UPR producing *XBP1u* mRNA with long poly(A) tails that spliced and undergoes rapid deadenylation to short poly(A) tails during the chronic phase of the UPR. Interestingly, the data revealed that transient stabilization of *XBP1* mRNA is coincident with accumulation of *XBP1* mRNA with long poly(A) tails during the acute UPR dependent on transcription and that these transcripts are destabilized as cells transition to the chronic UPR where short

poly(A) tails were common among tested genes. To investigate the correlation between mRNA stability and poly(A) tail length for *XBP1* mRNA, cordycepin treatment was used to block synthesis of long poly(A) tails on *XBP1* mRNA during the acute UPR and transcript half-life in the presence or absence of cordycepin was measured. Strikingly, I found that cordycepin treatment decreased accumulation of long poly(A) tails on *XBP1* mRNA, but stabilized *XBP1* transcripts during the acute UPR. Moreover, a comparison of the half-life of *XBP1* mRNA in phosphorylation competent and mutant eIF2α cells during the acute UPR revealed that the stability of *XBP1* mRNA is dependent on its translation status during the acute UPR. Given the observations that the length of poly(A) tail length is not directly involved in the increase in *XBP1* mRNA stability during the acute UPR, experiments to address whether long poly(A) tails facilitated *XBP1* mRNA translation during the acute UPR despite the eIF2α-P mediated translation repression were pursued.

CHAPTER 3: *XBP1* mRNA WITH LONG POLY(A) TAILS ESCAPES TRANSLATION REPRESSION DURING THE ACUTE PHASE OF UPR

The poly(A) tail length is dynamically regulated in the nucleus and cytoplasm (Bresson & Tollervey, 2018; Eckmann, Rammelt, & Wahle, 2011; Jalkanen, Coleman, & Wilusz, 2014; M. Stewart, 2019; Weill, Belloc, Bava, & Mendez, 2012). Studies on the role of poly(A) tails in mRNA translation are not conclusive. Some studies have indicated a positive correlation between long poly(A) tails and mRNA translation, while others have excluded such a relationship (Beilharz & Preiss, 2007; Eichhorn et al., 2016; Legnini, Alles, Karaiskos, Ayoub, & Rajewsky, 2019; Lim, Lee, Son, Chang, & Kim, 2016; Lima et al., 2017; Subtelny, Eichhorn, Chen, Sive, & Bartel, 2014). Upon ER stress, eIF2α phosphorylation severely impedes global mRNA translation, while promoting selective translation of ER stress mRNA such as *ATF4* via alternative mechanisms of translation (Figure 2.1A and Figure 2.3C) (Costa-Mattioli & Walter, 2020; Wek, 2018). Although selective mRNA translation predominantly utilizes specific features in mRNA 5′-UTRs including uORFs to escape the UPR-mediated translational repression, a few reports indicate the existence of additional uORF-independnet mechanisms during the acute stress phase (Guan et al., 2017; Jaud et al., 2020; Moro, Hermans, Ruiz-Orera, & Alba, 2021; Pavitt & Ron, 2012; van den Beucken et al., 2007; Wek, 2018). Here, I investigated the role of *XBP1* mRNA poly(A) tail length in mRNA translation during the acute and chronic UPR phases.

Regulation of poly(A) tails of *XBP1* mRNA during the acute UPR

To better understand what drives the observed changes in the poly(A) tail length during the UPR, UPR signaling events were tested. To investigate whether activation of PERK signaling that phosphorylates eIF2α leading to translation inhibition is involved in the observed increase in poly(A) tail length of *XBP1* mRNA during the acute phase of the UPR, the poly(A) tail length of *XBP1* and *GAPDH* mRNAs was evaluated under PERK inhibition. WT MEF cells were treated with PERKi, which is an ATP-competitive inhibitor of PERK enzymatic activity (Atkins et al., 2013; Guan et al., 2017), for 1 h prior to the end of DMSO or Tg treatment (for 1 h). Meanwhile, during the chronic UPR, WT MEF cells were treated with Tg for 12 h and added PERKi for additional 4 h. Under these conditions, no significant changes in the poly(A) tail length of *XBP1* and *GAPDH* transcripts compared to PERK-competent cells indicating that PERK-mediated translation inhibition was not essential for the increased poly(A) tail of *XBP1* mRNA during the acute UPR (compare Figure 2.6 and Figure 3.1). Next, the importance of *XBP1* mRNA splicing in regulation of *XBP1* mRNA poly(A) tails was addressed. IRE1α-deficient MEF cells, lacking the splicing activity, were treated with DMSO for 1 h or Tg for 1 or 16 h (K. Lee et al., 2002). The poly(A) tail length of *XBP1* and *GAPDH* mRNAs was found to be dynamic and the poly(A) tail length changes of *XBP1* and *GAPDH* mRNAs were independent of IRE1α splicing activity (Figure 3.1).

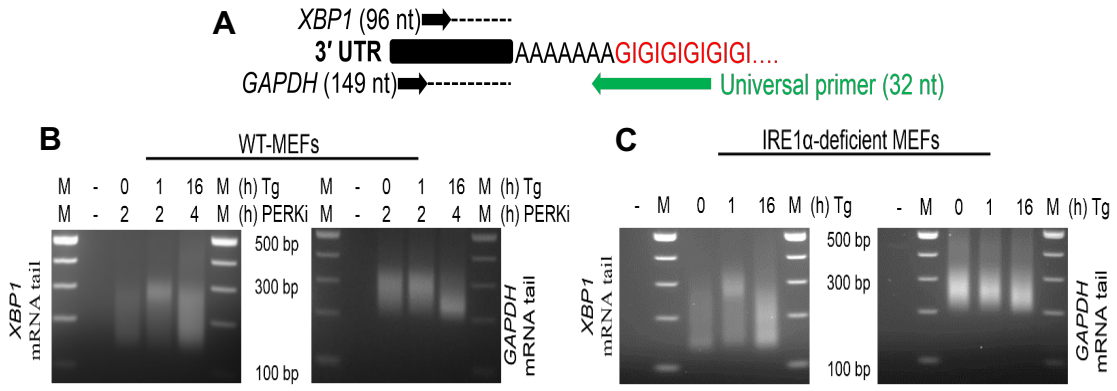

Figure 3. 1. Poly(A) tail length of *XBP1* and *GAPDH* mRNAs was independent of PERK activation and IRE1α splicing activity during UPR conditions.
(A) Schematic of the PCR-based poly(A) tailing assay for *XBP1* and *GAPDH* mRNAs. **(B)** Poly(A) tail length of *XBP1* (Left) and *GAPDH* (Right) mRNAs was analyzed in WT MEF cells treated with PERKi for 1 h prior to DMSO or Tg for 1 h. The chronic UPR was induced by Tg treatment for 16 h when PERKi was added in the last 4 h. **(C)** Poly(A) tail length of *XBP1* (Left) and *GAPDH* (Right) mRNAs was analyzed in IRE1α-deficient MEF cells treated with Tg for the indicated time. M indicates 100 base-pair DNA ladder.

Although cytoplasmic polyadenylation functions predominantly in specific cellular contexts such as early embryonic development and synaptic plasticity to activate specific mRNA translation (Charlesworth, Meijer, & de Moor, 2013), a recent study has shown the upregulation of Cytoplasmic Polyadenylation Element-Binding 4 (CPEB4) in response to ER stress in hepatocytes to mediate translational control of mRNA containing CPE-binding sites (Maillo et al., 2017). CPEB4 translation was also upregulated in WT MEF cells during the acute UPR (Guan et al., 2017). Therefore, I addressed whether CPEB4 involved in the observed increase in poly(A) tail length of *XBP1* mRNA during the acute UPR. With the courtesy of Dr. Mendez who provided CPEB4-deficient MEF cells, the poly(A)

tail length of *XBP1* mRNA under UPR conditions was evaluated in these cells. In the absence of

CPEB4, I did not observe any significant difference in the poly(A) tail length of *XBP1* and *GAPDH* mRNAs during the acute UPR (Figure 3.2). Therefore, this finding does not rule out the involvement of cytoplasmic polyadenylation during the acute UPR but shows that *XBP1* mRNA is not regulated by CPEB4 proteins.

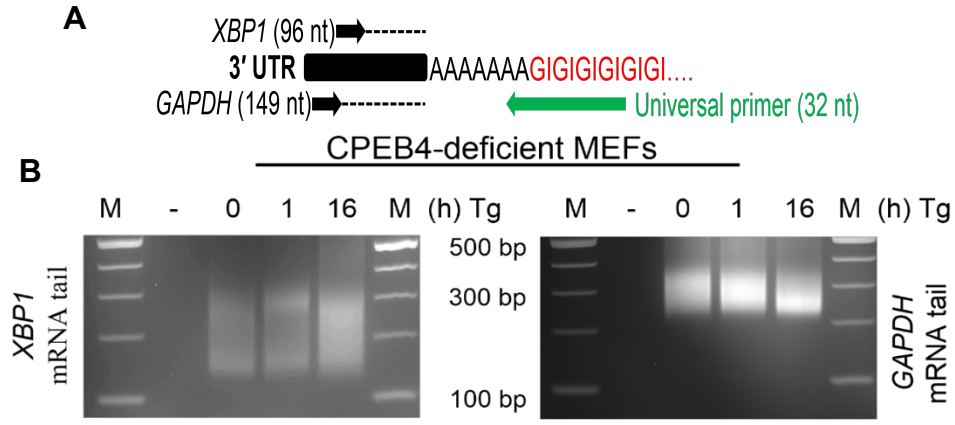

Figure 3. 2. CPEB4-mediated cytoplasmic polyadenylation does not regulate the poly(A) tail length of *XBP1* and *GAPDH* mRNAs during the UPR.
(A) Schematic of the PCR-based poly(A) tailing assay for *XBP1* and *GAPDH* mRNAs. **(B)** Poly(A) tail length of *XBP1* (Left) and *GAPDH* (Right) mRNAs in CPEB4-deficient MEF cells treated with Tg for the indicated time. M indicates 100 base-pair DNA ladder.

Long poly(A) tails of *XBP1* mRNA are preferentially associated with polyribosomes during the acute UPR

XBP1 mRNA was found to harbor long poly(A) tails during the acute UPR characterized by global translation inhibition (Figure 2.6). Investigating the impact of long poly(A) tails on *XBP1* mRNA translation would shed light on the importance

of poly(A) tail length during the acute UPR. To address the impact of poly(A) tail length on mRNA translation during the acute PR, polysome profiles of WT MEF under UPR conditions were analyzed. Polysome profile analysis utilizes ultracentrifugation to isolate complexes of the mRNA with ribosomes. Efficiently translated mRNA associate with more ribosomes and form larger complexes (polyribosomes/heavy polysomes). In contrast, inefficiently translated mRNA associate with fewer ribosomes and therefore form smaller complexes. This methodology can be used to determine changes in the translational efficiency of specific mRNA during stress, by monitoring the distribution of mRNA on polyribosomes with polysome profile analysis. With the help of Dr. Jobava, WT MEF cells were treated with DMSO (control), Tg for 1 h (acute UPR) or Tg for 16 h (chronic UPR) and cellular extracts were fractionated through sucrose gradients (Figure 3.3). As expected, polysome profiles show a dramatic decrease in heavy polysomes and an accumulation of monosomes in Tg-treated cells for 1 h, supporting the severe inhibition of translation during the acute UPR. The decreased percentage of monosomes and increased percentage of polyribosomes in Tg-treated cells for 16 h suggest a partial translational recovery during the chronic UPR as previously described (Figure 3.3) (Guan et al., 2017).

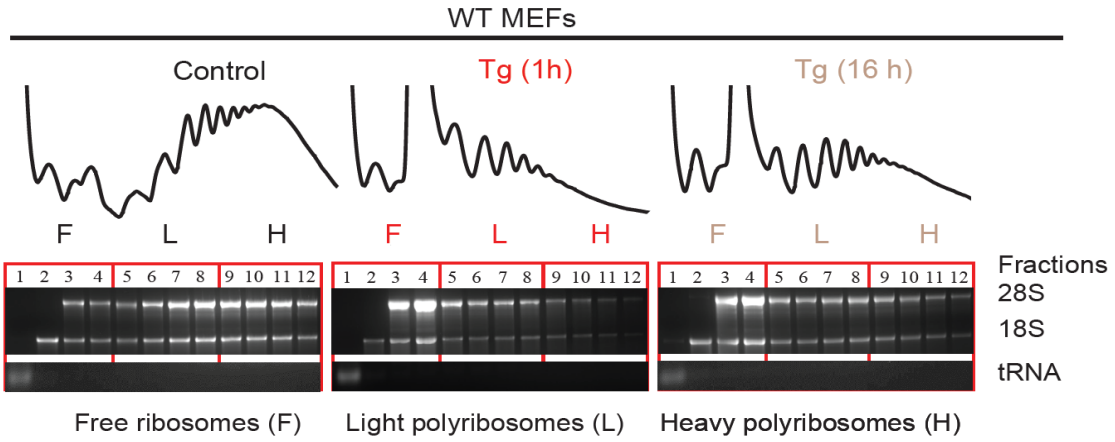

Figure 3. 3. Polysome profiles of WT MEF cells during UPR conditions.
(Top) Polysome profiles of WT MEF cells treated with Tg for 0, 1 and 16 h. (Bottom) RNA isolated from polysome fractions after cell extracts being subject to sucrose gradient ultracentrifugation and analyzed on agarose gels. Polysome fractions were later combined into 3 pools per cell treatment as shown: Polyribosome-Free Fractions (F), Light Polyribosomes (L), Heavy Polyribosomes (H).

Moreover, the PCR-based poly(A) tailing assay was performed for *XBP1* mRNA in RNA isolated from combined gradient fractions as explained in Figure 3.3 [Polyribosome-Free (F), Light Polyribosomes (L), and Heavy Polyribosomes (H)]. Strikingly, the long poly(A) tail of *XBP1* mRNA was associated with heavy polysomes during the acute UPR, at a time when global translation initiation is compromised (Figure 3.4). In contrast, a broader range of *XBP1* mRNA poly(A) tails was observed during the chronic UPR when inhibition of translation showed a partial recovery (Figure 3.4). This dynamic change of poly(A) tail length of *XBP1* mRNA on polyribosomes as cells transition from the acute to chronic UPR, may reflect co-translational deadenylation during the chronic UPR, as has been previously described in other systems (Duan, Jiao, He, & Yan, 2020; Vindry et al.,

2012). Taken together, these data suggest that two populations of *XBP1* mRNA exist during the acute UPR: one with relatively long poly(A) tails that escapes translational repression and can be found on polyribosomes, and the other with short poly(A) tails is translationally attenuated (Figure 3.4).

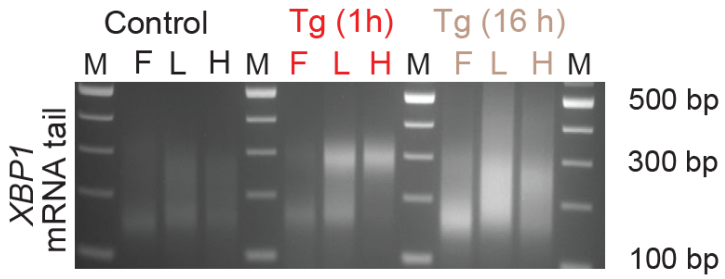

Figure 3. 4. Long poly(A) tailed *XBP1* mRNA escapes translational repression in WT MEF cells during the acute UPR.
PCR-based poly(A) tailing assay for *XBP1* mRNA in RNA isolated from the combined polysome fractions (i.e., F, L, and H fractions as explained in Figure 3.3) of WT MEF cells treated with Tg for 0 h (control), 1 h (acute UPR), and 16 h (chronic UPR). M indicates 100 base-pair DNA ladder.

The importance of long poly(A) tailed *XBP1* mRNA during the acute UPR

Induction of *XBP1* gene expression in response to ER stress result in the long poly(A) tails of the *XBP1* mRNA as confirmed by the transcriptional inhibition experiment (Figure 2.2A and Figure 2.10B). To further confirm whether long poly(A) tails of *XBP1* mRNA represent newly synthesized mRNA, RNA metabolic labeling was performed during the acute UPR. WT MEF cells were grown in control, acute, and chronic UPR conditions and pulse-labeled with 5-Ethynyl Uridine (5EU), an analog of uridine, for 1 h. The PCR-based poly(A) tailing assay was performed for *XBP1* mRNA in RNA isolated from both flow-through (old RNA)

and eluted (newly synthesized RNA) fractions (Figure 3.5). A homogeneous population of *XBP1* mRNA with long poly(A) tails was enriched in the eluted fraction, whereas the flow-through contained *XBP1* mRNA with shorter and heterogeneous poly(A) tail lengths (Figure 3.5). Strikingly, the data demonstrate that the newly synthesized *XBP1* mRNA during the acute UPR predominantly harbor long poly(A) tails, while those during the chronic UPR, present with different poly(A) tail length of *XBP1* mRNA (compare Figure 3.4 with Figure 3.5). I concluded that newly synthesized *XBP1* mRNA with long poly(A) tails escaped translational repression during the acute UPR. This finding reveals a potential new mechanism for select mRNA translation during the acute UPR dependent upon mRNA poly(A) tail length.

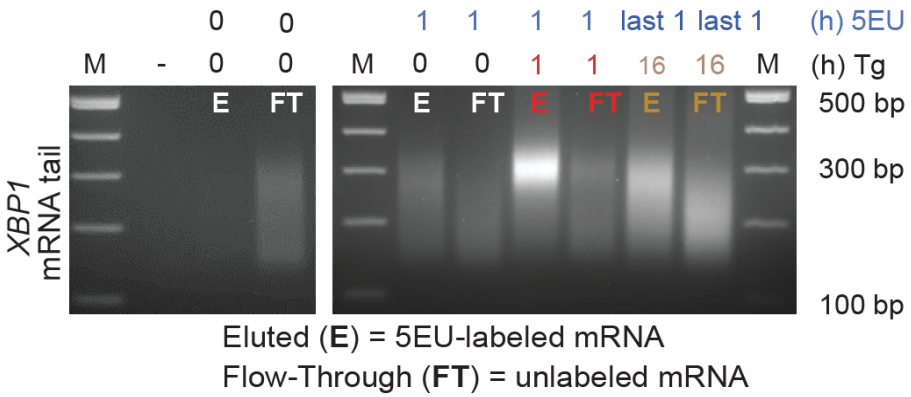

Figure 3. 5. Measurement of poly(A) tail length of 5EU-labeled and unlabeled *XBP1* mRNA in WT MEF cells during the UPR.
PCR-based poly(A) tailing assay for *XBP1* mRNA was evaluated in 5EU-labeled RNA isolated from WT MEF cells treated with Tg for 1, or 16 h, and pulse-labeled with 5EU (400 μM) in the last 1 h of Tg treatment. Vehicle (DMSO) was added in control cells for 1 h in the presence or absence of 5EU. Following the click chemistry reaction, 5EU-labeled RNA was immobilized by streptavidin beads and was eluted (E). The flow-through (FT) was also collected as unlabeled RNA. The PCR-based poly(A) tailing assay was performed on both E and FT fractions as previously described in Figure 2.6. M indicates 100 base-pair DNA ladder.

To investigate whether 5EU treatment can cause stress resulting in *XBP1* induction, 5EU-labeled *XBP1* pre-mRNA abundance was first measured in WT MEF cells pulse-labeled with 400 μM 5EU in the presence or absence of Tg treatments as indicated. In this experiment, forward primers designed at the junction of the last intron and exon of *XBP1* and *GAPDH* genes were used (Figure 3.6A). Compared to the unchanged 5EU-*GAPDH* pre-mRNA, 5EU-labeled *XBP1* pre-mRNA expression was found to be the least in control, while gradually increased during the acute UPR conditions followed by a decrease in expression under the chronic UPR (Compare Figure 3.6A with Figure 2.2A). The data suggest that 5EU labeling does not induce stress or interfere with UPR induction of *XBP1* mRNA. To further validate the data, protein synthesis in WT MEF cells treated with DMSO, 5EU, or Tg for 1 h was evaluated. Under these conditions, the protein synthesis was comparable between DMSO-treated and 5EU-treated MEF cells but decreased dramatically in Tg-treated MEF cells, as expected (Figure 3.6B). This finding confirms that 5EU treatment does not evoke stress and consequently translation repression.

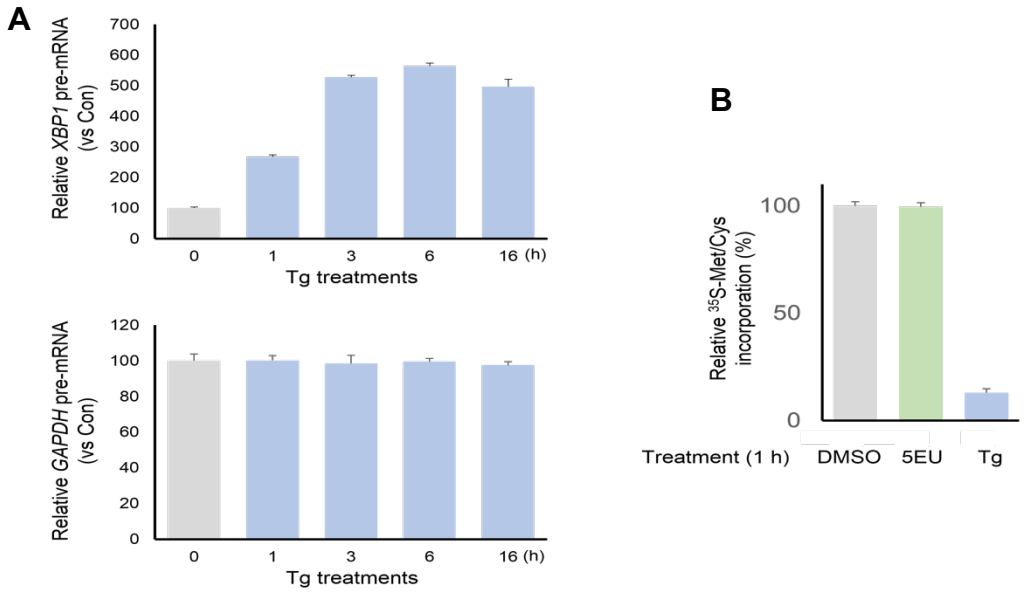

Figure 3. 6. The effect of 5EU-RNA labeling on XBP1 and GAPDH gene expression and global protein synthesis in WT MEF cells.
(A) RT-qPCR analysis of *XBP1* (Top) and *GAPDH* (Bottom) pre-mRNA abundance, after being normalized to total *GAPDH* mRNA, in WT MEF cells pulse-labeled with 5EU for 1 h prior to the end of Tg treatment as indicated. Vehicle (DMSO) was used in control cells for 1 h in the presence of 5EU. **(B)** Protein synthesis was measured using [^{35}S]-Met/Cys incorporation into proteins of WT MEF cells treated with DMSO or 5EU or Tg for 1 h.

Furthermore, the contribution of long poly(A) tails of *XBP1* mRNA to the produced XBP1s proteins during the acute UPR was assessed by inhibiting the production of newly synthesized *XBP1* mRNA with long poly(A) tails using transcriptional inhibitor actinomycin D as shown previously (Figure 2.10B). WT MEF cells were treated with DMSO or CPA in the presence or absence of actinomycin D for 3 h and XBP1s protein expression was analyzed. XBP1s protein expression during the acute UPR was negatively influenced despite the presence of other UPR markers such as ATF4 and eIF2α-P (Figure 3.7). Taken together, the data indicate the acute phase of the UPR involves an unrecognized

mechanism of selective mRNA translation via the synthesis of mRNA with long poly(A) tails that escapes eIF2α-P-mediated translational repression and allows synthesis of proteins encoded by transcriptionally-induced genes.

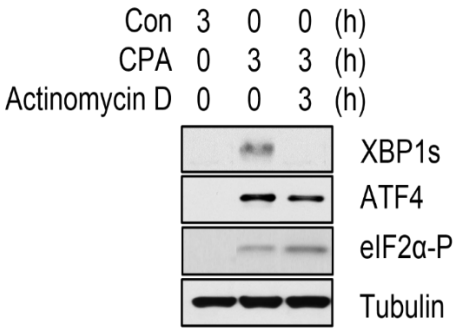

Figure 3. 7. The importance of newly synthesized mRNA on XBP1s protein expression in WT MEF cells during the acute UPR.
Western blot analysis of a few ER stress markers including XBP1s, eIF2α-P and ATF4 proteins in WT MEF cells treated with DMSO (Con) or CPA (acute UPR) for 3 h in the presence or absence of actinomycin D.

To address the fate of the *XBP1s* mRNA during recovery from acute UPR, WT MEF cells were exposed to ER stress for 1 h using CPA treatment and then CPA was washed away from these cells for up to 4 h. First, protein synthesis inhibition was restored fast by removing CPA from CPA-treated cells (i.e., washouts), as expected (Figure 3.8A). The increase in *XBP1s* mRNA steady state levels and poly(A) tail length decreased gradually during recovery from stress (Figure 3.8B and Figure 3.8C), in contrast to the XBP1s protein which showed increased accumulation during recovery from stress, at a time that the stress-induced signaling proteins declined (Figure 3.8D). Specifically, the lower molecular weight of PERK proteins after phosphorylation-dependent shift under the acute UPR and dephosphorylation of eIF2α are indicative of UPR deactivation. Following

that, ATF4 protein expression disappeared earlier than XBP1s protein (Figure 3.8D). Together, these data imply the increased accumulation of translationally repressed *XBP1s* mRNA during the acute UPR, generates a cellular reserve mRNA pool for efficient translation and XBP1s protein synthesis during recovery from acute ER stress. In contrast, the accumulation of long poly(A) tails of *XBP1* mRNA during the acute UPR, is the result of stress-induced transcription and serves as a translationally competent mRNA pool allowing synthesis of XBP1s protein during stress (Figure 3.8D). Of note, stress-induced mRNAs that have long half-lives, such as *BiP*, are translated better during the recovery from acute stress leading to the accumulation of their encoded proteins (Figure 3.8D).

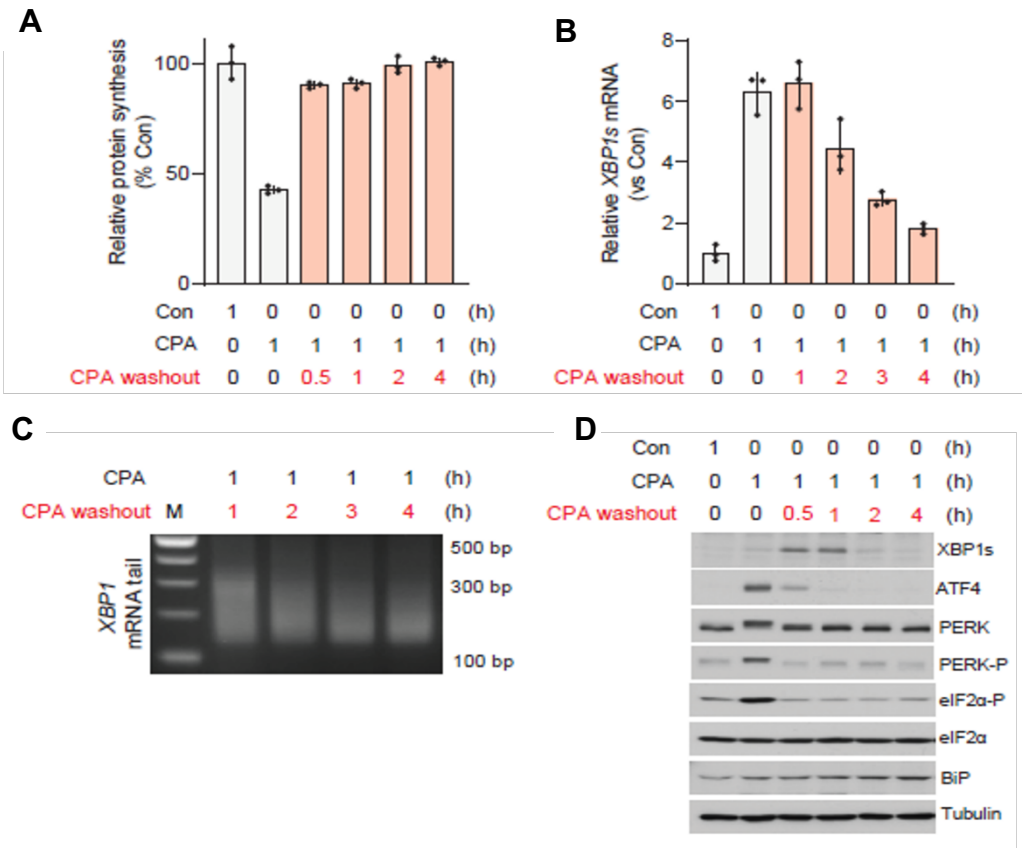

Figure 3. 8. Recovery from the acute UPR involves termination of the PERK-mediated signaling and induction of XBP1s protein.
(A) Protein synthesis was measured using [^{35}S]-Met/Cys incorporation into proteins of WT MEF cells treated with either DMSO (Con) or CPA for 1 h, or CPA-treated cells for 1 h followed by the removal of CPA (CPA washouts) for 0.5, 1, 2, and 4 h. **(B)** RT-qPCR analysis of *XBP1s* mRNA steady state levels in MEF cells treated with DMSO (Con), CPA for 1 h, or CPA washouts for 1, 2, 3, 4 h. **(C)** PCR-based poly(A) tailing assay for *XBP1* mRNA in MEF cells treated with CPA for 1 h followed by washing away CPA from CPA-treated cells (CPA washouts) for 1, 2, 3, 4 h. **(D)** Western blot analysis of the indicated proteins in WT MEF cells treated with DMSO (Con), CPA for 1 h, or CPA washouts for 0.5, 1, 2, 4 h. M indicates 100 base-pair DNA ladder.

In summary, possible regulations involved in *XBP1* mRNA poly(A) tail length during UPR conditions were examined. The long poly(A) tail of *XBP1* mRNA was found to be not regulated by the PERK signaling pathway nor IRE1α splicing of *XBP1* mRNA. In addition, CPEB4, an RNA-binding protein that recruits cytoplasmic PAPs to extend mRNA poly(A) tails, does not play a role in the poly(A) tail length of *XBP1* mRNA during the acute UPR. Importantly, the induced transcription of the *XBP1* gene drives the long poly(A) tail of *XBP1* transcripts during the acute UPR as shown by 5EU-labeled *XBP1* mRNA. Notably, 5EU labeling does not inhibit mRNA translation or interfere with *XBP1* gene expression during the UPR. In addition to the well-known uORF mechanism of translation during acute stress conditions (Wek, 2018), I propose that the long poly(A) tail is a novel mechanism to escape translational inhibition during the acute UPR. This notion is supported by the association of long poly(A) tails of *XBP1* mRNA with polyribosomes and the diminished XBP1s protein in response to the treatment of transcriptional inhibitor actinomycin D during the acute UPR. Interestingly, the XBP1s protein was persistent during recovery from acute ER stress. This study illustrates the temporal regulation of *XBP1* gene as a model during the UPR. Experiments to compare regulation of other gene expressions were pursued to demonstrate how pervasive this regulation is during the UPR.

CHAPTER 4: BROAD SIGNIFICANCE OF TEMPORAL REGULATION OF GENE EXPRESSION DURING THE UPR

UPR reprogramming of gene expression involves different mechanisms, including transcription, mRNA translation, and mRNA decay (Arensdorf et al., 2013; Jaud et al., 2020; Le Thomas et al., 2021; Namkoong, Ho, Woo, Kwak, & Lee, 2018). Although many studies have focused on the importance of transcriptional control in adaptation to chronic ER stress and translational control during acute ER stress, the importance of acute UPR-induced transcription is less well-studied (Gonen et al., 2019; Guan et al., 2017). A recent study has demonstrated a correlation between long poly(A) tail mRNA and increased stability and translation for a number of stress-induced mRNAs (Woo et al., 2018). Here, I investigated the prevalence of the UPR temporal regulation highlighting the importance of newly synthesized UPR transcripts during the acute phase of the UPR.

Long poly(A) tails are a characteristic of ER stress-induced transcripts during the acute phase of the UPR

To identify whether the temporal regulation of poly(A) tail length of *XBP1* mRNA was a feature of other UPR-induced gene transcripts, *ATF4* and *BiP* mRNAs were selected as UPR-induced genes from our previous study (Guan et al., 2017). First, the UPR induction of these genes was confirmed by treating WT MEF cells with Tg for the indicated durations and quantifying the steady state levels of *ATF4* and *BiP* transcripts by RT-qPCR. Although the *ATF4* mRNA was induced in response to the UPR, its steady state levels declined during the chronic

UPR. On the other hand, *BiP* mRNA expression remained induced even following the transition to the chronic UPR (Figure 4.1A). These data are in agreement with previous reports that concluded unstable *ATF4* mRNA compared to the long half-life of *BiP* mRNA during UPR conditions (Rutkowski et al., 2006). Under acute and chronic UPR conditions, the poly(A) tail length for *ATF4* and *BiP* transcripts was estimated using the PCR-based tailing assay. The poly(A) tail length of *ATF4* and *BiP* mRNAs was long in response to the acute UPR, similar to long poly(A) tail of *XBP1* mRNA (compare Figure 2.6 with Figure 4.1B). During the chronic UPR, these transcripts had heterogeneous size of poly(A) tail lengths. Of note, BiP mRNA had two populations of poly(A) tail during the chronic UPR and that could be reflected by the continuous gene expression of *BiP* (Figure 4.1A).

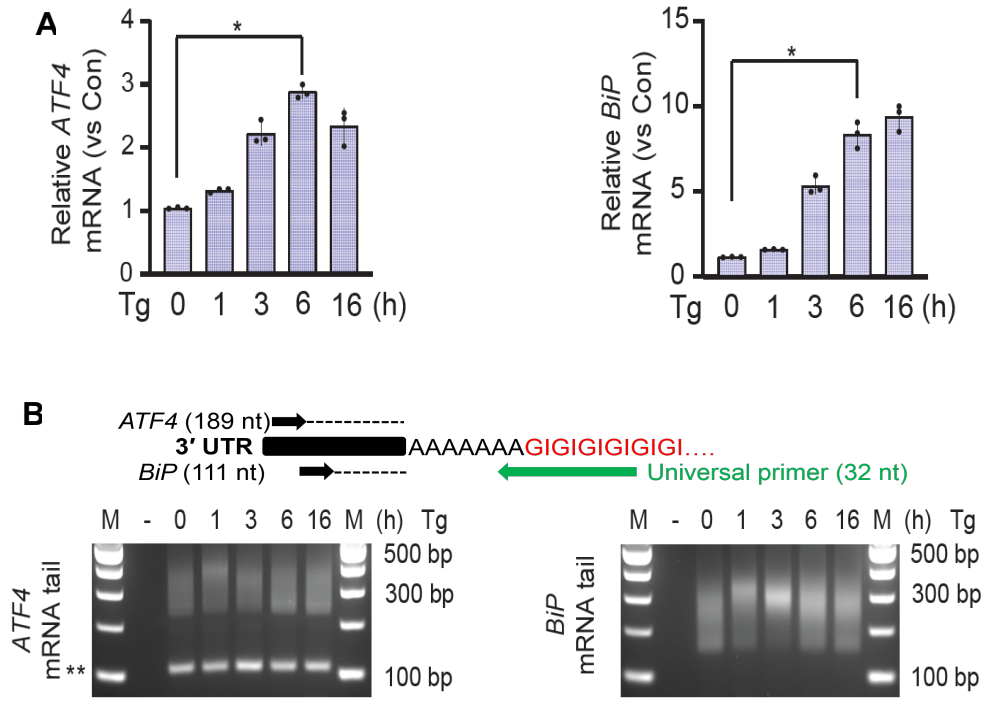

Figure 4. 1. Temporal regulation of UPR-regulated gene expression in WT MEF cells during UPR conditions.
(A) RT-qPCR analysis of *ATF4* and *BiP* mRNA steady state levels in WT MEF cells treated with Tg as indicated. **(B)** (Top) Schematic of the PCR-based poly(A) tailing assay for *ATF4* and *BiP* mRNAs. (Bottom) Poly(A) tail length of *ATF4* (Left) and *BiP* (Right) mRNAs in WT MEF cells treated with Tg for the indicated time was analyzed as explained in Figure 2.6. Asterisks (*) indicate statistical significance of replicates with $P < 0.0005$ for *ATF4* mRNA and $P < 0.005$ for *BiP* mRNA. Double asterisks (**) indicate artifact bands. M indicates 100 base-pair DNA ladder.

Based on our reported study (Guan et al., 2017), a few non UPR-regulated genes were selected to compare with the regulation of *GAPDH* mRNA, previously used as a control in the experimental system. Under the same UPR conditions, the steady state levels of non UPR-regulated *SEC24D* and *ATP Synthase F1 Subunit-β* (*ATP5B)* mRNAs were found with negligible changes in their levels (Figure 4.2A). Similarly, the poly(A) tail length of these transcripts did not show any significant change in response to the acute UPR. Interestingly, their poly(A) tail length was

either unchanged or shorter during the chronic UPR compared to the acute UPR indicating that some mRNAs are specifically regulated during the chronic UPR. The latter finding of short poly(A) tail during the chronic UPR is consistent with the poly(A) tail of *GAPDH* mRNA (compare Figure 2.6 with Figure 4.2B for *ATP5B* mRNA). Overall, these data indicate that the UPR-induced mRNA show an increase in mRNA poly(A) tails that may serve a functional significance post-transcriptionally, especially when bulk mRNA translation is repressed during the acute UPR.

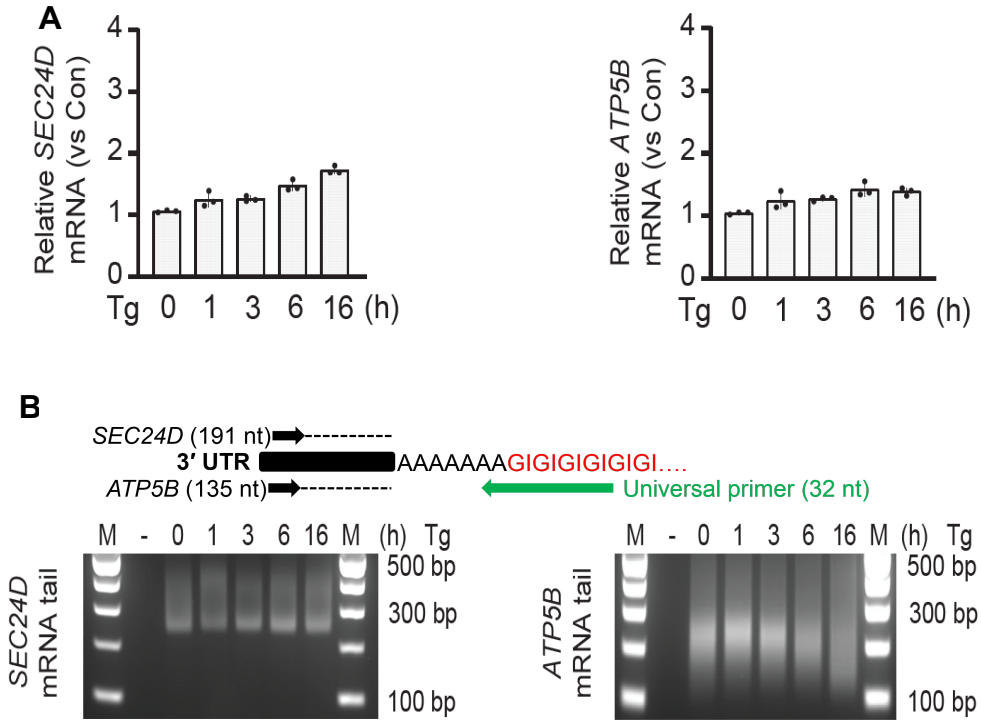

Figure 4. 2. Temporal regulation of non UPR-induced genes in WT MEF cells during UPR conditions.
(A) RT-qPCR analysis of *SEC24D* and *ATP5B* mRNA steady state levels in WT MEF cells treated with Tg as indicated. **(B)** (Top) Schematic of the PCR-based poly(A) tailing assay for *SEC24D* and *ATP5B* mRNAs. (Bottom) Poly(A) tail length of *SEC24D* (Left) and *ATP5B* (Right) mRNAs in WT MEF cells treated with Tg for the indicated time was analyzed as explained in Figure 2.6. M indicates 100 base-pair DNA ladder.

The UPR temporal regulation of gene expression is recapitulated in different cell types

Recently, we published that CPA-treated Mouse Pancreatic β (MIN6) cells induced the UPR that negatively regulated the well-known β-cell-specific markers (C. W. Chen et al., 2022). To demonstrate that the UPR temporal regulation of *XBP1* expression was not limited to WT MEF cells, MIN6 cells were exposed to CPA for up to 12 h and estimated the *XBP1* mRNA steady state levels and poly(A) tail length during UPR conditions. As expected, *XBP1* gene expression was induced upon CPA treatment and the poly(A) tail length of *XBP1* mRNA was dynamic, similar to *XBP1* gene expression in CPA-treated WT MEF cells (compared Figure 4.3 with Figure 2.6). Similar to *GAPDH* regulation in WT MEF cells during the chronic UPR, the poly(A) tail length of *GAPDH* mRNA in MIN6 cells was decreased under the chronic UPR (compare Figure 4.3B with Figure 2.6). These data reinforce that temporal regulation of poly(A) tail length is pervasive in different cell types during the UPR.

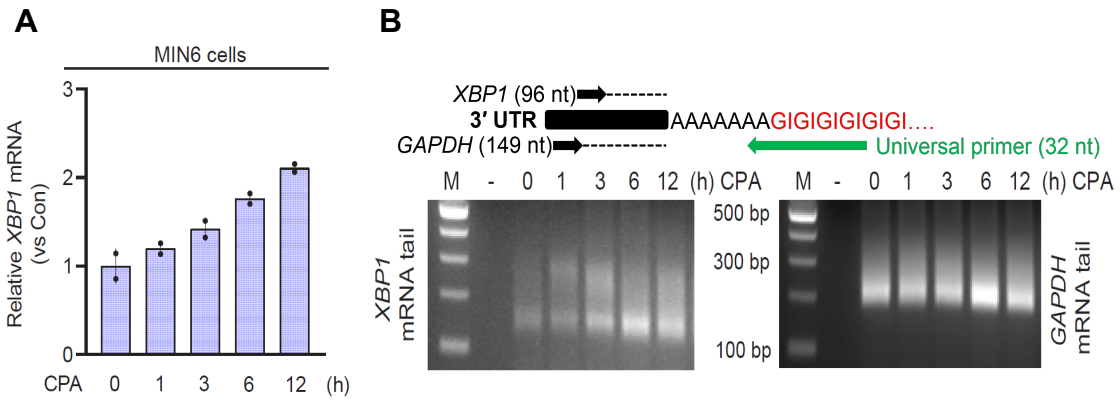

Figure 4. 3. Temporal regulation of *XBP1* mRNA during the UPR in mouse pancreatic β cells (MIN6) cells.
(A) RT-qPCR analysis of *XBP1* mRNA steady state levels in MIN6 treated with CPA for the indicated time. **(B)** (Top) Schematic of the PCR-based poly(A) tailing assay for *XBP1* and *GAPDH* mRNAs. (Bottom) Poly(A) tail length of *XBP1* and *GAPDH* mRNAs in MIN6 cells treated with CPA for the indicated time was analyzed as in Figure 2.6. M indicates 100 base-pair DNA ladder.

Furthermore, I evaluated the poly(A) tail length of *MAF bZIP Transcription Factor A* (*MAFA*), a β-cell-specific marker that is downregulated during the UPR as discussed in our paper (C. W. Chen et al., 2022). *MAFA* mRNA steady state levels and poly(A) tail length were estimated in CPA-treated MIN6 cells. *MAFA* expression was gradually decreased after 1 h of CPA treatment as MIN6 cells transition to the chronic UPR (Figure 4.4A). Interestingly, the poly(A) tail length of *MAFA* mRNA was observed with minimal changes among UPR conditions except that it became shorter and less expressed during the chronic UPR (Figure 4.4B). The short poly(A) tails of *MAFA* mRNA are consistent with the low MAFA protein expression during the chronic UPR likely due to mRNA degradation. In a separate experiment, the half-life of *MAFA* mRNA in MIN6 cells treated with DMSO (Con) and CPA (chronic UPR) for 12 h was compared. With the assumption that the short

poly(A) tail length would decrease the half-life of *MAFA* mRNA, *MAFA* mRNA was found to be less stable in control than CPA-treated MIN6 cells for 12 h despite *MAFA* mRNA being more abundant in control than chronic UPR (Figure 4.4C). This striking observation was consistent with other downregulated β-cell-specific markers such as *Pancreas/Duodenum Homeobox Protein 1* (*PDX1*) and *NK2 Homeobox 2* (*NKX2-2*) during the chronic UPR in MIN6 cells (Figure 4.5). The subtle increase in the stability of β-cell-specific mRNA may reflect their translation status that is downregulated during the chronic UPR (C. W. Chen et al., 2022). These data suggest an anti-correlation between mRNA translation and stability. Furthermore, the decreased steady state level of β-cell identity mRNAs during the chronic UPR suggests the involvement of nuclear gene regulation mechanisms which will be explored in future studies.

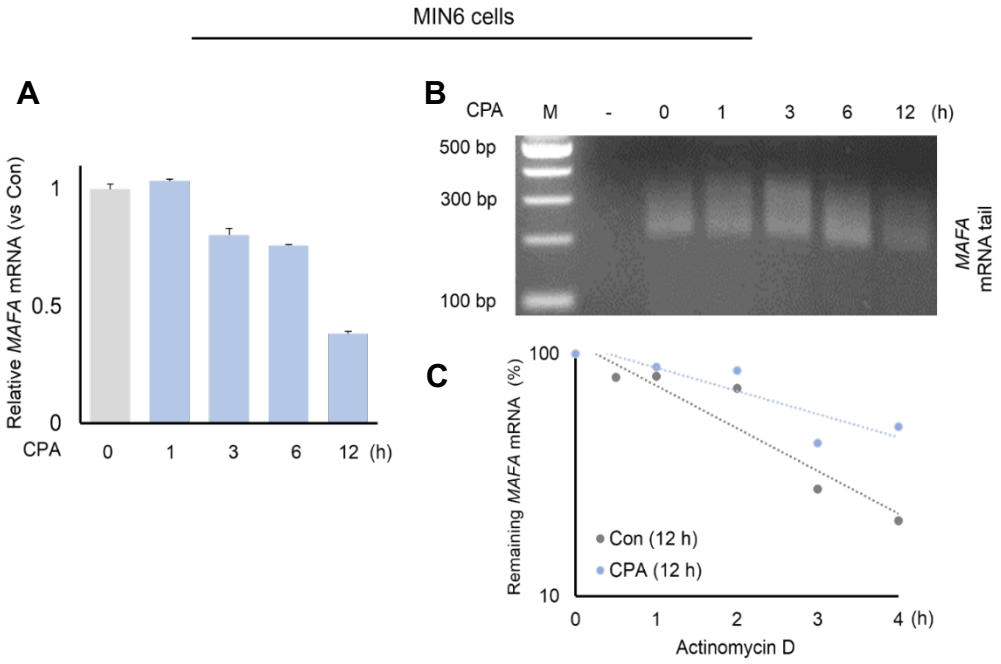

Figure 4. 4. Temporal regulation of *MAFA* mRNA steady state levels and poly(A) tail length during UPR conditions in MIN6 cells.
(A) RT-qPCR analysis of *MAFA* mRNA steady state levels in MIN6 treated with CPA for the indicated time. **(B)** Poly(A) tail length of *MAFA* mRNA in MIN6 cells treated with CPA as indicated. The assay was performed as explained in Figure 2.6. **(C)** *MAFA* mRNA half-life was determined by treating MIN6 cells with DMSO (Con) or CPA for 12 h. Following DMSO and CPA treatment, actinomycin D was added for 0, 0.5, 1, 2, 3, and 4 h, and *MAFA* mRNA half-life was calculated as DMSO: 2.3 +/- 0.6 h, and CPA: 3.5 +/- 0.8 h. M indicates 100 base-pair DNA ladder.

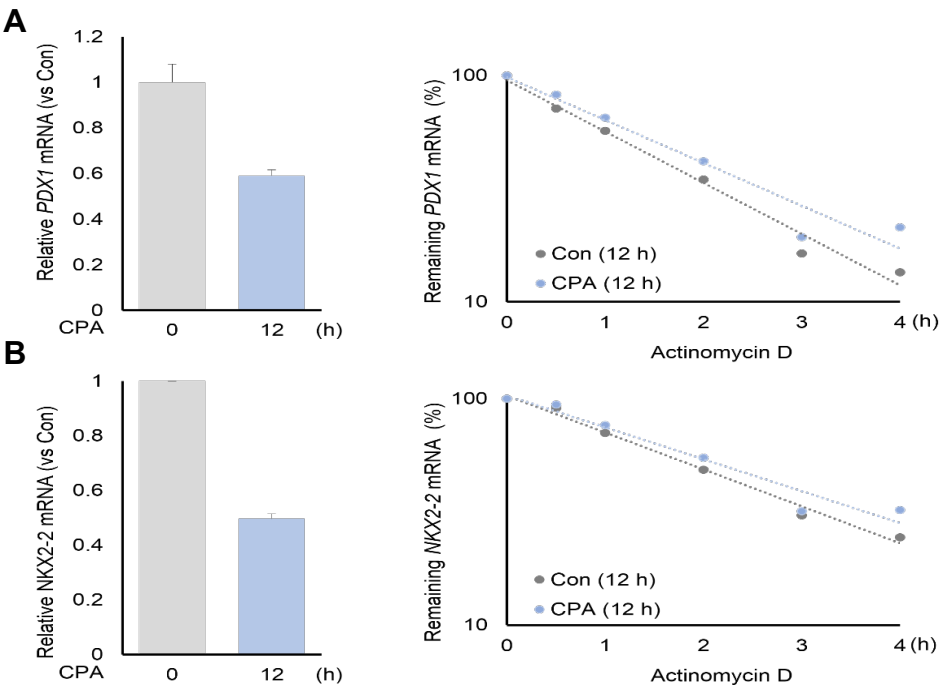

Figure 4. 5. β-cell-specific mRNA steady state level and stability during the chronic UPR in MIN6 cells.
(A) (Left) RT-qPCR analysis of *PDX1* mRNA steady state levels in MIN6 treated with DMSO or CPA for 12 h. (Right) *PDX1* mRNA half-life in MIN6 cells under control and chronic UPR conditions was calculated as $t_{1/2}$ = Con: 1.1 +/- 0.1 h, CPA: 1.5 +/- 0.1 h. **(B)** RT-qPCR analysis and half-life of *NKX2-2* mRNA in MIN6 treated with DMSO or CPA for 12 h. The half-life of *NKX2-2* mRNA was calculated as $t_{1/2}$ = Con: 1.7 +/- 0.1 h, CPA: 2.3 +/- 0.2 h.

Polyadenylation of UPR-induced transcripts promotes cell survival during the acute UPR

To explore the effect of newly synthesized mRNA on cell survival during the acute phase of the UPR, the cell viability of WT MEF cells in response to cordycepin treatment during acute UPR was measured. In this experiment, polyadenylation was inhibited in these cells by supplementing the growth media with cordycepin in the presence or absence of CPA for 3 h. Surprisingly, cell viability was not affected after DMSO, cordycepin, or CPA treatment for 3 h in WT

MEF cells (Figure 4.6). In contrast, cell viability under a simultaneous treatment of CPA and cordycepin for 3 h was decreased (Figure 4.6). This finding highlights the importance of gene expression regulation during the acute UPR.

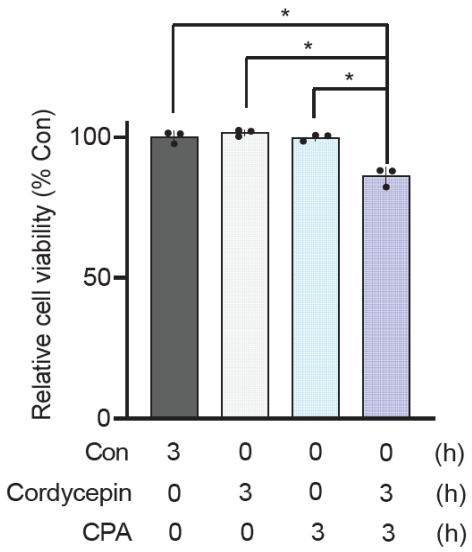

Figure 4. 6. Nascent RNA polyadenylation promotes cell survival during the acute UPR in WT MEF cells.
Cell survival assay was evaluated in MEF cells treated with DMSO (Con), CPA, cordycepin, or combined CPA and cordycepin for 3 h. Asterisks (*) indicate statistical significance of replicates with $P < 0.05$.

To determine whether *XBP1* expression alone is required for stress recovery, cell viability of WT- and XBP1-deficient MEF cells, obtained from Dr. Kaufman, was tested after being treated with DMSO (Con), CPA for 3 h, or CPA for 3 h followed by CPA removal for 6 h and 16 h. Under these conditions, cell survival in these cells was indistinguishable between DMSO (Con) and CPA treatment for 3 h (Figure 4.7), confirming previous results (Figure 4.6). Although the viability of these cells was decreased during the first 6 h of recovery following the acute UPR, they gradually returned after 16 h of CPA removal from media

(Figure 4.7). Together, these data indicate no difference in the recovery from the acute UPR between WT and XBP1-deficient MEF cells suggesting that the entire newly synthesized transcriptome assists recovery from the acute UPR and that a single protein such XBP1s is not sufficient for stress recovery.

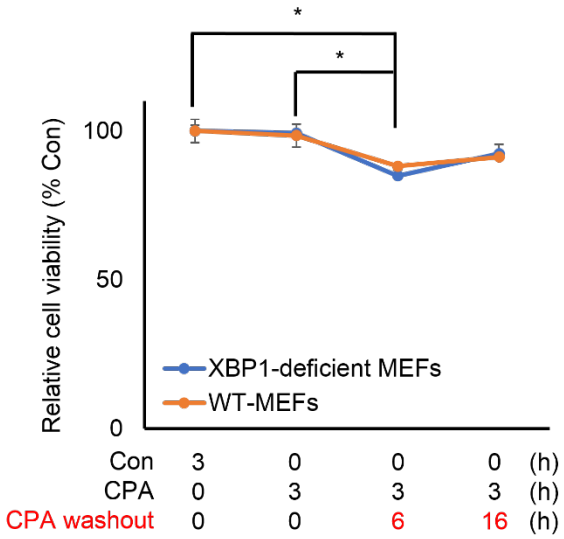

Figure 4. 7. The absence of XBP1s protein alone does not affect the recovery from acute UPR in WT MEF cells.

Cell survival assay was evaluated in WT and XBP1-deficient MEF cells treated with DMSO (Con), CPA for 3 h or CPA for 3 h followed by CPA washouts for 6 or 16 h. Asterisks (*) indicate statistical significance of replicates with $P < 0.05$ for WT and $P < 0.005$ for XBP1-deficient MEFs.

In summary, the long poly(A) tails are a feature of UPR-induced transcripts during the acute UPR. However, short poly(A) tails are common among tested transcripts during the chronic UPR that needs further investigations to unravel the mechanisms controlling the poly(A) tail length under the chronic UPR. In addition, regulation of poly(A) tail length was specific to the induction of gene expression during the UPR regardless of cell types tested. Interestingly, UPR-downregulated β-cell-specific mRNAs in MIN6 cells are slightly more stable compared to control

conditions, despite their decreased steady state levels. These findings may indicate an inverse correlation between mRNA stability and mRNA accumulation during the chronic UPR for selected transcripts. Finally, I demonstrated that the UPR-induced mRNA with long poly(A) tails are critical for cell survival during the acute UPR. This finding was not specific to the absence of a single UPR marker such as the XBP1s protein. Therefore, the entire UPR-induced gene expression during the acute UPR is important for cell survival and restoration of ER homeostasis.

CHAPTER 5: DISCUSSION AND FUTURE DIRECTIONS

Discussion

A new mechanism of translational control is identified for *XBP1* gene expression during the UPR through the length of the poly(A) tail. During the acute UPR, two discrete populations of *XBP1* mRNA, with either short or long poly(A) tails, are observed. The long poly(A) tailed *XBP1* mRNA is derived from newly synthesized mRNA generated by stress-induced transcription of the *XBP1* gene and escapes translational inhibition. The short poly(A) tailed *XBP1* mRNA, on the other hand, is translationally repressed and stabilized. Because the half-life of *XBP1* mRNA is short and its transcription is massively upregulated, progression from acute to chronic ER stress involves continuous enrichment with long poly(A) tail *XBP1* mRNA, while the mRNA with short poly(A) tails produced pre-stress is gradually depleted. Interestingly, during the chronic UPR, heterogeneous poly(A) tail length *XBP1* mRNA was translationally de-repressed and destabilized, as described below (Model 1). Although the focus of this work was the regulation of the *XBP1* gene, I also showed similar biphasic regulation of poly(A) tail length of other stress-induced mRNAs, suggesting a more global mechanism of gene regulation during the UPR. I conclude that cells exhibit biphasic regulation of translation and stability during ER stress; during the acute phase of ER stress, newly synthesized mRNA is protected from translational repression via the long poly(A) tails, thus initiating synthesis of pro-adaptive proteins. In the second phase of adaptation to chronic ER stress, expression of adaptive proteins is limited most

likely via co-translational mRNA deadenylation and degradation. This biphasic response limits the UPR threshold and prolongs adaptation to chronic ER stress.

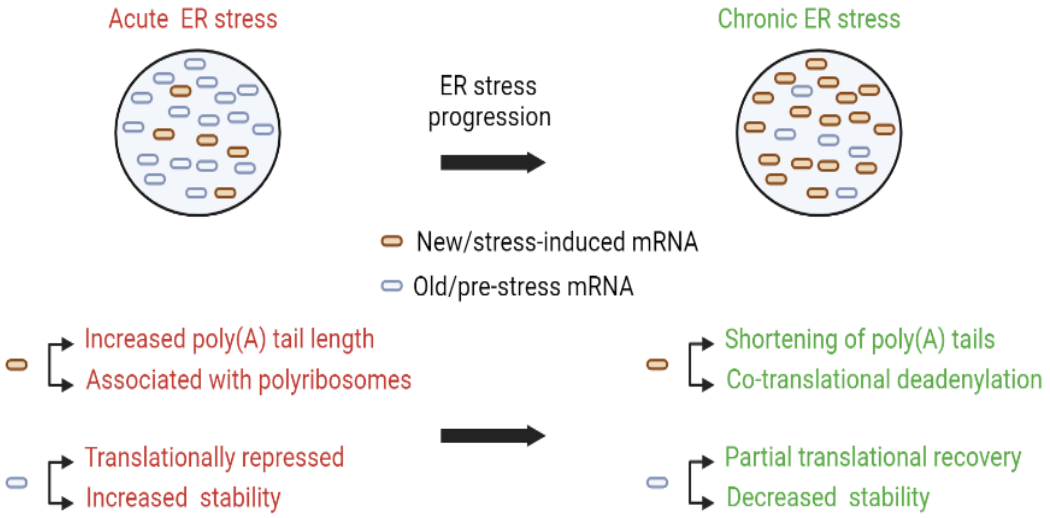

Model 1. *XBP1* mRNA regulation during acute and chronic ER stress.
The steady state of the acute ER stress consists of different populations of *XBP1* mRNA. During the acute phase of ER stress, the pre-ER stress (old) mRNA is translationally repressed and stabilized. However, the newly synthesized (new) mRNA has long poly(A) tails and escapes translational repression. During the chronic phase of ER stress, the pre-ER stress (old) mRNA is partially translationally derepressed and becomes unstable. Meanwhile, the newly synthesized (new) mRNA is subject to poly(A) tail shortening due to co-translational deadenylation. This figure was created by Biorender.com.

The phenomenon of coupling mRNA translation to stability was first described decades ago (Peltz, Donahue, & Jacobson, 1992; Stimac, Groppi, & Coffino, 1984). Physiological processes such as mitosis or stress conditions that involve transient inhibition of protein synthesis are also characterized by transient mRNA stabilization (Kawai et al., 2004; Majumder et al., 2012; Ross, 1997; Tanenbaum, Stern-Ginossar, Weissman, & Vale, 2015). The mechanisms for this regulation are still obscure; however, they are likely to involve the suggested loss

of interaction between the stabilized mRNA and factors of the degradation machinery when their translation is inhibited (Heck & Wilusz, 2018; Morris, Cluet, & Ricci, 2021). This would agree with more current reports of mRNA degradation occurring co-translationally (Pelechano, Wei, & Steinmetz, 2015). An alternative mechanism of regulation of mRNA stability via poly(A) tail length during the UPR may be via addition of non-A nucleotides of the poly(A) tail. Recent reports suggest that poly(A) tails may contain other nucleotides than A′s, such as G′s and U′s; guanylated poly(A) tails tend to be associated with long poly(A) tails and positively correlate with mRNA half-life, whereas uridylation is more common in short poly(A) tails and negatively correlates with mRNA half-life (H. Chang, Lim, Ha, & Kim, 2014; Lim et al., 2018). It will be interesting to study if heterogenous poly(A) tails are involved in the biphasic mechanism of the regulation of poly(A) tail length during the UPR. For example, the assay shown in Figure 2.7A could be used to identify if the different poly(A) tail lengths during the UPR consist of heterogeneous populations of modified poly(A) tails.

One striking observation in this study was the presence of two *XBP1* mRNA pools with different translational fates during the acute phase of the UPR; *XBP1* mRNA with short poly(A) tails was translationally attenuated as compared to newly synthesized pool harboring long poly(A) tails, which escaped translational inhibition. The generation of long poly(A) tail *XBP1* mRNA was shown to involve transcriptional mechanisms during the UPR. However, it is unlikely to occur via regulation of polyadenylation because I have shown that the poly(A) tail length of newly synthesized *XBP1* mRNA is not significantly different between the

unstressed (control), acute, and chronic UPR (Figure 3.5). The accumulation of a long poly(A) tail *XBP1* mRNA parallels its increased synthesis during ER stress and therefore it does not discriminate between spliced and unspliced *XBP1* mRNA species. Mechanisms linking transcription to mRNA translation, stability, and poly(A) tail length have recently been reported (Slobodin et al., 2020; Slobodin & Dikstein, 2020; Slobodin et al., 2017). It was shown that reduced transcription dynamics correlated with enhanced m^6A base modification, increased deadenylation activity, shorter poly(A) tails, and decreased mRNA stability of the target mRNA (Slobodin et al., 2020). On the other hand, enhanced transcription correlated with less m^6A deposition on mRNA and positive regulation of translational efficiency (Slobodin et al., 2017). Such mechanisms can be investigated for the temporal regulation of *XBP1* mRNA poly(A) tail length during the UPR (Figure 2.2 and Figure 2.6). Although most studies indicate weak correlations between translation efficiency and poly(A) tail length in somatic cells (H. Chang et al., 2014; J. E. Park, Yi, Kim, Chang, & Kim, 2016; Subtelny et al., 2014), there is evidence that poly(A) tail length-mediated regulation of translation is likely dependent on the cellular context. For example, in zebrafish and frog embryos, poly(A) tail length is coupled to translation efficiency, but a developmental switch diminished this regulation during gastrulation (Subtelny et al., 2014). In this study, the preferential association of long poly(A) tail *XBP1* mRNA with heavy polyribosomes was illustrated during the acute phase of the UPR (Figure 3.4). A possible explanation for this phenomenon might be that long poly(A) tail mRNA are more competitive for the limited availability of poly(A) binding

protein (PABP) (Xiang & Bartel, 2021). Several studies have shown that PABPC is a critical factor mediating translation initiation in mammalian cells (Martineau et al., 2008; Smith et al., 2017), and that during stress conditions that induce eIF2α-P, PABPC is sequestered in SGs (Child, Chen, Reid, Jagannathan, & Nicchitta, 2021; Vanderweyde, Youmans, Liu-Yesucevitz, & Wolozin, 2013). The latter can explain the limited PABPC availability during the acute UPR, which can lead to competition among mRNA and therefore selective mRNA translation. Systematic analysis of published data from genome-wide studies can determine poly(A) tail length requirements for the mRNA under translational control during the acute UPR (Woo et al., 2018).

I showed here that during the chronic UPR, most transcripts tend to have short poly(A) tails (Figure 2.6, Figure 4.1B and Figure 4.2B) at a time that their translation is de-repressed (Guan et al., 2017). This agrees with a previous report that short poly(A) tailed mRNA is a characteristic of well-expressed genes (Lima et al., 2017; J. E. Park et al., 2016). However, the finding of decreased poly(A) tail length correlating with better translational efficiency during the chronic UPR seems contrary to the “dogma” that longer poly(A) tail mRNA is better translated (Webster et al., 2018). If we consider findings of this study that shorter poly(A) tails of the *XBP1* mRNA were found on polyribosomes, the “dogma” may be correct, and the mechanism of generating shorter poly(A) tail mRNA may involve co-translational deadenylation, as was shown previously (Vindry et al., 2012; Webster et al., 2018). Identifying the mechanism of co-translational deadenylation during the chronic UPR will suggest better experimental approaches to address the relationship

between poly(A) tail length and efficiency of translation. Additional mechanisms for shortening of the poly(A) tails during the chronic phase could involve cis- and trans-regulatory elements such as miRNA and RBPs recruited to mRNA during ER stress, or release of PABPC from SGs (Backlund et al., 2020; Cairrao et al., 2022; Duan et al., 2020; Good & Stoffers, 2020; Malhi, 2014).

I described here the temporal regulation of poly(A) tail length of the newly synthesized *XBP1* mRNA during the UPR. A biphasic response to ER stress has previously been described (Han et al., 2013; Hetz & Papa, 2018; Krokowski et al., 2013). The stress-induced gene regulation programs are shown as an important mechanism of controlling the UPR threshold, which needs to be carefully controlled to maintain adaptation to chronic ER stress (Hetz & Papa, 2018). Although partial recovery of the acute phase translational inhibition is necessary for adaptation to chronic ER stress (Guan et al., 2017), recovery of protein synthesis to normal pre-stress levels decreases adaptation to chronic ER stress via mechanisms involving the UPR-induced transcription program (Han et al., 2013; Krokowski et al., 2013). Furthermore, during chronic ER stress, selective translation initiation in the absence of active eIF4E involves the translation initiation factor eIF3 (Guan et al., 2017), which may be involved in the mechanism of ribosome-associated deadenylation of mRNA during the chronic UPR. In this work, I propose that the long poly(A) tails of newly synthesized mRNA during the acute phase of the UPR escape translational repression, and the shortening of the poly(A) tails during the chronic phase of the UPR may be a mechanism to limit the threshold of the UPR. The ribosome-associated shortening of poly(A) tails can contribute to both

decreased translation efficiency and increased mRNA decay. Elegant studies by (Eisen et al., 2020) have shown that mRNA degradation occurs predominantly via deadenylation and identified that most mRNA are committed to degradation once the poly(A) tail is 25 nt or shorter. However, I cannot exclude the possibility that the gradient of poly(A) tail length during the chronic UPR also serves to decrease translational efficiency of mRNA in subsequent rounds of translation initiation. Therefore, I propose that deadenylation during the chronic UPR can regulate either mRNA degradation or translation efficiency (Figure 2.7). This regulation of gene expression via poly(A) tail length is consistent with the adaptive response to chronic ER stress by keeping the UPR in homeostatic levels (Gomez & Rutkowski, 2016; Guan et al., 2017).

The significance of the stabilization of the pre-existing *XBP1* mRNA under the acute phase of the UPR can be considered as a mechanism to amplify the chronic UPR response. An alternative function of the acute phase stress response may be the anticipation of recovery from transient exposure to stress (Figure 3.8). mRNA stabilization during the acute UPR may therefore preserve the capacity of the cells to synthesize proteins to facilitate faster recovery of ER function when exposure to stress is transient. This explanation is supported by other physiological responses such as cell cycle progression, where translation is inhibited transiently during mitosis and recovers as cells enter the G1 phase (Hume, Dianov, & Ramadan, 2020; Tanenbaum et al., 2015). Similar to the increased stability of translationally repressed mRNA during the acute phase of ER stress (Kawai et al.,

2004; Majumder et al., 2012), translationally repressed mRNA in mitosis are also stabilized (Marzluff, Wagner, & Duronio, 2008; J. E. Park et al., 2016; Ross, 1997).

In conclusion, the findings of this study suggest an exciting hypothesis that establishing a steady state of adaptation to chronic ER stress involves a pre-steady state UPR phase of changes in transcription, translation, and mRNA stability. In the pre-steady state UPR, regulation of mRNA stability and translation promotes recovery from acute stress. In the steady-state adaption phase, the massive transcriptional induction and reprogramming of translation initiation protects cells during chronic ER stress. This biphasic response provides plasticity in the cellular response, allowing recovery from stress after acute or chronic episodes of ER stress with minimal commitment of resources and energy. Therefore, the coordinated transcriptional and post-transcriptional mechanisms of gene regulation in the pre-steady state and steady-state UPR is a critical cellular response to duration and intensity of environmental cues.

Future Directions

I presented my study showing the temporal regulation of the *XBP1* gene in response to ER stress in WT MEF cells as well as MIN6 cells using different UPR inducers such as Tg and CPA. This study revealed a novel mechanism of *XBP1* gene regulation during the UPR. During the acute ER stress, the long poly(A) tails of newly transcribed mRNA are found to be critical for cell survival and *XBP1* mRNA with long poly(A) tails escape the eIF2α-P mediated translation inhibition. In this study, the *XBP1* gene was used as a model of transcriptionally-induced

genes during ER stress to study the mechanism of gene regulation. The identification of regulated mRNA poly(A) tail length during ER stress opened avenues of questions to be addressed in the future concerning selectivity of this regulation in cellular adaptation and survival to ER stress.

Investigating the role of poly(A) tail length in mRNA translation during ER stress

Upon ER stress, the uORF feature of a subset of mRNA has been suggested to selectively regulate translation (Guan et al., 2017; Wek, 2018). However, little is known about the role of poly(A) tails during the UPR. In this work, I showed *XBP1* mRNA with long poly(A) tails escaped translational inhibition during acute ER stress (Figure 3.4). The long poly(A) tails of *XBP1* mRNA represented newly synthesized *XBP1* mRNA as determined by the metabolic 5EU labeling (Figure 3.5). Metabolic RNA labeling has been widely used in measuring the rate of RNA synthesis, especially in specific contexts such as cellular stress response (Singha, Spitalny, Nguyen, Vandewalle, & Spitale, 2021; Wissink et al., 2019). Although some reports indicated metabolic labeling caused stress (Altieri & Hertel, 2021; Burger et al., 2010; Burger et al., 2013; Duffy, Schofield, & Simon, 2019), I did not observe stress in MEF cells treated with 5EU as determined by the rate of protein synthesis and expression of *XBP1* mRNA (Figure 3.6). To identify a global mechanism of translation regulation via the poly(A) tail length, it would be worth determining the poly(A) tail length of 5EU pulse-labeled mRNA associated with polyribosomes during the unstressed (control), acute, and chronic ER stress conditions as described in other systems (H. Chang et al., 2014; Legnini et al.,

2019; Subtelny et al., 2014). Compared to the unlabeled mRNA, the poly(A) tail length of 5EU-labeled mRNA is predominantly long because they represent newly synthesized mRNA. During acute ER stress, two predominant groups of unlabeled trnscripts are expected: (1) translational repressed mRNA that shift from heavy polyribosomes to the free pool of polysome fractions. (2) mRNA that escape translation inhibition via the uORFs or other mechanisms of translation. Meanwhile, the 5EU-labeled mRNA will be associated with polyribosomes indicative of preferential translation during eIF2α-P mediated translation inhibition. During chronic ER conditions as compared to acute ER stress, the unlabeled mRNA would be short and (1) translationally repressed or (2) translationally recovered if they are subject to reprogramming mRNA translation during chronic ER stress. The 5EU-labeled mRNA during chronic ER stress, however, is expected to be present with various poly(A) tail lengths that associate with polyribosomes due to the assumption of co-translational deadenylation that functions to decrease mRNA stability, mRNA translation or both. Co-translational deadenylation and degradation of mRNA has been documented in other systems (Vindry et al., 2012; Webster et al., 2018). During chronic ER stress, mRNA co-translational deadenylation could be an important mechanism to limit the UPR threshold. The identification of genes, representing the 5EU-labeled mRNA, will not only provide targets that are preferentially translated during acute ER stress, but also highlight genes important for recovery from acute ER stress. In conclusion, the suggested experiments involving 5EU-labeled transcripts will examine whether the

phenomenon that mRNA long poly(A) tails escaping translation inhibition during acute ER stress is a general cellular response to stress.

Role of mRNA poly(A) tails in mRNA stability during ER stress

Studies of the relationship between mRNA stability and the length of mRNA poly(A) tail have yielded different conclusions. This discrepancy may be explained by different methods used in sequencing the poly(A) tails and their comparison of mRNA poly(A) tail length to published values of mRNA half-lives (H. Chang et al., 2014; Subtelny et al., 2014). Although chemical inhibition of transcription has been applied as a methodology to measure mRNA half-lives for decades, alternative approaches are currently emerging. A recent study compared the mRNA stability in a continuous 5EU labeling experiment in 3T3 cells in the presence or absence of the chemical transcriptional inhibitor actinomycin D. Compared to 5EU labeling, the study shows that addition of actinomycin D did not affect the rank order of mRNA half-life (Eisen et al., 2020). Upon ER stress, several studies indicated global and individual mRNA stabilization upon ER stress (Kawai et al., 2004; Majumder et al., 2012; Rutkowski et al., 2006; Woo et al., 2018). In my study, I showed the biphasic regulation of *XBP1* mRNA stability and its dynamic poly(A) tail length during acute and chronic ER stress conditions. Interestingly, the *XBP1* mRNA is stabilized and has long poly(A) tails during acute ER stress, while it is destabilized during control and chronic ER stress characterized by short poly(A) tails of *XBP1* mRNA (Figure 2.6, Figure 2.2, and Figure 2.3). Of note, Tg-treated MEF cells for 1 h exhibited two populations of *XBP1* mRNA with long and short poly(A) tails representing new (newly synthesized) and old (pre-existing) mRNA,

respectively, as determined by the 5EU labeling experiment (Figure 3.5). To better understand the contribution of poly(A) tail length in mRNA stability and during ER stress, I would suggest using a comparison between the mRNA half-life and poly(A) tail length in a 5EU-chase experiment under the unstressed, acute, and chronic ER stress conditions. Compared to the unlabeled mRNA, I expect that the poly(A) tails of 5EU-labeled transcripts are longer and more stable in all conditions. For example, during acute ER stress, I expect that the poly(A) tail length of 5EU labeled mRNA (new) representing stress-induced genes is long and more stable. In contrast, the unlabeled mRNA (old) will be shorter than 5EU labeled mRNA and likely to be more stable in agreement with this thesis's findings. During the control and chronic ER stress, although the newly synthesized *XBP1* mRNA are observed to have a varied length of poly(A) tails, I expect that newly synthesized mRNAs have different poly(A) tail lengths and are more stable than unlabeled mRNA. mRNA stability is dependent on the rate of deadenylation that varies among transcripts (Eisen et al., 2020). However, contributors such as heterogenous poly(A) tails and their effects to the observed mRNA half-lives during ER stress are not well studied. The terminal nucleotide of poly(A) tail has been documented to contain non-A nucleotides influencing the rate of mRNA deadenylation (H. Chang et al., 2014; Lim et al., 2018). I would suggest studying poly(A) tails containing non-A nucleotides to highlight the mechanisms contributing to the observed mRNA stability during ER stress.

The mechanisms controlling poly(A) tail length during ER stress

During acute ER stress, the long poly(A) tail of *XBP1* mRNA was shown to be independent of PERK activation and *XBP1* splicing (Figure 3.1). Since *XBP1* gene expression is induced upon ER stress, labeling of newly synthesized *XBP1* mRNA appeared with long poly(A) tails (Figure 3.5) and blocking transcription with actinomycin D decreased the length of *XBP1* mRNA poly(A) tails (Figure 2.10B). Several reports indicate that *XBP1* gene expression is enhanced by a few transcription factors such as XBP1s and ATF6 (He et al., 2010; Yoshida, Matsui, Yamamoto, Okada, & Mori, 2001). To date, there is no comprehensive list of transcriptional activators of *XBP1* expression. Therefore, I suggest an inducible system (Kallunki, Barisic, Jaattela, & Liu, 2019) of *XBP1* expression in XBP1-deficient cells to study the *XBP1* mRNA fate in response to ER stress. XBP1-deficient cells can be reconstructed with (1) a transcriptionally induced reporter of the *XBP1* gene such as under the control of *ATF4* promoter, and (2) a transcriptionally non-induced reporter of the *XBP1* gene under the control of *ATP5B* promoter, an example of non-induced UPR target. If the system is designed to induce or not induce *XBP1* gene expression under ER stress, the newly synthesized and pre-existing *XBP1* mRNA fate can be determined. Induction of *XBP1* reporters controlled by *ATF4* promoter, for example, is expected to show various poly(A) tail lengths of newly synthesized *XBP1* mRNAs under control and chronic ER stress, while predominantly long poly(A) tails during acute ER stress. The *XBP1* reporter controlled by the non-induced promoters such as *ATP5B* is expected to have short poly(A) tails during ER stress conditions. On the other

hand, I suggest designing another experimental system in which *XBP1* transcriptional induction is absent by depleting ATF6 in IRE1α-deficient cells. These cells serve to attenuate *XBP1* transcriptional induction during ER stress. Inhibition of *XBP1* expression under acute and chronic ER stress conditions will show that the pre-existing *XBP1* mRNAs have short poly(A) tails. In addition, the pre-existing *XBP1* mRNAs during acute ER stress may be stored in a translationally inhibited complex leading to their degradation. Alternative mechanisms may apply such as poly(A) tails can be re-extended by the cytoplasmic polyadenylation during ER stress transitioning from acute to chronic phases (Maillo et al., 2017).

During chronic ER stress, short poly(A) tails of mRNA were observed among tested genes including the stable *GAPDH* mRNA (Figure 2.6, Figure 4.1A and Figure 4.2A). This observation is worth further investigation to establish the mechanisms controlling mRNA poly(A) tail length during chronic ER stress. Interestingly, IRE1 has been proposed to cleave other mRNAs besides *XBP1* mRNA and thus, participates in the decreased ER load to restore ER proteostasis (Maurel et al., 2014). In IRE1α-deficient MEF cells, shortening of mRNA poly(A) tails was independent of IRE1α activation regardless of the tested transcripts including *XBP1* and *GAPDH* mRNAs (Figure 3.1). However, other canonical targets of RIDD such as *BLOS1* mRNA (Bashir et al., 2021) and mRNA targeted co-translationally to the ER (X. A. Cui & Palazzo, 2014) should be tested. In addition, the observed short poly(A) tails of mRNA during chronic ER stress were

attributed to the partial recovery of protein synthesis during the chronic ER stress (Figure 2.4A) (Guan et al., 2017). The partial recovery of mRNA translation is achieved by the induced GADD34 that recruits the PP1 phosphatase to dephosphorylate eIF2α-P during chronic ER stress (Novoa et al., 2003). Therefore, I would ask if co-translational deadenylation and degradation of mRNA, as explained previously, contributes to the poly(A) tail length during chronic ER stress. To determine the poly(A) tail length in conditions of blocked translational recovery during chronic ER stress, I suggest estimating the poly(A) tail length of mRNA during chronic ER stress in GADD34-deficient cells. I expect two outcomes: (1) The poly(A) tail length is not decreased due to the diminished GADD34 required for translation recovery during chronic ER stress. This will indicate that poly(A) tail shortening is the result of co-translational deadenylation mechanisms. (2) The poly(A) tail length is decreased indicating that the poly(A) tail length is independent of translation. In addition, I showed that *XBP1* mRNA is destabilized during chronic ER stress (Figure 2.2). Therefore, I would evaluate the mRNA half-life under such conditions to further validate the correlation between mRNA stability and translation status (Figure 2.5) and understand the contribution of poly(A) tail length to mRNA stability. Based on the outcomes of the GADD34 depletion during chronic ER stress, mRNA stability would be enhanced in the absence of GADD34 and decreased in the presence of GADD34. Next, I would investigate the association of mRNA with components of the deadenylase complex. CCR4-NOT complex is the major cytoplasmic deadenylase controlling the poly(A) tail length (Eisen et al., 2020; Heck & Wilusz, 2018; Webster et al., 2018). From a mechanistic point of

view, a possible mechanism might be the decreased association of the deadenylase complex with mRNA during acute ER stress and return association during chronic ER stress. RNA-binding proteins are expected to mediate these associations. I suggest RNA sequencing of tagged CCR4 proteins-immunoprecipitated mRNA to identify targets regulated by the deadenylase complex during acute and chronic ER stress conditions.

APPENDIX: EXPERIMENTAL METHODS

Cell Lines, Cell Culture Conditions, and Chemicals

Established cell lines of WT, eIF2α-P-deficient, IRE1α-deficient, and XBP1-deficient MEF cells were grown in Dulbecco's modified Eagle's medium enriched with 10% fetal bovine serum (Gibco), 100 units/mL penicillin, 100 µg/mL streptomycin, and 2 mM L-Gln. Mouse pancreatic β cells (MIN6) were purchased (AddexBio-C0018008) and grown as described (Krokowski et al., 2013). Cells were grown at 37° C under 5% CO_2. ER stress was induced by treating cells with either 400 nM Tg (Sigma-Aldrich) or 100 µM CPA (Tocris Bioscience) for the indicated durations. Other chemicals used in this study include 4µ8C (Torris Bioscience, 50 µM), Cycloheximide (100 µg/mL) (Sigma-Aldrich), Puro (5 µg/mL) (Thermo Fisher Scientific), Actinomycin D (10 µg/mL), and cordycepin (10 µg/mL) (Sigma-Aldrich).

RNA Isolation, splicing reaction, and RT-qPCR

To measure mRNA steady state levels and half-life, cells were seeded at 0.5×10^6 cells in 60-mm culture dishes and grown to 80% confluency. Following the indicated treatments, total RNA was isolated using TRIzol (Invitrogen) according to the manufacturer's instructions. The relative mRNA abundance was measured by RT-qPCR and normalized to steady state mRNA levels of house-keeping genes such as *GAPDH*. Briefly, cDNA was synthesized using ProtoScript® II Reverse Transcriptase with random primer mix (New England Biolabs). This cDNA was also used for a conventional PCR using Go-Taq® Master Mix (Promega) with *XBP1* splicing primers. To illustrate whether *XBP1* mRNA was

spliced, 2.5% ethidium bromide-stained agarose gels (Sigma) were prepared and run for 45 Min at 150 V. Also, mRNA abundance was quantitively determined using VeriQuest SYBR Green qPCR Master Mix (Affymetrix) with the StepOnePlus Real-Time PCR System (Applied Biosystems). Half-lives were calculated by fitting the data points to a nonlinear curve for the decay exponential of each target. Primers used in this study are listed in Table 1.

RNA Labeling, Biotinylation, and Purification

WT MEF cells were seeded at 3×10^6 cells in 150-mm culture dishes and were grown to 80% confluency. To metabolically label RNA, 400 μM 5EU (Click Chemistry Tools) was added for 1 h as indicated. Following total RNA isolation of labeled RNA with 5EU, I performed click chemistry using the CuAAC Biomolecule Reaction Buffer Kit-BTTAA based (Jena Biosciences). Following click chemistry, RNA was purified using spin columns (Zymo Research). RNA was resuspended in 50 μL nuclease-free water and mixed with equal volumes of 1X High Salt Wash Buffer (10 mM Tris pH 7.5, 1 mM ethylenediaminetetraacetic acid (EDTA) pH 8, 0.1 M NaCl, 0.01% Tween-20). To capture the labeled RNA, 100 μL of Dynabeads™ MyOne™ Streptavidin T1 beads (Invitrogen) were used after being washed as described previously (Eisen et al., 2020). RNA from flow-through and elution was isolated using TRIzol LS (Invitrogen).

PCR-based poly(A) tailing assay

Total RNA (10 μg) was incubated with recombinant RNAse-free deoxyribonuclease I (Sigma) in 50 μL-reaction tubes at 37° C for 20 Min. The reaction was terminated by adding 200 μL of nuclease-free water and 750 μL of

TRIzol LS (Invitrogen), and RNA was then isolated and quantified. To add an artificial tail to the mRNA poly(A) tail, 1.5 µg of the isolated RNA (up to 14.5 µL) was mixed with 2 µL of recombinant yeast PAP together with 5 µL of 5X PAP buffer (Thermo Fisher Scientific), 2.5 µL of 10 µM GTP/ITP/$MgCl_2$ (Jena Bioscience), and 1 µL of RNase inhibitor (New England Biolabs). The 25 µL-reaction was incubated in a thermocycler set at 37° C for 1 h. G/I nucleotide-tailed RNA was then purified using spin columns (Zymo Research). The RNA, eluted in 9 µL, was used in a reverse transcription reaction as described previously (Patil et al., 2014) using the poly(C) primer (CCCCCCCCCCTT) in the reverse transcription reaction. The resulting cDNA was used in a conventional PCR reaction to estimate the poly(A) tail length. Primers used in this study are listed in Table 2. PCR products were run on 2.5 % ethidium bromide-stained agarose gels, and bands were visualized and captured under UV light (Syngene).

RNA fractionation based on the length of poly(A) tails

The protocol used to visualize poly(A) tail lengths was based on the poly(A) tail fractionation (Chorghade et al., 2017). Briefly, total RNA from untreated or Tg-treated cells for 3 or 16 h was isolated. 20 µL of total RNA (~10-50 µg) was mixed with 200 µL of guanidine thiocyanate buffer (4 M guanidine thiocyanate, 25 mM sodium citrate, pH 7.1), 4 µL of beta-mercaptoethanol (β-ME), 5 µL of 50 pmol/µL biotinylated oligo (dT) probes (Promega), and 408 µL of diffusion buffer (3X saline-sodium citrate (SSC), 5 mM Tris, pH 7.5, 0.5 mM EDTA, 0.125% sodium dodecylsulfate (SDS), 5% β-ME). The mixture was heated at 70° C for 5 Min followed by a 10-Min centrifugation at 12,000 x g at room temperature. The

supernatant was added to 150 µL of Dynabeads™ MyOne™ Streptavidin C1 beads (Invitrogen) that had been washed 3 times with 0.5X SSC buffer containing 0.02% Tween20. The beads were rotated slowly at room temperature for 15 Min followed by 3 washes with 0.5X SSC buffer containing 0.02% Tween20. RNAs with the shortest poly(A) tails were eluted from the beads by adding 400 µL of 0.07X SSC followed by a 20-Min incubation at room temperature. The remaining fractions were eluted in the same way with the following SSC concentrations: 0.06X, 0.05X and 0.04X. The RNA from these fractions was purified by RNA-phenol/chloroform extraction, precipitated with sodium acetate and glycoblue (ThermoFisher) overnight, pelleted, and resuspended in 25 µL of water. 4 µL of RNA was 3′-end-labeled with [5′-^{32}p] pCp (prepared by incubating 16.5 µL of [γ-^{32}p] ATP (PerkinElmer), 1 µL of T4 polynucleotide Kinase, 2 µL of 10X buffer (New England Biolabs), and 833 µM of cytidine 3′-phosphate at 37° C for 1 h, followed by 10 Min at 65° C). The ^{32}pCp was ligated using T4 RNA ligase 1 (New England Biolabs) and incubated overnight at 4° C. Following clean up with Micro Bio-Spin 6 columns (Bio-Rad), the 3′-end-labeled RNA was incubated with RNase A (Thermo Scientific™) at 37° C for 30 Min in a 100 µL-reaction containing 20 mM Tris pH 8, 1.25 mM $MgCl_2$, 550 mM NaCl, 1.25 mM *E. coli* tRNA, and 0.125 mM RNase A. Radiolabeled poly(A) tails were purified by RNA-phenol/chloroform extraction and overnight precipitation with sodium acetate and glycoblue. The distribution of poly(A) tail length was visualized by running the RNA on an 8.5% polyacrylamide gel with 7 M urea.

Western Blot analysis

Cell extracts and western blot were performed as previously described (Guan et al., 2017). Briefly, treated MEF cells were washed twice in cold Phosphate-Buffer Saline (PBS) and lysed using a lysis buffer (50 mM Tris-HCl at pH 7.5, 150 mM NaCl, 2 mM EDTA, 1% NP-40, 0.1% SDS and 0.5% sodium deoxycholate) supplemented with EDTA-free protease inhibitor (Roche Applied Science) and PhosSTOP phosphatase inhibitor (Roche Applied Science). Cell lysates were placed on ice and sonicated 10 times. The supernatants of cold lysates were transferred to fresh tubes after centrifugation at 13,000 rpm for 10 Min at 4° C. The supernatants were used for protein quantification via the use of the DC™ Protein Assay Kit (Bio-Rad). Equal loading of proteins (10–20 μg) was analyzed in SDS-PAGE and primary antibodies were applied after a standard western blotting was performed. These antibodies were listed in Table 3.

Metabolic Labeling of Cells with [^{35}S] Met/Cys

eIF2α-P-deficient MEF cells were seeded at 5 × 10^4 cells/well in 24-well plates. Cells were grown overnight and treated as described above. Prior to the end of each treatment, [^{35}S]-Met/Cys was added (30 μCi/mL EXPRE^{35}S Protein Labeling Mix, PerkinElmer) for 30 Min. Next, cells were washed twice with cold PBS and total proteins were precipitated in 5% trichloroacetic acid (TCA) with 1 mM Met (Sigma-Aldrich) for 15 Min on ice. The precipitation step was repeated overnight at 4° C. After careful removal of TCA and free Met, 200 μL of 1 N NaOH and 0.5% sodium deoxycholate were added for 30 Min. To determine the incorporation of [^{35}S]-Met/Cys into total cellular proteins, liquid scintillation

counting, and DC Protein Assay (Bio-Rad) were used to quantify radioactivity and protein concentration, respectively.

Polysome Profile Analysis and PCR-based tailing assay

Wild type MEF cells were seeded at 3×10^6 cells/150-mm culture dishes (2 dishes per treatment) and grown to reach 80% confluency. Cells were washed twice with cold PBS containing 100 μg/mL cycloheximide and placed on ice. 1 mL of lysis buffer (10 mM 4-(2-Hydroxyethyl)-1-Piperazineethanesulfonic Acid (HEPES)-potassium hydroxide (KOH) (pH 7.4), 5 mM $MgCl_2$, 100 mM KCl, 1% Triton, 100 μg/mL cycloheximide, 2 mM DTT, 200 units/mL RNase inhibitor (New England Biolabs), EDTA-free protease inhibitor (Roche Applied Science) was added to each plate after removing the remaining PBS carefully. Next, cells were scraped, and then passed 5 times through a 26-gauge needle. Lysates were spun at 13,000 x g for 15 Min, and supernatants containing cytosolic cell extracts were collected. Approximately 10 *A* units (260 nm) of lysates were layered over 10%–50% cold sucrose gradients in buffer (10 mM HEPES-KOH (pH 7.4), 2.5 mM $MgCl_2$, 100 mM KCl). Gradients were centrifuged at 31,000 rpm in a Beckman SW32 rotor for 2.5 h at 4° C. After centrifugation, gradients were fractionated and collected into 12 tubes (~1 mL/fraction). RNA from each fraction was isolated using TRIzol LS (Invitrogen), and an equal volume of RNA from each fraction was used for cDNA synthesis. The relative quantities of specific mRNA were measured by RT-qPCR as described above. To measure the poly(A) tail length of mRNA, fractions were equally combined into 3 pools of free, light, and heavy

polyribosomes. After RNA isolation, the poly(A) tail length was measured using equal volumes from each pool of mRNA as described above.

Cell Viability Assay

WT MEF cells were seeded at 1×10^4 cells/well in 96-well plates. Cells were grown overnight and treated as indicated. Prior to the end of treatment, an equal volume of CellTiter-Glo® reagent (Promega) was added to the existing media volume. After mixing the reagent well, the plate was incubated at 37° C for 10 Min, followed by incubation at room temperature on a shaker for another 10 Min. Luminescence was recorded using a SpectraMAx M3 instrument.

Statistical Analysis

The mean of technical triplicate measurements was statistically evaluated using the two-tailed student's t-test, included in the GraphPad Prism software that generates most of figures, where asterisks (*) indicate statistical significance of replicates. Otherwise, results were considered non-significant (NS). Error bars indicate standard deviation of the mean.

TABLES

Table 1. Oligonucleotides used in RT-qPCR assays

Target/ Primers	Forward primer	Reverse Primer
ATP5B	GATGTGATGTTCTCT CTGAAGAG	CCACCACTGTGAGCT CAA
ATF4	GAGGCTCTGAAAGAG AAGGCAG	CAAGCACAAAGCACC TGACTAC
BiP	AGGGTGTGTGTTCAC CTTGG	AACATTTATTGGTGT CACTTATGGT
GAPDH	CGCCTGGAGAAACCT GCCAAGTATG	GGTGGAAGAATGGG AGTTGCTGTTG
*GAPDH pre-mRNA***	gttctagGTATGACAATG AATACGGC	GTCTGGGATGGAAAT TGTGAGG
MAFA	GAGGTCATCCGACTG AAACAGAAGC	TGGAGCTGGCACTTC TCGCT
PDX1	CCGAATGGAACCGA GCCTG	ACGGGTCCTCTTGTT TTCCT

Target/ Primers	Forward primer	Reverse Primer
NKX2-2	AGAGGAGGAGAGCGAAGG	CGTGCAGGGAGTATTGGAG
Sec24D	AGCCTGAAATCTGTCTGGTAGA	CCGTTTTATAGACAAAACAACTGG
XBP1 splicing*	ACACGCTTGGGAATGGACAC	CCATGGGAAGATGTTCTGGG
XBP1 total	GGCTGTCTGGCCTTAGAAGA	CTGTCAAATGACCCTCCCTG
XBP1 pre-mRNA**	gcctcttgtagTCTGATATCCTTTTG	CTTCCAGCTTGGCTGATGAG
XBP1s	GAGTCCGCAGCAGGTG	CTGGGAGTTCCTCCAGACTA
XBP1u	GACTATGTGCACCTCTGCAG	CTGGGAGTTCCTCCAGACTA

* *XBP1* splicing primers were used for RT-PCR.

** Small letters indicate a portion of sequence located within introns.

Table 2. Oligonucleotides used in poly(A) tailing assays

Target/ Primers	Forward primer	Reverse Primer
ATP5B	GATGTGATGTTCTCT CTGAAGAG	CCACCACTGTGAGCT CAA
ATF4	GAGGCTCTGAAAGAG AAGGCAG	CAAGCACAAAGCACC TGACTAC
BiP	AGGGTGTGTGTTCAC CTTGG	AACATTTATTGGTGTC ACTTATGGT
GAPDH	ACTGAGCAAGAGAGG CCCTATC	GTTATTATGGGGGTC TGGGATGG
GI-Tail		GAGTAGCGTTGAATA AGTTGCCCCCCCCCC TT
MAFA	CTCTCACTGAGTCTT CTGAAC	CAAATGAGTGAGTGA GTGAGAGAG
Sec24D	AGCCTGAAATCTGTC TGGTAGA	CCGTTTTATAGACAA AACAACTGG
XBP1	GTAAATGCTTGATGG ATCTTCTTGC	GCTGTGTTGCTTTTTT TTTAATTGC

Table 3. Antibodies used in western blotting assays

Antibodies	Company	Catalog Number
Rabbit monoclonal anti-ATF4	Cell Signaling Technology	#11815
Rabbit monoclonal anti-BiP	Cell Signaling Technology	#3177
Rabbit polyclonal anti-eIF2α	Cell Signaling Technology	#9722
Rabbit monoclonal anti-eIF2α-P (Phosphorylated at Ser-51)	Abcam	#ab32157
Mouse monoclonal anti-α-tubulin	Sigma-Aldrich	#T9026
Rabbit polyclonal anti-XBP1s	Cell Signaling Technology	#83418
Rabbit monoclonal anti-PERK	Cell Signaling Technology	#3192
Rabbit monoclonal anti-PERK-P (Phosphorylated at Thr-980)	Cell Signaling Technology	#3179

BIBLIOGRAPHY

Acevedo, J. M., Hoermann, B., Schlimbach, T., & Teleman, A. A. (2018). Changes in global translation elongation or initiation rates shape the proteome via the Kozak sequence. *Sci Rep, 8*(1), 4018. doi:10.1038/s41598-018-22330-9

Adams, B. M., Canniff, N. P., Guay, K. P., Larsen, I. S. B., & Hebert, D. N. (2020). Quantitative glycoproteomics reveals cellular substrate selectivity of the ER protein quality control sensors UGGT1 and UGGT2. *Elife, 9*. doi:10.7554/eLife.63997

Adomavicius, T., Guaita, M., Zhou, Y., Jennings, M. D., Latif, Z., Roseman, A. M., & Pavitt, G. D. (2019). The structural basis of translational control by eIF2 phosphorylation. *Nat Commun, 10*(1), 2136. doi:10.1038/s41467-019-10167-3

Aksenova, V., Smith, A., Lee, H., Bhat, P., Esnault, C., Chen, S., . . . Dasso, M. (2020). Nucleoporin TPR is an integral component of the TREX-2 mRNA export pathway. *Nat Commun, 11*(1), 4577. doi:10.1038/s41467-020-18266-2

Almanza, A., Carlesso, A., Chintha, C., Creedican, S., Doultsinos, D., Leuzzi, B., . . . Samali, A. (2019). Endoplasmic reticulum stress signalling - from basic mechanisms to clinical applications. *FEBS J, 286*(2), 241-278. doi:10.1111/febs.14608

Alone, P. V., & Dever, T. E. (2006). Direct binding of translation initiation factor eIF2gamma-G domain to its GTPase-activating and GDP-GTP exchange factors eIF5 and eIF2B epsilon. *J Biol Chem, 281*(18), 12636-12644. doi:10.1074/jbc.M511700200

Altieri, J. A. C., & Hertel, K. J. (2021). The influence of 4-thiouridine labeling on pre-mRNA splicing outcomes. *PLoS One, 16*(12), e0257503. doi:10.1371/journal.pone.0257503

Alzahrani, M. R., Guan, B. J., Zagore, L. L., Wu, J., Chen, C. W., Licatalosi, D. D., . . . Hatzoglou, M. (2022). Newly synthesized mRNA escapes translational repression during the acute phase of the mammalian unfolded protein response. *PLoS One, 17*(8), e0271695. doi:10.1371/journal.pone.0271695

Anda, S., Zach, R., & Grallert, B. (2017). Activation of Gcn2 in response to different stresses. *PLoS One, 12*(8), e0182143. doi:10.1371/journal.pone.0182143

Arensdorf, A. M., Diedrichs, D., & Rutkowski, D. T. (2013). Regulation of the transcriptome by ER stress: non-canonical mechanisms and physiological consequences. *Front Genet, 4*, 256. doi:10.3389/fgene.2013.00256

Atkins, C., Liu, Q., Minthorn, E., Zhang, S. Y., Figueroa, D. J., Moss, K., . . . Kumar, R. (2013). Characterization of a novel PERK kinase inhibitor with antitumor and antiangiogenic activity. *Cancer Res, 73*(6), 1993-2002. doi:10.1158/0008-5472.CAN-12-3109

Backlund, M., Stein, F., Rettel, M., Schwarzl, T., Perez-Perri, J. I., Brosig, A., . . . Kulozik, A. E. (2020). Plasticity of nuclear and cytoplasmic stress responses of RNA-binding proteins. *Nucleic Acids Res, 48*(9), 4725-4740. doi:10.1093/nar/gkaa256

Bagchi, P. (2020). Endoplasmic reticulum in viral infection. *Int Rev Cell Mol Biol, 350*, 265-284. doi:10.1016/bs.ircmb.2019.10.005

Bandla, S., Diaz, S., Nasheuer, H. P., & FitzGerald, U. (2019). ATPase activity of human binding immunoglobulin protein (BiP) variants is enhanced by signal sequence and physiological concentrations of Mn(2). *FEBS Open Bio, 9*(8), 1355-1369. doi:10.1002/2211-5463.12645

Bashir, S., Banday, M., Qadri, O., Bashir, A., Hilal, N., Nida, I. F., . . . Fazili, K. M. (2021). The molecular mechanism and functional diversity of UPR signaling sensor IRE1. *Life Sci, 265*, 118740. doi:10.1016/j.lfs.2020.118740

Beilharz, T. H., & Preiss, T. (2007). Widespread use of poly(A) tail length control to accentuate expression of the yeast transcriptome. *RNA, 13*(7), 982-997. doi:10.1261/rna.569407

Bhavnani, V., Swarnendu, K., Savergave, L., Raghuwanshi, A. S., Kumar, A., Kumar, A., & Pal, J. (2017). HRI, a stress response eIF2alpha kinase, exhibits structural and functional stability at high temperature and alkaline conditions. *Int J Biol Macromol, 95*, 528-538. doi:10.1016/j.ijbiomac.2016.11.071

Bommiasamy, H., & Popko, B. (2011). Animal models in the study of the unfolded protein response. *Methods Enzymol, 491*, 91-109. doi:10.1016/B978-0-12-385928-0.00006-7

Braakman, I., & Hebert, D. N. (2013). Protein folding in the endoplasmic reticulum. *Cold Spring Harb Perspect Biol, 5*(5), a013201. doi:10.1101/cshperspect.a013201

Breitling, J., & Aebi, M. (2013). N-linked protein glycosylation in the endoplasmic reticulum. *Cold Spring Harb Perspect Biol, 5*(8), a013359. doi:10.1101/cshperspect.a013359

Bresson, S., & Tollervey, D. (2018). Surveillance-ready transcription: nuclear RNA decay as a default fate. *Open Biol, 8*(3). doi:10.1098/rsob.170270

Burger, K., Muhl, B., Harasim, T., Rohrmoser, M., Malamoussi, A., Orban, M., . . . Eick, D. (2010). Chemotherapeutic drugs inhibit ribosome biogenesis at various levels. *J Biol Chem, 285*(16), 12416-12425. doi:10.1074/jbc.M109.074211

Burger, K., Muhl, B., Kellner, M., Rohrmoser, M., Gruber-Eber, A., Windhager, L., . . . Eick, D. (2013). 4-thiouridine inhibits rRNA synthesis and causes a nucleolar stress response. *RNA Biol, 10*(10), 1623-1630. doi:10.4161/rna.26214

Burwick, N., & Aktas, B. H. (2017). The eIF2-alpha kinase HRI: a potential target beyond the red blood cell. *Expert Opin Ther Targets, 21*(12), 1171-1177. doi:10.1080/14728222.2017.1397133

Buschauer, R., Matsuo, Y., Sugiyama, T., Chen, Y. H., Alhusaini, N., Sweet, T., . . . Beckmann, R. (2020). The Ccr4-Not complex monitors the translating ribosome for codon optimality. *Science, 368*(6488). doi:10.1126/science.aay6912

Buttner, S., Eisenberg, T., Carmona-Gutierrez, D., Ruli, D., Knauer, H., Ruckenstuhl, C., . . . Madeo, F. (2007). Endonuclease G regulates budding yeast life and death. *Mol Cell, 25*(2), 233-246. doi:10.1016/j.molcel.2006.12.021

Cairrao, F., Santos, C. C., Le Thomas, A., Marsters, S., Ashkenazi, A., & Domingos, P. M. (2022). Pumilio protects Xbp1 mRNA from regulated Ire1-dependent decay. *Nat Commun, 13*(1), 1587. doi:10.1038/s41467-022-29105-x

Carew, N. T., Nelson, A. M., Liang, Z., Smith, S. M., & Milcarek, C. (2018). Linking Endoplasmic Reticular Stress and Alternative Splicing. *Int J Mol Sci, 19*(12). doi:10.3390/ijms19123919

Carrocci, T. J., & Neugebauer, K. M. (2019). Pre-mRNA Splicing in the Nuclear Landscape. *Cold Spring Harb Symp Quant Biol, 84*, 11-20. doi:10.1101/sqb.2019.84.040402

Castilho, B. A., Shanmugam, R., Silva, R. C., Ramesh, R., Himme, B. M., & Sattlegger, E. (2014). Keeping the eIF2 alpha kinase Gcn2 in check. *Biochim Biophys Acta, 1843*(9), 1948-1968. doi:10.1016/j.bbamcr.2014.04.006

Chang, H., Lim, J., Ha, M., & Kim, V. N. (2014). TAIL-seq: genome-wide determination of poly(A) tail length and 3' end modifications. *Mol Cell, 53*(6), 1044-1052. doi:10.1016/j.molcel.2014.02.007

Chang, T. K., Lawrence, D. A., Lu, M., Tan, J., Harnoss, J. M., Marsters, S. A., . . . Ashkenazi, A. (2018). Coordination between Two Branches of the Unfolded Protein Response Determines Apoptotic Cell Fate. *Mol Cell, 71*(4), 629-636 e625. doi:10.1016/j.molcel.2018.06.038

Charlesworth, A., Meijer, H. A., & de Moor, C. H. (2013). Specificity factors in cytoplasmic polyadenylation. *Wiley Interdiscip Rev RNA, 4*(4), 437-461. doi:10.1002/wrna.1171

Chavez, S., Garcia-Martinez, J., Delgado-Ramos, L., & Perez-Ortin, J. E. (2016). The importance of controlling mRNA turnover during cell proliferation. *Curr Genet, 62*(4), 701-710. doi:10.1007/s00294-016-0594-2

Chen, C. A., & Shyu, A. B. (2017). Emerging Themes in Regulation of Global mRNA Turnover in cis. *Trends Biochem Sci, 42*(1), 16-27. doi:10.1016/j.tibs.2016.08.014

Chen, C. A., Strouz, K., Huang, K. L., & Shyu, A. B. (2020). Tob2 phosphorylation regulates global mRNA turnover to reshape transcriptome and impact cell proliferation. *RNA, 26*(9), 1143-1159. doi:10.1261/rna.073528.119

Chen, C. W., Guan, B. J., Alzahrani, M. R., Gao, Z., Gao, L., Bracey, S., . . . Hatzoglou, M. (2022). Adaptation to chronic ER stress enforces pancreatic beta-cell plasticity. *Nat Commun, 13*(1), 4621. doi:10.1038/s41467-022-32425-7

Chen, H. H., & Tarn, W. Y. (2019). uORF-mediated translational control: recently elucidated mechanisms and implications in cancer. *RNA Biol, 16*(10), 1327-1338. doi:10.1080/15476286.2019.1632634

Chen, Y., Tsai, B., Li, N., & Gao, N. (2022). Structural remodeling of ribosome associated Hsp40-Hsp70 chaperones during co-translational folding. *Nat Commun, 13*(1), 3410. doi:10.1038/s41467-022-31127-4

Cheng, L. C., Zheng, D., Baljinnyam, E., Sun, F., Ogami, K., Yeung, P. L., . . . Tian, B. (2020). Widespread transcript shortening through alternative polyadenylation in secretory cell differentiation. *Nat Commun, 11*(1), 3182. doi:10.1038/s41467-020-16959-2

Child, J. R., Chen, Q., Reid, D. W., Jagannathan, S., & Nicchitta, C. V. (2021). Recruitment of endoplasmic reticulum-targeted and cytosolic mRNAs into membrane-associated stress granules. *RNA, 27*(10), 1241-1256. doi:10.1261/rna.078858.121

Chorghade, S., Seimetz, J., Emmons, R., Yang, J., Bresson, S. M., Lisio, M., . . . Kalsotra, A. (2017). Poly(A) tail length regulates PABPC1 expression to tune translation in the heart. *Elife, 6*. doi:10.7554/eLife.24139

Chukwurah, E., Farabaugh, K. T., Guan, B. J., Ramakrishnan, P., & Hatzoglou, M. (2021). A tale of two proteins: PACT and PKR and their roles in inflammation. *FEBS J, 288*(22), 6365-6391. doi:10.1111/febs.15691

Costa-Mattioli, M., & Walter, P. (2020). The integrated stress response: From mechanism to disease. *Science, 368*(6489). doi:10.1126/science.aat5314

Cross, B. C., Bond, P. J., Sadowski, P. G., Jha, B. K., Zak, J., Goodman, J. M., . . . Harding, H. P. (2012). The molecular basis for selective inhibition of unconventional mRNA splicing by an IRE1-binding small molecule. *Proc Natl Acad Sci U S A, 109*(15), E869-878. doi:10.1073/pnas.1115623109

Cui, W., Li, J., Ron, D., & Sha, B. (2011). The structure of the PERK kinase domain suggests the mechanism for its activation. *Acta Crystallogr D Biol Crystallogr, 67*(Pt 5), 423-428. doi:10.1107/S0907444911006445

Cui, X. A., & Palazzo, A. F. (2014). Localization of mRNAs to the endoplasmic reticulum. *Wiley Interdiscip Rev RNA, 5*(4), 481-492. doi:10.1002/wrna.1225

Decroly, E., Ferron, F., Lescar, J., & Canard, B. (2011). Conventional and unconventional mechanisms for capping viral mRNA. *Nat Rev Microbiol, 10*(1), 51-65. doi:10.1038/nrmicro2675

Dever, T. E., Dinman, J. D., & Green, R. (2018). Translation Elongation and Recoding in Eukaryotes. *Cold Spring Harb Perspect Biol, 10*(8). doi:10.1101/cshperspect.a032649

Di Giammartino, D. C., Nishida, K., & Manley, J. L. (2011). Mechanisms and consequences of alternative polyadenylation. *Mol Cell, 43*(6), 853-866. doi:10.1016/j.molcel.2011.08.017

Dorotea, D., Koya, D., & Ha, H. (2020). Recent Insights Into SREBP as a Direct Mediator of Kidney Fibrosis via Lipid-Independent Pathways. *Front Pharmacol, 11*, 265. doi:10.3389/fphar.2020.00265

Dorrbaum, A. R., Alvarez-Castelao, B., Nassim-Assir, B., Langer, J. D., & Schuman, E. M. (2020). Proteome dynamics during homeostatic scaling in cultured neurons. *Elife, 9*. doi:10.7554/eLife.52939

Duan, T. L., Jiao, H., He, G. J., & Yan, Y. B. (2020). Translation Efficiency and Degradation of ER-Associated mRNAs Modulated by ER-Anchored poly(A)-Specific Ribonuclease (PARN). *Cells, 9*(1). doi:10.3390/cells9010162

Duffy, E. E., Schofield, J. A., & Simon, M. D. (2019). Gaining insight into transcriptome-wide RNA population dynamics through the chemistry of 4-thiouridine. *Wiley Interdiscip Rev RNA, 10*(1), e1513. doi:10.1002/wrna.1513

Duwaerts, C. C., Siao, K., Soon, R. K., Jr., Her, C., Iwawaki, T., Kohno, K., . . . Maher, J. J. (2021). Hepatocyte-specific deletion of XBP1 sensitizes mice to liver injury through hyperactivation of IRE1alpha. *Cell Death Differ, 28*(5), 1455-1465. doi:10.1038/s41418-020-00671-1

Eckmann, C. R., Rammelt, C., & Wahle, E. (2011). Control of poly(A) tail length. *Wiley Interdiscip Rev RNA, 2*(3), 348-361. doi:10.1002/wrna.56

Eden, E. R. (2016). The formation and function of ER-endosome membrane contact sites. *Biochim Biophys Acta, 1861*(8 Pt B), 874-879. doi:10.1016/j.bbalip.2016.01.020

Eichhorn, S. W., Subtelny, A. O., Kronja, I., Kwasnieski, J. C., Orr-Weaver, T. L., & Bartel, D. P. (2016). mRNA poly(A)-tail changes specified by deadenylation broadly reshape translation in Drosophila oocytes and early embryos. *Elife, 5*. doi:10.7554/eLife.16955

Eisen, T. J., Eichhorn, S. W., Subtelny, A. O., Lin, K. S., McGeary, S. E., Gupta, S., & Bartel, D. P. (2020). The Dynamics of Cytoplasmic mRNA Metabolism. *Mol Cell, 77*(4), 786-799 e710. doi:10.1016/j.molcel.2019.12.005

Eizirik, D. L., Pasquali, L., & Cnop, M. (2020). Pancreatic beta-cells in type 1 and type 2 diabetes mellitus: different pathways to failure. *Nat Rev Endocrinol, 16*(7), 349-362. doi:10.1038/s41574-020-0355-7

Eyries, M., Montani, D., Girerd, B., Perret, C., Leroy, A., Lonjou, C., . . . Soubrier, F. (2014). EIF2AK4 mutations cause pulmonary veno-occlusive disease, a recessive form of pulmonary hypertension. *Nat Genet, 46*(1), 65-69. doi:10.1038/ng.2844

Fan, A. C., & Leung, A. K. (2016). RNA Granules and Diseases: A Case Study of Stress Granules in ALS and FTLD. *Adv Exp Med Biol, 907*, 263-296. doi:10.1007/978-3-319-29073-7_11

Funato, K., Riezman, H., & Muniz, M. (2020). Vesicular and non-vesicular lipid export from the ER to the secretory pathway. *Biochim Biophys Acta Mol Cell Biol Lipids, 1865*(1), 158453. doi:10.1016/j.bbalip.2019.04.013

Gal-Ben-Ari, S., Barrera, I., Ehrlich, M., & Rosenblum, K. (2018). PKR: A Kinase to Remember. *Front Mol Neurosci, 11*, 480. doi:10.3389/fnmol.2018.00480

Galloway, A., & Cowling, V. H. (2019). mRNA cap regulation in mammalian cell function and fate. *Biochim Biophys Acta Gene Regul Mech, 1862*(3), 270-279. doi:10.1016/j.bbagrm.2018.09.011

Garcia-Barrio, M., Dong, J., Ufano, S., & Hinnebusch, A. G. (2000). Association of GCN1-GCN20 regulatory complex with the N-terminus of eIF2alpha kinase GCN2 is required for GCN2 activation. *EMBO J, 19*(8), 1887-1899. doi:10.1093/emboj/19.8.1887

Garneau, N. L., Wilusz, J., & Wilusz, C. J. (2007). The highways and byways of mRNA decay. *Nat Rev Mol Cell Biol, 8*(2), 113-126. doi:10.1038/nrm2104

Gerondopoulos, A., Brauer, P., Sobajima, T., Wu, Z., Parker, J. L., Biggin, P. C., . . . Newstead, S. (2021). A signal capture and proofreading mechanism for the KDEL-receptor explains selectivity and dynamic range in ER retrieval. *Elife, 10*. doi:10.7554/eLife.68380

Girardin, S. E., Cuziol, C., Philpott, D. J., & Arnoult, D. (2021). The eIF2alpha kinase HRI in innate immunity, proteostasis, and mitochondrial stress. *FEBS J, 288*(10), 3094-3107. doi:10.1111/febs.15553

Gomez, J. A., & Rutkowski, D. T. (2016). Experimental reconstitution of chronic ER stress in the liver reveals feedback suppression of BiP mRNA expression. *Elife, 5*. doi:10.7554/eLife.20390

Gonen, N., Sabath, N., Burge, C. B., & Shalgi, R. (2019). Widespread PERK-dependent repression of ER targets in response to ER stress. *Sci Rep, 9*(1), 4330. doi:10.1038/s41598-019-38705-5

Good, A. L., & Stoffers, D. A. (2020). Stress-Induced Translational Regulation Mediated by RNA Binding Proteins: Key Links to beta-Cell Failure in Diabetes. *Diabetes, 69*(4), 499-507. doi:10.2337/dbi18-0068

Grey, M. J., Cloots, E., Simpson, M. S., LeDuc, N., Serebrenik, Y. V., De Luca, H., . . . Lencer, W. I. (2020). IRE1beta negatively regulates IRE1alpha signaling in response to endoplasmic reticulum stress. *J Cell Biol, 219*(2). doi:10.1083/jcb.201904048

Guan, B. J., Krokowski, D., Majumder, M., Schmotzer, C. L., Kimball, S. R., Merrick, W. C., . . . Hatzoglou, M. (2014). Translational control during endoplasmic reticulum stress beyond phosphorylation of the translation initiation factor eIF2alpha. *J Biol Chem, 289*(18), 12593-12611. doi:10.1074/jbc.M113.543215

Guan, B. J., van Hoef, V., Jobava, R., Elroy-Stein, O., Valasek, L. S., Cargnello, M., . . . Hatzoglou, M. (2017). A Unique ISR Program Determines Cellular Responses to Chronic Stress. *Mol Cell, 68*(5), 885-900 e886. doi:10.1016/j.molcel.2017.11.007

Han, J., Back, S. H., Hur, J., Lin, Y. H., Gildersleeve, R., Shan, J., . . . Kaufman, R. J. (2013). ER-stress-induced transcriptional regulation increases protein synthesis leading to cell death. *Nat Cell Biol, 15*(5), 481-490. doi:10.1038/ncb2738

He, Y., Sun, S., Sha, H., Liu, Z., Yang, L., Xue, Z., . . . Qi, L. (2010). Emerging roles for XBP1, a sUPeR transcription factor. *Gene Expr, 15*(1), 13-25. doi:10.3727/105221610x12819686555051

Heck, A. M., & Wilusz, J. (2018). The Interplay between the RNA Decay and Translation Machinery in Eukaryotes. *Cold Spring Harb Perspect Biol, 10*(5). doi:10.1101/cshperspect.a032839

Hellen, C. U. T. (2018). Translation Termination and Ribosome Recycling in Eukaryotes. *Cold Spring Harb Perspect Biol, 10*(10). doi:10.1101/cshperspect.a032656

Herzel, L., Ottoz, D. S. M., Alpert, T., & Neugebauer, K. M. (2017). Splicing and transcription touch base: co-transcriptional spliceosome assembly and function. *Nat Rev Mol Cell Biol, 18*(10), 637-650. doi:10.1038/nrm.2017.63

Hetz, C., Chevet, E., & Oakes, S. A. (2015). Proteostasis control by the unfolded protein response. *Nat Cell Biol, 17*(7), 829-838. doi:10.1038/ncb3184

Hetz, C., & Papa, F. R. (2018). The Unfolded Protein Response and Cell Fate Control. *Mol Cell, 69*(2), 169-181. doi:10.1016/j.molcel.2017.06.017

Hillary, R. F., & FitzGerald, U. (2018). A lifetime of stress: ATF6 in development and homeostasis. *J Biomed Sci, 25*(1), 48. doi:10.1186/s12929-018-0453-1

Hinnebusch, A. G., & Lorsch, J. R. (2012). The mechanism of eukaryotic translation initiation: new insights and challenges. *Cold Spring Harb Perspect Biol, 4*(10). doi:10.1101/cshperspect.a011544

Hu, X. P., Dourado, H., Schubert, P., & Lercher, M. J. (2020). The protein translation machinery is expressed for maximal efficiency in Escherichia coli. *Nat Commun, 11*(1), 5260. doi:10.1038/s41467-020-18948-x

Hume, S., Dianov, G. L., & Ramadan, K. (2020). A unified model for the G1/S cell cycle transition. *Nucleic Acids Res, 48*(22), 12483-12501. doi:10.1093/nar/gkaa1002

Ingolia, N. T., Lareau, L. F., & Weissman, J. S. (2011). Ribosome profiling of mouse embryonic stem cells reveals the complexity and dynamics of mammalian proteomes. *Cell, 147*(4), 789-802. doi:10.1016/j.cell.2011.10.002

Jacquemyn, J., Cascalho, A., & Goodchild, R. E. (2017). The ins and outs of endoplasmic reticulum-controlled lipid biosynthesis. *EMBO Rep, 18*(11), 1905-1921. doi:10.15252/embr.201643426

Jalkanen, A. L., Coleman, S. J., & Wilusz, J. (2014). Determinants and implications of mRNA poly(A) tail size--does this protein make my tail look big? *Semin Cell Dev Biol, 34*, 24-32. doi:10.1016/j.semcdb.2014.05.018

Jaud, M., Philippe, C., Di Bella, D., Tang, W., Pyronnet, S., Laurell, H., . . . Touriol, C. (2020). Translational Regulations in Response to Endoplasmic Reticulum Stress in Cancers. *Cells, 9*(3). doi:10.3390/cells9030540

Jennings, M. D., Kershaw, C. J., Adomavicius, T., & Pavitt, G. D. (2017). Fail-safe control of translation initiation by dissociation of eIF2alpha phosphorylated ternary complexes. *Elife, 6*. doi:10.7554/eLife.24542

Junjappa, R. P., Patil, P., Bhattarai, K. R., Kim, H. R., & Chae, H. J. (2018). IRE1alpha Implications in Endoplasmic Reticulum Stress-Mediated Development and Pathogenesis of Autoimmune Diseases. *Front Immunol, 9*, 1289. doi:10.3389/fimmu.2018.01289

Kallunki, T., Barisic, M., Jaattela, M., & Liu, B. (2019). How to Choose the Right Inducible Gene Expression System for Mammalian Studies? *Cells, 8*(8). doi:10.3390/cells8080796

Kawai, T., Fan, J., Mazan-Mamczarz, K., & Gorospe, M. (2004). Global mRNA stabilization preferentially linked to translational repression during the endoplasmic reticulum stress response. *Mol Cell Biol, 24*(15), 6773-6787. doi:10.1128/MCB.24.15.6773-6787.2004

Kershaw, C. J., Jennings, M. D., Cortopassi, F., Guaita, M., Al-Ghafli, H., & Pavitt, G. D. (2021). GTP binding to translation factor eIF2B stimulates its guanine nucleotide exchange activity. *iScience, 24*(12), 103454. doi:10.1016/j.isci.2021.103454

Kiledjian, M. (2018). Eukaryotic RNA 5'-End NAD(+) Capping and DeNADding. *Trends Cell Biol, 28*(6), 454-464. doi:10.1016/j.tcb.2018.02.005

Kolitz, S. E., & Lorsch, J. R. (2010). Eukaryotic initiator tRNA: finely tuned and ready for action. *FEBS Lett, 584*(2), 396-404. doi:10.1016/j.febslet.2009.11.047

Kondrashov, A., Meijer, H. A., Barthet-Barateig, A., Parker, H. N., Khurshid, A., Tessier, S., . . . De Moor, C. H. (2012). Inhibition of polyadenylation reduces inflammatory gene induction. *RNA, 18*(12), 2236-2250. doi:10.1261/rna.032391.112

Koromilas, A. E. (2019). M(en)TORship lessons on life and death by the integrated stress response. *Biochim Biophys Acta Gen Subj, 1863*(3), 644-649. doi:10.1016/j.bbagen.2018.12.009

Krebs, J., Groenendyk, J., & Michalak, M. (2011). Ca2+-signaling, alternative splicing and endoplasmic reticulum stress responses. *Neurochem Res, 36*(7), 1198-1211. doi:10.1007/s11064-011-0431-4

Krokowski, D., Han, J., Saikia, M., Majumder, M., Yuan, C. L., Guan, B. J., . . . Hatzoglou, M. (2013). A self-defeating anabolic program leads to beta-cell apoptosis in endoplasmic reticulum stress-induced diabetes via regulation of amino acid flux. *J Biol Chem, 288*(24), 17202-17213. doi:10.1074/jbc.M113.466920

Kumar, A., Clerici, M., Muckenfuss, L. M., Passmore, L. A., & Jinek, M. (2019). Mechanistic insights into mRNA 3'-end processing. *Curr Opin Struct Biol, 59*, 143-150. doi:10.1016/j.sbi.2019.08.001

Kurosaki, T., Popp, M. W., & Maquat, L. E. (2019). Quality and quantity control of gene expression by nonsense-mediated mRNA decay. *Nat Rev Mol Cell Biol, 20*(7), 406-420. doi:10.1038/s41580-019-0126-2

Kwan, T., & Thompson, S. R. (2019). Noncanonical Translation Initiation in Eukaryotes. *Cold Spring Harb Perspect Biol, 11*(4). doi:10.1101/cshperspect.a032672

Lancaster, G. I., Kammoun, H. L., Kraakman, M. J., Kowalski, G. M., Bruce, C. R., & Febbraio, M. A. (2016). PKR is not obligatory for high-fat diet-induced obesity and its associated metabolic and inflammatory complications. *Nat Commun, 7*, 10626. doi:10.1038/ncomms10626

Le Thomas, A., Ferri, E., Marsters, S., Harnoss, J. M., Lawrence, D. A., Zuazo-Gaztelu, I., . . . Ashkenazi, A. (2021). Decoding non-canonical mRNA decay by the endoplasmic-reticulum stress sensor IRE1alpha. *Nat Commun, 12*(1), 7310. doi:10.1038/s41467-021-27597-7

Lee, H., Lee, Y. S., Harenda, Q., Pietrzak, S., Oktay, H. Z., Schreiber, S., . . . Engin, F. (2020). Beta Cell Dedifferentiation Induced by IRE1alpha Deletion Prevents Type 1 Diabetes. *Cell Metab, 31*(4), 822-836 e825. doi:10.1016/j.cmet.2020.03.002

Lee, K., Tirasophon, W., Shen, X., Michalak, M., Prywes, R., Okada, T., . . . Kaufman, R. J. (2002). IRE1-mediated unconventional mRNA splicing and S2P-mediated ATF6 cleavage merge to regulate XBP1 in signaling the unfolded protein response. *Genes Dev, 16*(4), 452-466. doi:10.1101/gad.964702

Legnini, I., Alles, J., Karaiskos, N., Ayoub, S., & Rajewsky, N. (2019). FLAM-seq: full-length mRNA sequencing reveals principles of poly(A) tail length control. *Nat Methods, 16*(9), 879-886. doi:10.1038/s41592-019-0503-y

Lemmens, R., Larsson, O., Berggren, P. O., & Islam, M. S. (2001). Ca2+-induced Ca2+ release from the endoplasmic reticulum amplifies the Ca2+ signal mediated by activation of voltage-gated L-type Ca2+ channels in pancreatic beta-cells. *J Biol Chem, 276*(13), 9971-9977. doi:10.1074/jbc.M009463200

Lim, J., Kim, D., Lee, Y. S., Ha, M., Lee, M., Yeo, J., . . . Kim, V. N. (2018). Mixed tailing by TENT4A and TENT4B shields mRNA from rapid deadenylation. *Science, 361*(6403), 701-704. doi:10.1126/science.aam5794

Lim, J., Lee, M., Son, A., Chang, H., & Kim, V. N. (2016). mTAIL-seq reveals dynamic poly(A) tail regulation in oocyte-to-embryo development. *Genes Dev, 30*(14), 1671-1682. doi:10.1101/gad.284802.116

Lima, S. A., Chipman, L. B., Nicholson, A. L., Chen, Y. H., Yee, B. A., Yeo, G. W., . . . Pasquinelli, A. E. (2017). Short poly(A) tails are a conserved feature of highly expressed genes. *Nat Struct Mol Biol, 24*(12), 1057-1063. doi:10.1038/nsmb.3499

Liu, G. Y., & Sabatini, D. M. (2020). mTOR at the nexus of nutrition, growth, ageing and disease. *Nat Rev Mol Cell Biol, 21*(4), 183-203. doi:10.1038/s41580-019-0199-y

Liu, R., & Proud, C. G. (2016). Eukaryotic elongation factor 2 kinase as a drug target in cancer, and in cardiovascular and neurodegenerative diseases. *Acta Pharmacol Sin, 37*(3), 285-294. doi:10.1038/aps.2015.123

Ma, Y., & Hendershot, L. M. (2004). ER chaperone functions during normal and stress conditions. *J Chem Neuroanat, 28*(1-2), 51-65. doi:10.1016/j.jchemneu.2003.08.007

Maillo, C., Martin, J., Sebastian, D., Hernandez-Alvarez, M., Garcia-Rocha, M., Reina, O., . . . Mendez, R. (2017). Circadian- and UPR-dependent control of CPEB4 mediates a translational response to counteract hepatic steatosis under ER stress. *Nat Cell Biol, 19*(2), 94-105. doi:10.1038/ncb3461

Majumder, M., Huang, C., Snider, M. D., Komar, A. A., Tanaka, J., Kaufman, R. J., . . . Hatzoglou, M. (2012). A novel feedback loop regulates the response to endoplasmic reticulum stress via the cooperation of cytoplasmic splicing and mRNA translation. *Mol Cell Biol, 32*(5), 992-1003. doi:10.1128/MCB.06665-11

Malhi, H. (2014). MICRORNAs IN ER STRESS: DIVERGENT ROLES IN CELL FATE DECISIONS. *Curr Pathobiol Rep, 2*(3), 117-122. doi:10.1007/s40139-014-0046-y

Maracci, C., & Rodnina, M. V. (2016). Review: Translational GTPases. *Biopolymers, 105*(8), 463-475. doi:10.1002/bip.22832

Martineau, Y., Derry, M. C., Wang, X., Yanagiya, A., Berlanga, J. J., Shyu, A. B., . . . Sonenberg, N. (2008). Poly(A)-binding protein-interacting protein 1 binds to eukaryotic translation initiation factor 3 to stimulate translation. *Mol Cell Biol, 28*(21), 6658-6667. doi:10.1128/MCB.00738-08

Martinez-Rucobo, F. W., Kohler, R., van de Waterbeemd, M., Heck, A. J., Hemann, M., Herzog, F., . . . Cramer, P. (2015). Molecular Basis of Transcription-Coupled Pre-mRNA Capping. *Mol Cell, 58*(6), 1079-1089. doi:10.1016/j.molcel.2015.04.004

Marzluff, W. F., Wagner, E. J., & Duronio, R. J. (2008). Metabolism and regulation of canonical histone mRNAs: life without a poly(A) tail. *Nat Rev Genet, 9*(11), 843-854. doi:10.1038/nrg2438

Masson, G. R. (2019). Towards a model of GCN2 activation. *Biochem Soc Trans, 47*(5), 1481-1488. doi:10.1042/BST20190331

Matsuki, Y., Matsuo, Y., Nakano, Y., Iwasaki, S., Yoko, H., Udagawa, T., . . . Inada, T. (2020). Ribosomal protein S7 ubiquitination during ER stress in yeast is associated with selective mRNA translation and stress outcome. *Sci Rep, 10*(1), 19669. doi:10.1038/s41598-020-76239-3

Maurel, M., Chevet, E., Tavernier, J., & Gerlo, S. (2014). Getting RIDD of RNA: IRE1 in cell fate regulation. *Trends Biochem Sci, 39*(5), 245-254. doi:10.1016/j.tibs.2014.02.008

McCaughey, J., & Stephens, D. J. (2018). COPII-dependent ER export in animal cells: adaptation and control for diverse cargo. *Histochem Cell Biol, 150*(2), 119-131. doi:10.1007/s00418-018-1689-2

Meijer, H. A., & de Moor, C. H. (2011). Fractionation of mRNA based on the length of the poly(A) tail. *Methods Mol Biol, 703*, 123-135. doi:10.1007/978-1-59745-248-9_9

Merrick, W. C., & Pavitt, G. D. (2018). Protein Synthesis Initiation in Eukaryotic Cells. *Cold Spring Harb Perspect Biol, 10*(12). doi:10.1101/cshperspect.a033092

Michels, A. A., & Bensaude, O. (2018). Hexim1, an RNA-controlled protein hub. *Transcription, 9*(4), 262-271. doi:10.1080/21541264.2018.1429836

Mollereau, B., Manie, S., & Napoletano, F. (2014). Getting the better of ER stress. *J Cell Commun Signal, 8*(4), 311-321. doi:10.1007/s12079-014-0251-9

Moncoq, K., Trieber, C. A., & Young, H. S. (2007). The molecular basis for cyclopiazonic acid inhibition of the sarcoplasmic reticulum calcium pump. *J Biol Chem, 282*(13), 9748-9757. doi:10.1074/jbc.M611653200

Moro, S. G., Hermans, C., Ruiz-Orera, J., & Alba, M. M. (2021). Impact of uORFs in mediating regulation of translation in stress conditions. *BMC Mol Cell Biol, 22*(1), 29. doi:10.1186/s12860-021-00363-9

Morris, C., Cluet, D., & Ricci, E. P. (2021). Ribosome dynamics and mRNA turnover, a complex relationship under constant cellular scrutiny. *Wiley Interdiscip Rev RNA, 12*(6), e1658. doi:10.1002/wrna.1658

Namkoong, S., Ho, A., Woo, Y. M., Kwak, H., & Lee, J. H. (2018). Systematic Characterization of Stress-Induced RNA Granulation. *Mol Cell, 70*(1), 175-187 e178. doi:10.1016/j.molcel.2018.02.025

Nanavaty, V., Abrash, E. W., Hong, C., Park, S., Fink, E. E., Li, Z., . . . Ting, A. H. (2020). DNA Methylation Regulates Alternative Polyadenylation via CTCF and the Cohesin Complex. *Mol Cell, 78*(4), 752-764 e756. doi:10.1016/j.molcel.2020.03.024

Nicholson, A. L., & Pasquinelli, A. E. (2019). Tales of Detailed Poly(A) Tails. *Trends Cell Biol, 29*(3), 191-200. doi:10.1016/j.tcb.2018.11.002

Novoa, I., Zhang, Y., Zeng, H., Jungreis, R., Harding, H. P., & Ron, D. (2003). Stress-induced gene expression requires programmed recovery from translational repression. *EMBO J, 22*(5), 1180-1187. doi:10.1093/emboj/cdg112

Nurenberg-Goloub, E., Kratzat, H., Heinemann, H., Heuer, A., Kotter, P., Berninghausen, O., . . . Beckmann, R. (2020). Molecular analysis of the ribosome recycling factor ABCE1 bound to the 30S post-splitting complex. *EMBO J, 39*(9), e103788. doi:10.15252/embj.2019103788

Oslowski, C. M., & Urano, F. (2011). Measuring ER stress and the unfolded protein response using mammalian tissue culture system. *Methods Enzymol, 490*, 71-92. doi:10.1016/B978-0-12-385114-7.00004-0

Ozcan, U., Cao, Q., Yilmaz, E., Lee, A. H., Iwakoshi, N. N., Ozdelen, E., . . . Hotamisligil, G. S. (2004). Endoplasmic reticulum stress links obesity, insulin action, and type 2 diabetes. *Science, 306*(5695), 457-461. doi:10.1126/science.1103160

Pakos-Zebrucka, K., Koryga, I., Mnich, K., Ljujic, M., Samali, A., & Gorman, A. M. (2016). The integrated stress response. *EMBO Rep, 17*(10), 1374-1395. doi:10.15252/embr.201642195

Park, J. E., Yi, H., Kim, Y., Chang, H., & Kim, V. N. (2016). Regulation of Poly(A) Tail and Translation during the Somatic Cell Cycle. *Mol Cell, 62*(3), 462-471. doi:10.1016/j.molcel.2016.04.007

Park, O. H., Park, J., Yu, M., An, H. T., Ko, J., & Kim, Y. K. (2016). Identification and molecular characterization of cellular factors required for glucocorticoid receptor-mediated mRNA decay. *Genes Dev, 30*(18), 2093-2105. doi:10.1101/gad.286484.116

Park, S. M., Kang, T. I., & So, J. S. (2021). Roles of XBP1s in Transcriptional Regulation of Target Genes. *Biomedicines, 9*(7). doi:10.3390/biomedicines9070791

Parker, R. (2012). RNA degradation in Saccharomyces cerevisae. *Genetics, 191*(3), 671-702. doi:10.1534/genetics.111.137265

Passmore, L. A., & Coller, J. (2022). Roles of mRNA poly(A) tails in regulation of eukaryotic gene expression. *Nat Rev Mol Cell Biol, 23*(2), 93-106. doi:10.1038/s41580-021-00417-y

Patil, D. P., Bakthavachalu, B., & Schoenberg, D. R. (2014). Poly(A) polymerase-based poly(A) length assay. *Methods Mol Biol, 1125*, 13-23. doi:10.1007/978-1-62703-971-0_2

Pavitt, G. D., & Ron, D. (2012). New insights into translational regulation in the endoplasmic reticulum unfolded protein response. *Cold Spring Harb Perspect Biol, 4*(6). doi:10.1101/cshperspect.a012278

Pelechano, V., Wei, W., & Steinmetz, L. M. (2015). Widespread Co-translational RNA Decay Reveals Ribosome Dynamics. *Cell, 161*(6), 1400-1412. doi:10.1016/j.cell.2015.05.008

Peltz, S. W., Donahue, J. L., & Jacobson, A. (1992). A mutation in the tRNA nucleotidyltransferase gene promotes stabilization of mRNAs in Saccharomyces cerevisiae. *Mol Cell Biol, 12*(12), 5778-5784. doi:10.1128/mcb.12.12.5778-5784.1992

Pobre, K. F. R., Poet, G. J., & Hendershot, L. M. (2019). The endoplasmic reticulum (ER) chaperone BiP is a master regulator of ER functions: Getting by with a little help from ERdj friends. *J Biol Chem, 294*(6), 2098-2108. doi:10.1074/jbc.REV118.002804

Preissler, S., Rato, C., Yan, Y., Perera, L. A., Czako, A., & Ron, D. (2020). Calcium depletion challenges endoplasmic reticulum proteostasis by destabilising BiP-substrate complexes. *Elife, 9*. doi:10.7554/eLife.62601

Presnyak, V., Alhusaini, N., Chen, Y. H., Martin, S., Morris, N., Kline, N., . . . Coller, J. (2015). Codon optimality is a major determinant of mRNA stability. *Cell, 160*(6), 1111-1124. doi:10.1016/j.cell.2015.02.029

Proudfoot, N. J. (2016). Transcriptional termination in mammals: Stopping the RNA polymerase II juggernaut. *Science, 352*(6291), aad9926. doi:10.1126/science.aad9926

Puhringer, T., Hohmann, U., Fin, L., Pacheco-Fiallos, B., Schellhaas, U., Brennecke, J., & Plaschka, C. (2020). Structure of the human core transcription-export complex reveals a hub for multivalent interactions. *Elife, 9*. doi:10.7554/eLife.61503

Radhakrishnan, A., Chen, Y. H., Martin, S., Alhusaini, N., Green, R., & Coller, J. (2016). The DEAD-Box Protein Dhh1p Couples mRNA Decay and Translation by Monitoring Codon Optimality. *Cell, 167*(1), 122-132 e129. doi:10.1016/j.cell.2016.08.053

Rambout, X., & Maquat, L. E. (2020). The nuclear cap-binding complex as choreographer of gene transcription and pre-mRNA processing. *Genes Dev, 34*(17-18), 1113-1127. doi:10.1101/gad.339986.120

Reid, D. W., & Nicchitta, C. V. (2015). Diversity and selectivity in mRNA translation on the endoplasmic reticulum. *Nat Rev Mol Cell Biol, 16*(4), 221-231. doi:10.1038/nrm3958

Roep, B. O., Thomaidou, S., van Tienhoven, R., & Zaldumbide, A. (2021). Type 1 diabetes mellitus as a disease of the beta-cell (do not blame the immune system?). *Nat Rev Endocrinol, 17*(3), 150-161. doi:10.1038/s41574-020-00443-4

Ross, J. (1997). A hypothesis to explain why translation inhibitors stabilize mRNAs in mammalian cells: mRNA stability and mitosis. *Bioessays, 19*(6), 527-529. doi:10.1002/bies.950190612

Rothenberg, D. A., Taliaferro, J. M., Huber, S. M., Begley, T. J., Dedon, P. C., & White, F. M. (2018). A Proteomics Approach to Profiling the Temporal Translational Response to Stress and Growth. *iScience, 9*, 367-381. doi:10.1016/j.isci.2018.11.004

Ruggiano, A., Foresti, O., & Carvalho, P. (2014). Quality control: ER-associated degradation: protein quality control and beyond. *J Cell Biol, 204*(6), 869-879. doi:10.1083/jcb.201312042

Rutkowski, D. T., Arnold, S. M., Miller, C. N., Wu, J., Li, J., Gunnison, K. M., . . . Kaufman, R. J. (2006). Adaptation to ER stress is mediated by differential stabilities of pro-survival and pro-apoptotic mRNAs and proteins. *PLoS Biol, 4*(11), e374. doi:10.1371/journal.pbio.0040374

Schuller, A. P., Wu, C. C., Dever, T. E., Buskirk, A. R., & Green, R. (2017). eIF5A Functions Globally in Translation Elongation and Termination. *Mol Cell, 66*(2), 194-205 e195. doi:10.1016/j.molcel.2017.03.003

Schwarz, D. S., & Blower, M. D. (2016). The endoplasmic reticulum: structure, function and response to cellular signaling. *Cell Mol Life Sci, 73*(1), 79-94. doi:10.1007/s00018-015-2052-6

Sen, N. D., Zhou, F., Harris, M. S., Ingolia, N. T., & Hinnebusch, A. G. (2016). eIF4B stimulates translation of long mRNAs with structured 5' UTRs and low closed-loop potential but weak dependence on eIF4G. *Proc Natl Acad Sci U S A, 113*(38), 10464-10472. doi:10.1073/pnas.1612398113

Shalgi, R., Hurt, J. A., Krykbaeva, I., Taipale, M., Lindquist, S., & Burge, C. B. (2013). Widespread regulation of translation by elongation pausing in heat shock. *Mol Cell, 49*(3), 439-452. doi:10.1016/j.molcel.2012.11.028

Shanmuganathan, V., Schiller, N., Magoulopoulou, A., Cheng, J., Braunger, K., Cymer, F., . . . Beckmann, R. (2019). Structural and mutational analysis of the ribosome-arresting human XBP1u. *Elife, 8*. doi:10.7554/eLife.46267

Singha, M., Spitalny, L., Nguyen, K., Vandewalle, A., & Spitale, R. C. (2021). Chemical methods for measuring RNA expression with metabolic labeling. *Wiley Interdiscip Rev RNA, 12*(5), e1650. doi:10.1002/wrna.1650

Slobodin, B., Bahat, A., Sehrawat, U., Becker-Herman, S., Zuckerman, B., Weiss, A. N., . . . Dikstein, R. (2020). Transcription Dynamics Regulate Poly(A) Tails and Expression of the RNA Degradation Machinery to Balance mRNA Levels. *Mol Cell, 78*(3), 434-444 e435. doi:10.1016/j.molcel.2020.03.022

Slobodin, B., & Dikstein, R. (2020). So close, no matter how far: multiple paths connecting transcription to mRNA translation in eukaryotes. *EMBO Rep, 21*(9), e50799. doi:10.15252/embr.202050799

Slobodin, B., Han, R., Calderone, V., Vrielink, J., Loayza-Puch, F., Elkon, R., & Agami, R. (2017). Transcription Impacts the Efficiency of mRNA Translation via Co-transcriptional N6-adenosine Methylation. *Cell, 169*(2), 326-337 e312. doi:10.1016/j.cell.2017.03.031

Smith, R. W. P., Anderson, R. C., Larralde, O., Smith, J. W. S., Gorgoni, B., Richardson, W. A., . . . Gray, N. K. (2017). Viral and cellular mRNA-specific activators harness PABP and eIF4G to promote translation initiation downstream of cap binding. *Proc Natl Acad Sci U S A, 114*(24), 6310-6315. doi:10.1073/pnas.1610417114

Sonenberg, N., & Hinnebusch, A. G. (2009). Regulation of translation initiation in eukaryotes: mechanisms and biological targets. *Cell, 136*(4), 731-745. doi:10.1016/j.cell.2009.01.042

Sonneveld, S., Verhagen, B. M. P., & Tanenbaum, M. E. (2020). Heterogeneity in mRNA Translation. *Trends Cell Biol, 30*(8), 606-618. doi:10.1016/j.tcb.2020.04.008

Sreejith, R. K., Suresh, C. G., Bhosale, S. H., Bhavnani, V., Kumar, A., Gaikwad, S. M., & Pal, J. K. (2012). Conformational transitions of the catalytic domain of heme-regulated eukaryotic initiation factor 2alpha kinase, a key translational regulatory molecule. *J Fluoresc, 22*(1), 431-441. doi:10.1007/s10895-011-0976-2

Starck, S. R., & Shastri, N. (2016). Nowhere to hide: unconventional translation yields cryptic peptides for immune surveillance. *Immunol Rev, 272*(1), 8-16. doi:10.1111/imr.12434

Stewart, C., Estrada, A., Kim, P., Wang, D., Wei, Y., Gentile, C., & Pagliassotti, M. (2017). Regulation of IRE1alpha by the small molecule inhibitor 4mu8c in hepatoma cells. *Endoplasmic Reticulum Stress Dis, 4*(1), 1-10. doi:10.1515/ersc-2017-0001

Stewart, M. (2019). Polyadenylation and nuclear export of mRNAs. *J Biol Chem, 294*(9), 2977-2987. doi:10.1074/jbc.REV118.005594

Stimac, E., Groppi, V. E., Jr., & Coffino, P. (1984). Inhibition of protein synthesis stabilizes histone mRNA. *Mol Cell Biol, 4*(10), 2082-2090. doi:10.1128/mcb.4.10.2082-2090.1984

Subtelny, A. O., Eichhorn, S. W., Chen, G. R., Sive, H., & Bartel, D. P. (2014). Poly(A)-tail profiling reveals an embryonic switch in translational control. *Nature, 508*(7494), 66-71. doi:10.1038/nature13007

Susorov, D., Zakharov, N., Shuvalova, E., Ivanov, A., Egorova, T., Shuvalov, A., . . . Alkalaeva, E. (2018). Eukaryotic translation elongation factor 2 (eEF2) catalyzes reverse translocation of the eukaryotic ribosome. *J Biol Chem, 293*(14), 5220-5229. doi:10.1074/jbc.RA117.000761

Tam, A. B., Koong, A. C., & Niwa, M. (2014). Ire1 has distinct catalytic mechanisms for XBP1/HAC1 splicing and RIDD. *Cell Rep, 9*(3), 850-858. doi:10.1016/j.celrep.2014.09.016

Tan, J. L., Fogley, R. D., Flynn, R. A., Ablain, J., Yang, S., Saint-Andre, V., . . . Zon, L. I. (2016). Stress from Nucleotide Depletion Activates the Transcriptional Regulator HEXIM1 to Suppress Melanoma. *Mol Cell, 62*(1), 34-46. doi:10.1016/j.molcel.2016.03.013

Tanenbaum, M. E., Stern-Ginossar, N., Weissman, J. S., & Vale, R. D. (2015). Regulation of mRNA translation during mitosis. *Elife, 4*. doi:10.7554/eLife.07957

Thompson, D. M., & Parker, R. (2009). The RNase Rny1p cleaves tRNAs and promotes cell death during oxidative stress in Saccharomyces cerevisiae. *J Cell Biol, 185*(1), 43-50. doi:10.1083/jcb.200811119

Ujvari, A., & Luse, D. S. (2004). Newly Initiated RNA encounters a factor involved in splicing immediately upon emerging from within RNA polymerase II. *J Biol Chem, 279*(48), 49773-49779. doi:10.1074/jbc.M409087200

Ule, J., & Blencowe, B. J. (2019). Alternative Splicing Regulatory Networks: Functions, Mechanisms, and Evolution. *Mol Cell, 76*(2), 329-345. doi:10.1016/j.molcel.2019.09.017

van den Beucken, T., Magagnin, M. G., Savelkouls, K., Lambin, P., Koritzinsky, M., & Wouters, B. G. (2007). Regulation of Cited2 expression provides a functional link between translational and transcriptional responses during hypoxia. *Radiother Oncol, 83*(3), 346-352. doi:10.1016/j.radonc.2007.04.026

Vanderweyde, T., Youmans, K., Liu-Yesucevitz, L., & Wolozin, B. (2013). Role of stress granules and RNA-binding proteins in neurodegeneration: a mini-review. *Gerontology, 59*(6), 524-533. doi:10.1159/000354170

Vindry, C., Lauwers, A., Hutin, D., Soin, R., Wauquier, C., Kruys, V., & Gueydan, C. (2012). dTIS11 Protein-dependent polysomal deadenylation is the key step in AU-rich element-mediated mRNA decay in Drosophila cells. *J Biol Chem, 287*(42), 35527-35538. doi:10.1074/jbc.M112.356188

Viphakone, N., Hautbergue, G. M., Walsh, M., Chang, C. T., Holland, A., Folco, E. G., . . . Wilson, S. A. (2012). TREX exposes the RNA-binding domain of Nxf1 to enable mRNA export. *Nat Commun, 3*, 1006. doi:10.1038/ncomms2005

Watanabe, T., Imamura, T., & Hiasa, Y. (2018). Roles of protein kinase R in cancer: Potential as a therapeutic target. *Cancer Sci, 109*(4), 919-925. doi:10.1111/cas.13551

Webster, M. W., Chen, Y. H., Stowell, J. A. W., Alhusaini, N., Sweet, T., Graveley, B. R., . . . Passmore, L. A. (2018). mRNA Deadenylation Is Coupled to Translation Rates by the Differential Activities of Ccr4-Not Nucleases. *Mol Cell, 70*(6), 1089-1100 e1088. doi:10.1016/j.molcel.2018.05.033

Weill, L., Belloc, E., Bava, F. A., & Mendez, R. (2012). Translational control by changes in poly(A) tail length: recycling mRNAs. *Nat Struct Mol Biol, 19*(6), 577-585. doi:10.1038/nsmb.2311

Wek, R. C. (2018). Role of eIF2alpha Kinases in Translational Control and Adaptation to Cellular Stress. *Cold Spring Harb Perspect Biol, 10*(7). doi:10.1101/cshperspect.a032870

Wende, W., Friedhoff, P., & Strasser, K. (2019). Mechanism and Regulation of Co-transcriptional mRNP Assembly and Nuclear mRNA Export. *Adv Exp Med Biol, 1203*, 1-31. doi:10.1007/978-3-030-31434-7_1

Wissink, E. M., Vihervaara, A., Tippens, N. D., & Lis, J. T. (2019). Nascent RNA analyses: tracking transcription and its regulation. *Nat Rev Genet, 20*(12), 705-723. doi:10.1038/s41576-019-0159-6

Wolf, D. A., Lin, Y., Duan, H., & Cheng, Y. (2020). eIF-Three to Tango: emerging functions of translation initiation factor eIF3 in protein synthesis and disease. *J Mol Cell Biol, 12*(6), 403-409. doi:10.1093/jmcb/mjaa018

Wolozin, B., & Ivanov, P. (2019). Stress granules and neurodegeneration. *Nat Rev Neurosci, 20*(11), 649-666. doi:10.1038/s41583-019-0222-5

Woo, Y. M., Kwak, Y., Namkoong, S., Kristjansdottir, K., Lee, S. H., Lee, J. H., & Kwak, H. (2018). TED-Seq Identifies the Dynamics of Poly(A) Length during ER Stress. *Cell Rep, 24*(13), 3630-3641 e3637. doi:10.1016/j.celrep.2018.08.084

Xiang, K., & Bartel, D. P. (2021). The molecular basis of coupling between poly(A)-tail length and translational efficiency. *Elife, 10*. doi:10.7554/eLife.66493

Xu, B., Liu, L., & Song, G. (2021). Functions and Regulation of Translation Elongation Factors. *Front Mol Biosci, 8*, 816398. doi:10.3389/fmolb.2021.816398

Yamamoto, K., Sato, T., Matsui, T., Sato, M., Okada, T., Yoshida, H., . . . Mori, K. (2007). Transcriptional induction of mammalian ER quality control proteins is mediated by single or combined action of ATF6alpha and XBP1. *Dev Cell, 13*(3), 365-376. doi:10.1016/j.devcel.2007.07.018

Yan, X., Hoek, T. A., Vale, R. D., & Tanenbaum, M. E. (2016). Dynamics of Translation of Single mRNA Molecules In Vivo. *Cell, 165*(4), 976-989. doi:10.1016/j.cell.2016.04.034

Yoshida, H., Matsui, T., Yamamoto, A., Okada, T., & Mori, K. (2001). XBP1 mRNA is induced by ATF6 and spliced by IRE1 in response to ER stress to produce a highly active transcription factor. *Cell, 107*(7), 881-891. doi:10.1016/s0092-8674(01)00611-0

Yucel, S. S., Stelzer, W., Lorenzoni, A., Wozny, M., Langosch, D., & Lemberg, M. K. (2019). The Metastable XBP1u Transmembrane Domain Defines Determinants for Intramembrane Proteolysis by Signal Peptide Peptidase. *Cell Rep, 26*(11), 3087-3099 e3011. doi:10.1016/j.celrep.2019.02.057

Zhang, P., McGrath, B., Li, S., Frank, A., Zambito, F., Reinert, J., . . . Cavener, D. R. (2002). The PERK eukaryotic initiation factor 2 alpha kinase is required for the development of the skeletal system, postnatal growth, and the function and viability of the pancreas. *Mol Cell Biol, 22*(11), 3864-3874. doi:10.1128/MCB.22.11.3864-3874.2002

Zomot, E., Achildiev Cohen, H., Dagan, I., Militsin, R., & Palty, R. (2021). Bidirectional regulation of calcium release-activated calcium (CRAC) channel by SARAF. *J Cell Biol, 220*(12). doi:10.1083/jcb.202104007